The Messenger

ALMA Antenna Production
New Filters for VISIR
Polarimetry of Gaseous Planets
Long Night of Science

ESO

A Science Vision for European Astronomy in the Next 20 Years

Guy Monnet[1]
Frank Molster[2]
Jorge Melnick[1]

[1] ESO
[2] Netherlands Organisation for Scientific Research (NWO), Den Haag, the Netherlands

By the end of the last century, European astronomers had secured large access to world-class facilities and produced cutting-edge science at all wavelengths, both from the ground and in space. To maintain that position and to ensure the necessary high level of international coordination and collaboration, it is essential to set up a European astrophysical strategic plan for the next two decades. This task is currently carried out by the ASTRONET network of funding Agencies, sponsored by the European Commission. A comprehensive Science Vision has now been produced. It will be followed in the autumn of 2008 by a prioritised roadmap of the facilities needed to implement this Vision.

European astronomy today is fully competitive on the global scene and at the forefront in many domains, with such recent breakthroughs as the first detection of an earth-like planet in the habitable zone around its parent star, the successful landing of a probe on Titan, the evidence for a massive black hole in the centre of our own Galaxy, the discovery of gravitational arcs in galaxy clusters and the proof that most gamma-ray bursts are caused by massive exploding stars at cosmological distances. The rise of European astronomy to this top position by the end of the last century has been achieved through extensive cooperation and coordination of efforts, in particular – but not only – through ESO for optical astronomy and ESA for space astronomy.

The ASTRONET programme

To strengthen Europe's position and extend it to all branches of astronomy and all nations of the enlarged European Research Area, a group of European funding agencies set up an ERA-Net programme, called ASTRONET and coordinated by INSU-CNRS, with the goal of establishing a comprehensive long-term strategic plan for European astronomy. The ASTRONET mandate covers all astrophysical domains from cosmology to the Solar System, and every observing window to the Universe, from space and from ground, and from electromagnetic radiation to particles and gravitational waves, to in situ exploration of the objects in our Solar System. It encompasses the links with neighbouring disciplines and, in particular, with the astroparticle community which is also developing its own strategic plan within the ASPERA ERA-Net programme (*http://www.aspera-eu.org/*). Cross membership of panels and overlapping interests of scientists ensure a fruitful collaboration in both endeavours.

ASTRONET addresses the whole astronomical 'food chain' from infrastructure and technology development to observation, data access, modelling, laboratory data and theory, and the human resources needed to make it all work. It also covers public awareness via education and public outreach. This effort is actually quite similar in scope to the 'decadal surveys' produced in the USA over the last fifty years, although conducted within a different setting. Extensive information on the full ASTRONET programme, currently supported by ESO, ESA and 18 funding agencies from across Europe is available from *http://www.astronet-eu.org/*.

Within this overall programme, a two-step procedure has been adopted. The first step was to produce an integrated Science Vision, an essential input to the subsequent task of drawing up a prioritised infrastructure roadmap to implement the Vision. Together they will provide the full strategic plan for the next two decades.

The Science Vision

The Science Vision document was released at the end of September 2007. This is the result of intense work by the Science Vision Working Group, aided by four thematic panels, a total of 50 scientists drawn from the community of European astronomers. Detailed mid-term feedback from the community was secured through a web forum and an open symposium that took place last January in Poitiers, France, in which 228 astronomers from 31 countries participated. The resulting scientific landscape was finally distilled by the Science Vision Working Group.

The Science Vision provides a comprehensive overview of the scientific issues that European astronomy should address in the next twenty years. The four key themes retained are: the extremes of the Universe, from the nature of dark matter and dark energy that comprise over 95 % of the Universe to the physics of extreme objects such as black holes, neutron stars, and gamma-ray bursts; the formation and evolution of galaxies from the first seeds to our Milky Way; the formation of stars and planetary systems and their evolution up to the origin of life; and the major question of how do we (and our Solar System) fit in the global picture of the Universe. These themes reach well beyond the realm of traditional astronomy into the frontiers of physics and biology.

Each of the four themes was further broken into five or six critical science questions that were analysed in depth. One important aspect of the effort was to identify the goals that we aim for and the
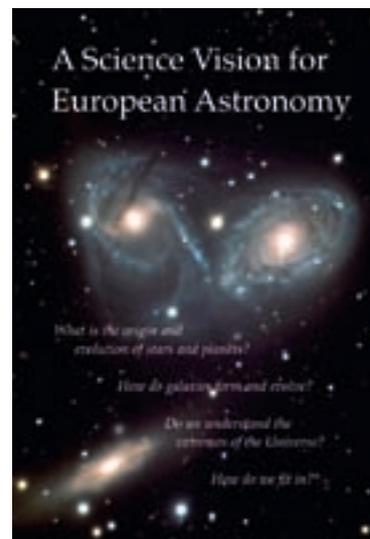
Figure 1: Cover of the ASTRONET Science Vision book.

Figure 2a: Current ground-based observatories. From left to right and from top to bottom: VLT, APEX, GREGOR, Gemini North, Gemini South, Magic, WSRT, La Palma, IRAM, SMA, Merlin, SST, La Silla and Effelsberg.

Figure 2b: Current space-based observatories. From left to right: HST, Integral, Mars Express, Venus Express, CoRoT, Rosetta, SOHO and XMM-Newton.

Figure 2c: Observatories under construction. From left to right and from top to bottom: Herschel, Planck, Gaia, JWST, Sofia, Bepi Colombo, GTC, ALMA, VST, LBT, VISTA, LOFAR and Auger.
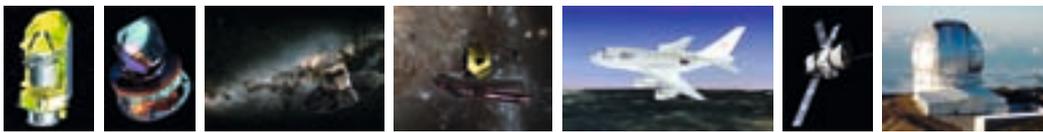
generic key technologies and facilities that are needed to tackle the scientific issues. Detailed recommendations were made, covering essential observing needs as well as complementary ones, i.e. not absolutely needed to solve a key issue but nevertheless bringing a strong scientific added value. Most importantly, this exercise took into account both current facilities, including those under development and fully funded, like ALMA, Herschel, Planck, LOFAR, JWST, GAIA, Rosetta and Bepi Colombo, as well as future needs. The panels and the Science Vision Working Group also outlined and stressed the need for parallel developments in theory and numerical simulations, high-performance computing resources, efficient astronomical data archiving, as well as a substantial commitment on laboratory astrophysics.

The ASTRONET Science Vision book (Figure 1) has been distributed to the funding agencies for further dissemination and is available on-line either in low-resolution format (17 MB) at *http://www.eso.org/public/outreach/press-rel/pr-2007/Astronet_ScienceVision_lowres.pdf* or in normal format (47 MB) at *http://www.eso.org/public/outreach/press-rel/pr-2007/Astronet_ScienceVision.pdf*.

The two-year Science Vision development was managed by ESO and NWO, with the scientific effort led by Tim de Zeeuw, then at Leiden Observatory, and Frank Molster of NWO.

Figure 2 offers a bird's eye view of current and planned observational facilities with significant or large European involvement.

The Infrastructure Roadmap

Preparation of the detailed Infrastructure Roadmap process began in the spring of 2007. The approach very much resembles the Science Vision's one with five Panels and an Infrastructure Roadmap Working Group. Programmatic breakdown is as follows. Panel A: High energy, astroparticle astrophysics and gravitational waves; Panel B: UV/Optical/IR and radio/mm, including survey instruments; Panel C: Solar telescopes, 'in situ' (Solar System) missions, laboratory studies; Panel D: Theory, computing facilities and networks, Virtual Observatory; Panel E: Education, recruitment and training, public outreach. Two major milestones ahead are the release of the first draft of the roadmap with the opening of a web-

based forum in the spring of 2008, and a community-wide open meeting in Liverpool on 16–19 June 2008.

The Infrastructure Roadmap development, is managed by Michael Bode and Maria Cruz of Liverpool University and Frank Molster of NWO.

Conclusions

With the September 2007 release of the Science Vision and the subsequent Infrastructure Roadmap effort now in full gear, European astronomy is for the first time ever fully engaged in the production of a global strategic plan, an essential prerequisite to ensure a vibrant future. Getting the community to agree by the end of 2008 on a common set of priorities, hard choices, and delicate balances is bound to be a tough task, but there is no other option open other than success.

A view from inside
the dome of VLT UT2
(Kueyen)

Coming Soon on Stage: X-shooter

Joel Vernet[1]
Hans Dekker[1]
Sandro D'Odorico[1]
Roberto Pallavicini[2]
Per Kjærgaard Rasmussen[3]
Lex Kaper[4]
François Hammer[5]
Paul Groot[6]
and the X-shooter team (see Table 2)

[1] ESO
[2] INAF – Osservatorio Astronomico di Palermo, Italy
[3] Niels Bohr Institute for Astronomy, Physics and Geophysics/Astronomical Observatory, Denmark
[4] Sterrenkundig Instituut, University of Amsterdam, the Netherlands
[5] Département Galaxies Etoiles Physique et Instrumentation (GEPI), Observatoire de Paris, France
[6] Department of Astrophysics, Radboud University Nijmegen, the Netherlands

X-shooter is a single-target, intermediate-resolution, wide-wavelength-range (*UV*- to *K*-band) spectrograph. It will be the first of the second-generation VLT instruments to go to the telescope. First light is planned in the second half of 2008. Here we give an update on the integration status and on the expected performance.

X-shooter overview

X-shooter is a high-efficiency spectrograph with a spectral resolution of 4 000–10 000 (dependent on wavelength and slit width) capable of simultaneously observing the complete spectral range 300–2 500 nm. It will be located at the Cassegrain focus of one of the VLT UTs. The instrument is designed for a rapid response and has a fixed spectral format.

X-shooter consists of a central structure (backbone) which supports three prism-cross-dispersed echelle spectrographs optimised for the UV-Blue, Visible and Near-IR wavelength ranges respectively. The backbone contains the calibration and acquisition units, an IFU that can be inserted in the light path, two dichroics to split the beam among the three arms, and relay optics to feed the entrance slits

of the three spectrographs. A functional diagram summarising all the functions of X-shooter is shown in Figure 1; the main instrument parameters are listed in Table 1.

The instrument concept has not changed since PDR and interested readers will find more information in the Messenger article of 2005 (Dekker and D'Odorico, The Messenger 120, page 2). The only modification, already hinted at, has been the implementation of three active flexure-correction mirrors in the light paths to the three spectrograph slits.

The larger fraction of the X-shooter hardware, as well as labour, is funded by the external members of the consortium. ESO is responsible for the detector systems, project management, and final system test and commissioning. More than 60 people are currently involved in the project at nine different institutes distributed over four ESO member states and at ESO (see Table 2). The overall cost of the project is 6.4 M€ and the staff effort 69 FTEs. Even with a complex distribution of the work tasks over many different sites, the X-shooter project has advanced well and on a relatively short time scale.

Table 1: X-shooter characteristics

Spectral format	Prism cross-dispersed echelle (order separation > 12″)
Wavelength range	300–2 500 nm, split in three arms using dichroics
	UVB: 300–550 nm
	VIS: 550–1 000 nm
	NIR: 1 000–2 500 nm
Spectral resolution	5 000 (UVB, NIR) and 7 000 (VIS) for a one arcsec slit
Slits/Image slicer	slit 12″ × 1″ (standard), 12″ × 0.6″ (high R), 12″ × 5″ (flux cal.)
	IFU 4 × 1.8″ input area, 12 × 0.6″ exit slit (3 slices)
Detectors	UVB: 2K × 4K E2V CCD
	VIS: 2X × 4K MIT/LL CCD
	IR: 2K × 2K Rockwell Hawaii2RG MBE (used area 1K × 2K)
Auxiliary functions	Calibration Unit; A & G unit with 1′ × 1′ field and comprehensive filter set; ADC for the UVB and VIS arms.
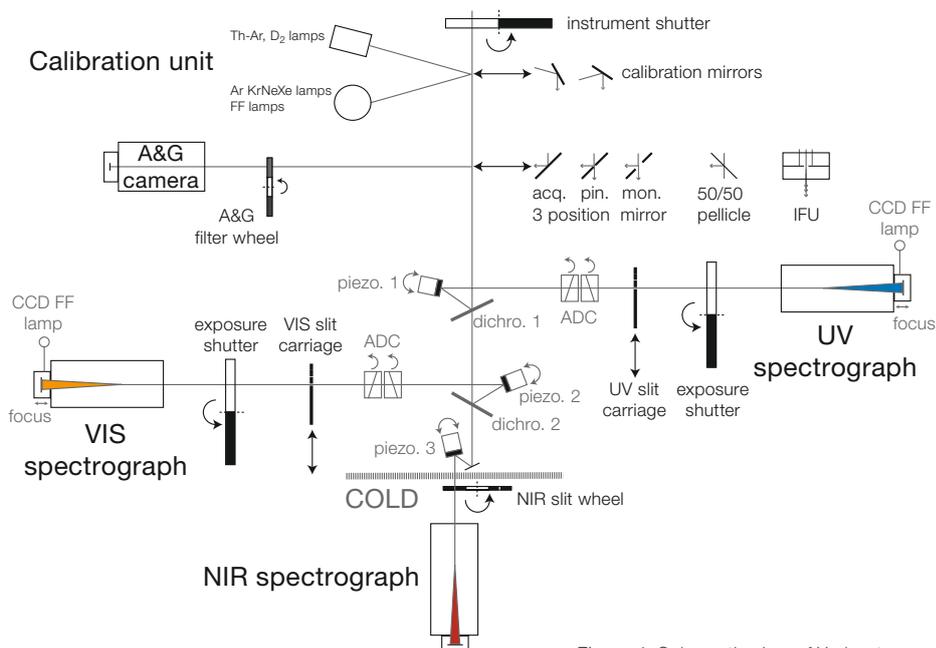
Figure 1: Schematic view of X-shooter

Project status

Since the FDR, which was completed in June 2006, all hardware items have been manufactured or ordered from industry and have been delivered (with two exceptions: the UVB camera and the NIR grating; now on the critical path). Since early 2007, subsystem integration and testing has been in progress at all six partner sites responsible for hardware deliveries (see Table 2). In the mean time, ESO has completed the handling carriage procurement and the detector systems for Acquisition and Guiding, as well as for each of the three spectrographs, and the Observatoire de Paris has completed and delivered the Integral Field Unit.

At the time of writing, the Backbone is under final system test at the Niels Bohr Institute in Copenhagen, while the UVB and VIS spectrographs are under test at INAF Brera-Merate Observatory near Milan. Figure 2 shows an early 'laboratory 1st light' image of the VIS spectrograph.

In the late summer of 2007, the vacuum/cryogenic test of the NIR spectrograph vessel was successfully completed at the University of Nijmegen. The vessel is now at Astron (Dwingeloo) for assembly with the cold bench that carries the optics and detector. First light is expected for November and delivery to ESO-Garching is projected to take place in February 2008.

Regarding software, coding and testing of the first modules of the Data Reduction Software was completed by the observatories of Paris and Amsterdam, who are closely working with the ESO pipeline group. A beta version of the Instrument Control Software, made available and supported by Trieste Observatory, is used for hardware testing at the various integration sites. ESO has completed and released early versions of the instrument model (see Figure 2) and of the Exposure Time Calculator (see Figure 4).

Expected efficiencies

Compared to efficiencies predicted at the Final Design Review in June 2006, most delivered optical components are well above specifications in terms of efficiency. In particular, critical components such as dichroics and gratings are of extremely good quality. As a result, the predicted total efficiency, obtained by multiplying actual measured efficiencies of individual components, is very high as can be judged from Figure 3. Based on these values, we have computed the expected limiting AB magnitudes at blaze peak in 1 hour for a S/N of 10 per spectral bin using a first version of the ETC (Figure 4). The ETC model uses the as-built values for optics (for UVB and VIS) and detector efficiency/noise, but still contains some

assumptions that need confirmation during commissioning, like the quality of the spectral extraction and sky subtraction, and the values of the background in the infrared bands. The decrease in efficiency to the blue of the UVB range (Figure 3) is due to the atmospheric absorption; at the red side of the VIS band it is due to the decrease in efficiency of the CCD; while on the long-wavelength side of the NIR range it is due to the rise of the thermal background.

Future steps toward installation at the telescope

Following the testing and acceptance of the subsystems at their integration sites, the final assembly of the single spectrographs into the instrument backbone will take place at ESO in Garching as of January 2008. As for all ESO instruments, the system test phase will be concluded with the so-called PAE (Provisional Acceptance Europe) review, now planned to occur in June 2008. The final installation at the telescope is planned for the second half of 2008, the exact date depending on the successful completion of the PAE and the availability of a commissioning slot at one Cassegrain focus at the VLT. Stay tuned in the next months. The goal is to offer the instrument for regular observing by 1 April 2009 at the latest.

X-Shooter VIS first light images 19/07/2007

Simulated (ESO/P. Bristow)   Actual (INAF)
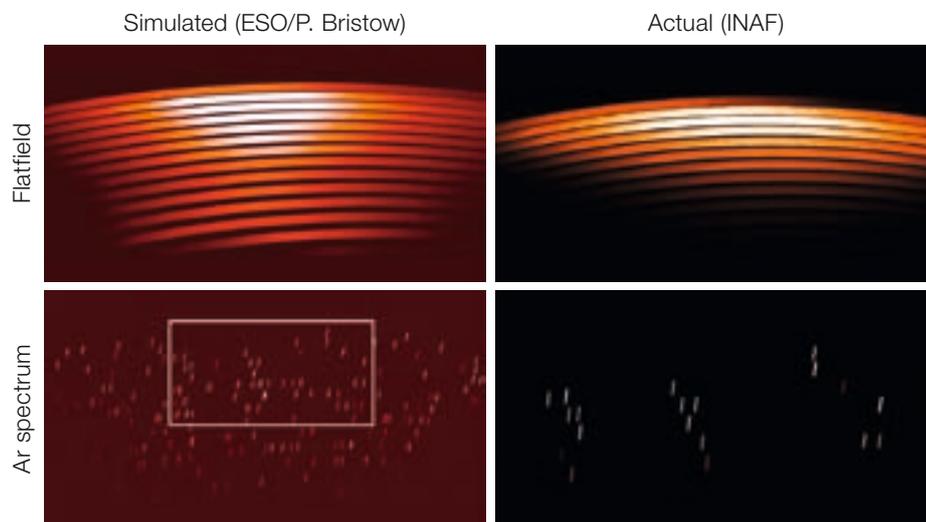
Figure 2: Halogen Flatfields and Ar line spectra in VIS spectrograph. Right column: first light images of July 19. Left column: simulated images, prepared in advance using the ESO instrument model. The first light Ar spectrum corresponds to the white-boxed region in the simulated spectrum. The agreement between the simulated spectral format and first light data is remarkable.
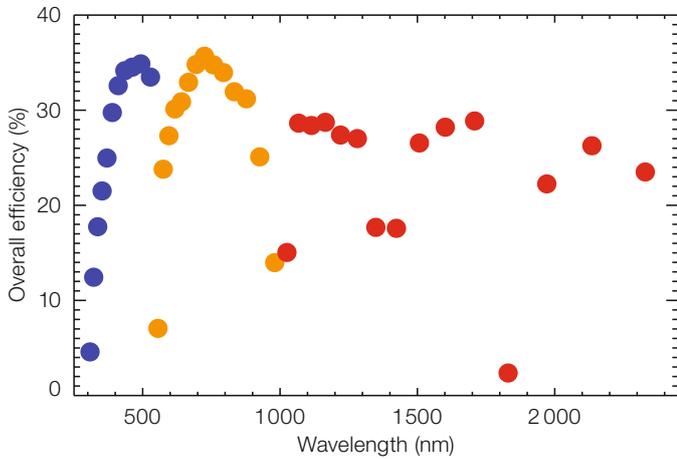
Figure 3: Total efficiency at blaze (atmosphere + telescope + instrument, excluding slit losses) obtained by combining actual measured (for UVB and VIS) or expected (for NIR) efficiencies of individual optical components.
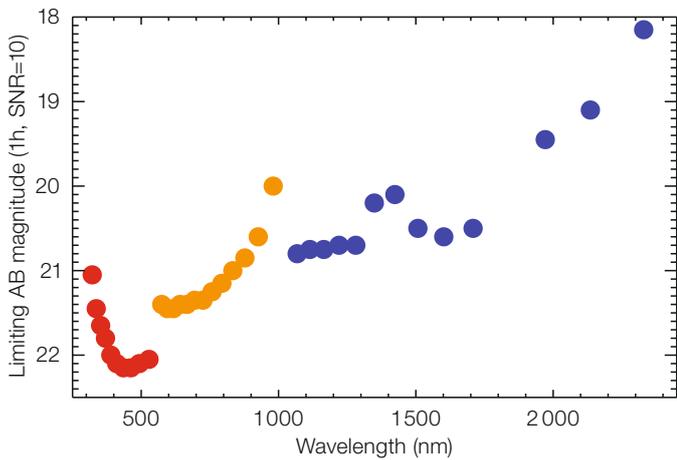
Figure 4: Limiting AB magnitude of X-shooter per spectral bin at S/N=10 in a 1 hour exposure. Other parameters: air mass 1.2, 0.8″ seeing, 1″ slit, 2× binning in spectral direction. The first version of the ESO ETC was used to compute these values.

Table 2: Participating institutes and staff currently working on the X-shooter project

ITALY	INAF Obs. Palermo: Roberto Pallavicini (Co-PI)	NETHERLANDS	Amsterdam Univ.: Lex Kaper (Co-PI), Matthew Horrobin, Ron Manuputy
	INAF Obs. Brera: Filippo Maria Zerbi (Project Manager), Vincenzo De Caprio, Antonio De Ugarte Postigo, Marco Riva, Paolo Spanò, Matteo Tintori		Nijmegen Univ.: Paul Groot (Chair Science Team), Thijs Adolfse, Peter Albers, Pieter Van Dael, Ivo Hendriks, Edwin Sweers, Han van der Vliet, Gerben Wulterkens
	INAF Obs. Trieste: Paolo Santin (Project Manager), Paolo Di Marcantonio, Igor Coretti, Andrea Zacchei		ASTRON: Ramon Navarro (Project Manager), Raymond van den Brink, Eddy Elswijk, Jan Idserda, Menno de Haan, Hiddo Hanenburg, Hendry Hof, Rik Ter Horst, Jan Kragt, Sjouke Kuindersma, Florence Rigal, Ronald Roelfsema, Ton Schoenmaker, Menno Schuil, Arjen Stam, Niels Tromp, Auke Veninga
	INAF Obs. Catania: Rosario Casentino, Pietro Bruno		
FRANCE	Obs. Paris Meudon : François Hammer (Co-PI), Isabelle Guinouard (Project Manager), Jean-Philippe Amans, Fanny Chemla, Patrick François, Régis Haigron, David Horville, Frédéric Royer	DENMARK	Niels Bohr Institute: Per Kjærgaard Rasmussen (Co-PI, Project Manager), Jeppe Joench Andersen, Hans Henrik Larsen, Niels Michaelsen, Dennis Wistisen, Anton Norup Sorensen, Preben Nørregaard
	AstroParticle and Cosmology: Paolo Goldoni (Project Manager of DRS), Guillaume Blanc, Laurent Guglielmi. Cyril Dufour		Danish National Space Centre: Niels Christian Jessen
ESO	Sandro D'Odorico (Co-PI), Hans Dekker (Project Manager, System Engineer), Joël Vernet (Instrument Scientist), Andrea Balestra, Pascal Ballester, Paul Bristow, Ralf Conzelmann, Bernard Delabre, Mark Downing, Gerd Finger, Florian Kerber, Jean-Louis Lizon, Henning Lorch, Christian Lucuix, Ruben Mazzoleni, Andrea Modigliani, Francesco Saitta, Jakob Vinther		

Peering into the Dust: News from VISIR

Hans Ulrich Käufl[1]
Dieter Nürnberger[1]
Leonardo Vanzi[1]
Pedro Baksai[1]
Danuta Dobrzycka[1]
Jorge Jimenez[1]
Alfredo Leiva[1]
Lars Lundin[1]
Massimiliano Marchesi[1]
Pedro Mardones[1]
Leander Mehrgan[1]
Jean-François Pirard[1]
Chester Rojas[1]
Daniel Salazar[1]
Ralf Siebenmorgen[1]
Armin Silber[1]
Mario van den Ancker[1]
Ueli Weilenmann[1]
Gilles Durand[2]
Eric Pantin[2]
Margaret Moerchen[3]

[1] ESO
[2] Service d'Astrophysique/DAPNIA/DSM, CEA Saclay, France
[3] University of Florida, Gainesville, Florida, USA

VISIR – ESO's VLT Imager and Spectrometer for mid-InfraRed – is a combined imager and echelle spectrograph, providing access to the atmospheric N and Q-band windows (7.7–13.3 and 16–24 μm) with a great variety of observing modes. Starting in Period 81 a new set of filters is available to the users of VISIR, and the characteristics of the filters and their science verification are described. The installation of the filters is the most visible result of a technical intervention performed at Paranal between April 24 and May 8, 2007, however more upgrades were also performed.

The Intervention

To minimise downtime, the re-coating slot of UT3 (Melipal) in 2007 was used to dismount VISIR. This operation, and the opening of the instrument, was aimed at realising a number of upgrades and repairs, but, at the same time, served also as a training for the technical staff. VISIR (*http://www.eso.org/instruments/visir/* and Lagage et al. 2004, Pantin et al.

2005) has up to now been operated in principle fully under ESO's responsibility. In fact in 2004 the instrument was shipped to Paranal completely assembled and so little practical experience in handling it existed at ESO. During the 2007 intervention it was also possible to include some envisaged upgrades in the instrument long-term plan, such as the installation of a new IRACE system and a new temperature controller for the detectors. Moreover the thermal inertia of the detector cooling system was increased by adding a disk of lead (note that the VISIR detectors operate at ~ 6–8 K where the thermal capacity of normal metals tends to become very small). As for the first intervention that took place in Paranal in October 2005, the activities were performed with the support of the VISIR Consortium.

Removal of the instrument, vessel opening and separation of imager and spectrometer are already standard procedures in Paranal (see Figure 1). On this occasion it was possible to review new tools to further improve the procedures. One of the key subsystems of VISIR, the rotational cable wrap, which routes a fibre bundle, cables, pipes and flexible helium lines (up to 25 bar!), is normally not accessible and so is subject to inspection and maintenance every time we have the necessity to access it. Covers to improve the operational safety of the unit were added. A new procedure to directly remove the optical bench, which holds both the spectrometer and imager (see Figure 1), from the cryostat, with the latter remaining at the telescope, is in progress. The mechanical interfaces for this operation were tested. Various upgrades in the cryogenic assemblies were performed but the most relevant was the installation of a new optical baffle – completely redesigned and manufactured by CEA/Saclay – in the imager three-mirror anastigmats (see Figure 2). This new baffle is made of metallic plates perpendicular to the optical beam, thus avoiding the spurious reflections which had produced a strong imager ghost. The effect was quite remarkable, the ghost has disappeared.
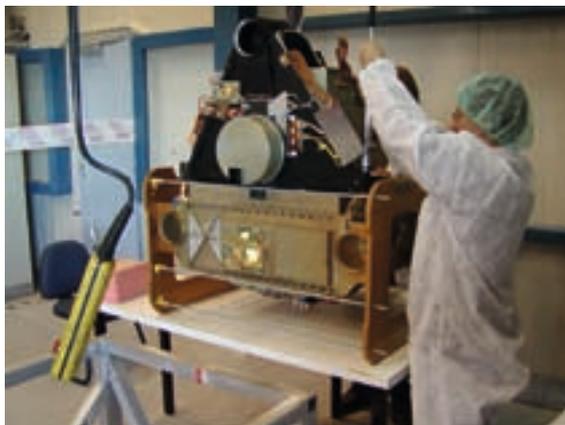
Figure 1: The VISIR optical bench in the laboratory, awaiting further disassembly. The lower (shiny) part contains the spectrometer, while the triangular, black anodised structure on top contains the imager. The three cup-like structures, forming an isosceles triangle, are the mechanical fixation to the telescope reference frame via the cryostat. In the future it is planned to dismount only this unit for interventions, while the vacuum vessel of the cryostat would stay on the telescope, thus simplifying the operation and minimising the impact on telescope operations substantially.
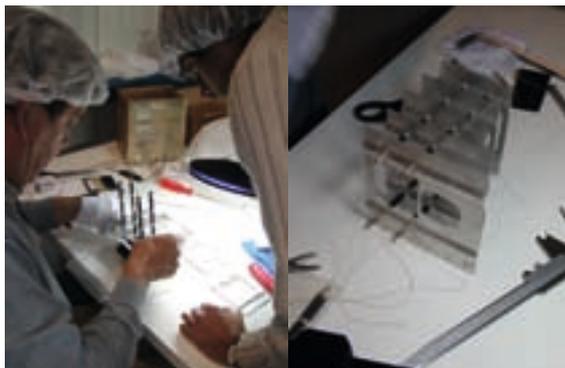
Figure 2: The new imager baffle. **Left:** being assembled by Gilles Durand, the VISIR project engineer of CEA/DAPNIA. **Right:** after assembly but before integration into the camera assembly.

The scientific filters originally delivered with VISIR were a "model pay-load" dating back from 1992/93 and did not include a silicate filter set. The plan was to add such a set, similar to the one in TIMMI2 (known in the community as the "OCLI filter set"), and which could be ordered on short notice for a relatively moderate price. Unfortunately, however, without advance warning the supplier disappeared from the market about two years before VISIR's first light. Thus a new supplier had to be found, so that the entire process took much longer than initially expected. Silicate dust has a very strong feature in the atmospheric 10-μm window. This feature is frequently observed in dusty objects as different as comets or active galactic nuclei; depending on circumstances the feature is sometimes in absorption, sometimes in emission. The absence of a filter set dedicated to this feature was seriously affecting the scientific productivity of VISIR. The main characteristics of the new filters are listed in Table 1.

In this process another special filter (J7.9) was added at the suggestion of Glenn Orton (JPL/Caltech). This filter is sensitive to methane and can be used to measure the temperature in the Jovian and Saturnian atmospheres. The potential of VISIR in this context has recently been demonstrated for Neptune where thermal infrared imaging allowed the temperature above the South pole of Neptune to be determined (see ESO Press Release 41/07 and the article on page 21).

The thermal control of the detectors was improved by relocating the thermal sensor and heaters as close as possible to the imager detector, through the use of a new fast high-quality thermal controller, an intervention to the cooling braid and by adding 342 grams of lead as thermal buffer to the cold head.

A new version of ESO's front-end electronics for detector read-out (IRACE) and a Linux workstation were installed, to put VISIR into the same configuration as the more recent IR instruments (SINFONI, CRIRES and HAWK-I), but also to correct some recurring operational errors. After some problems in connecting a VISIR special interlock to the detector power supply, the system was tested and is working according to specifications. To accommodate the burst-mode, an operational mode very similar to Speckle mode in optical instruments, the bandwidth for the data transfer was also improved by upgrading the communications.

The warm calibration unit was maintained and upgraded. This unit is located between the instrument and the telescope adaptor and in normal operation is not accessible. The main actions were to repair a vacuum line, to replace a linear slide for switching between the calibration sources, and the fine tuning of the monochromator, for wavelength verification of the VISIR astronomical filters, which is located deep in the instrument and thus normally inaccessible.

Finally in line with the UT3 recoating schedule, VISIR was mounted back to the Cassegrain flange to start the cool-down process. Then the VISIR special controller for vacuum and cryogenics (an industrial PLC[1]) autonomously started the procedures to achieve the operational temperatures: 3–4 K at the cold fingers and around 20 K for the optics and the instrument structure.

Commissioning

The recommissioning began off-sky starting on May 18 and on-sky during the nights of May 21 and 22, unfortunately not with the best atmospheric conditions. All the new filters mounted in the imager where checked with the monochromator of the calibration unit, and in particular the 50% cut-on and cut-off wavelengths were measured.

A test with the extended calibration source for all three magnifications (0.075, 0.127 and 0.2 arcsec/pixel) showed, that there is no indication of the imager ghost anymore, while there is positively no vignetting. We found instead that the J7.9 filter creates a noticeable filter ghost (~ 5%) and the J8.9 filter introduces an offset so substantial that the field mask produces a shadow. This shadow affects the detector and hence this filter is of questionable use.

The observing parameters required for operations (optimal combination of the detector on-chip integration time (DIT) and detector capacity) were determined on sky. Standard stars were observed and reduced with the pipeline to determine sensitivities. Table 1 presents the results. The measurements were repeated

[1] A PLC (Programmable Logic Controller) is a small special-purpose computer used to automate machines and considered as reliable as a pure hardware solution.

Filter Name	Cut on 50% [μm]	Cut off 50% [μm]	Sensitivity Small Field Best [mJy, 10 σ in 1 h]	Sensitivity Small Field Median [mJy, 10 σ in 1 h]	Sensitivity Intermed. Field Best [mJy, 10 σ in 1 h]	Sensitivity Intermed. Field Median [mJy, 10 σ in 1 h]
J 7.9	7.483	8.035	12	15.2	21	39
J 8.9	8.338	9.068	2.5	3.0	5	6.9
J 9.8	9.123	10.059	5.5	6.3	10	13.9
J 12.2	11.700	12.216	11.0	11.0	no data yet	no data yet
B 8.7	8.436	9.410	no data yet	no data yet	no data yet	no data yet
B 9.7	9.402	10.242	8	9.8	20	27.7
B 10.7	9.970	11.338	4.5	5.1	8	11.8
B 11.7	11.098	11.950	4	4.6	6.5	9.4
B 12.4	11.971	12.961	8	9.3	11	14.9

Table 1: The characteristics of the new filters and the sensitivities measured since commissioning. Sensitivities, as usual at ESO for the mid-infrared, are given in milli-Jansky for a 10 σ detection in 1 hour detector exposure time. To actually execute the whole Observing Block would take, including acquisition, approximately 1 h 40 m. These filters are also incorporated into the VISIR Exposure Time Calculator.

in the following months to improve the statistics so that the filters could also be reliably incorporated into the VISIR Exposure Time Calculator.

The spectrograph detector temperature is now quite stable, however, there is little margin to change it[2]. The imager detector is still oscillating with typically ±10–30 mK. While the detector artifacts are now less prominent, it is obvious that there is further room for improvement, before the planned fundamental detector upgrade takes place. At the next opportunity we will add a disk of Neodymium[3], having a specific heat ~ 5 times that of lead in the relevant temperature regime. An attempt was made to assess the performance of the imager-detector as a function of operating temperature by taking ramps with the flat-field (extended) source and analysing the pixel-to-pixel variance of ~ 50 × 50 pixel in the centre. This did not result in conclusive findings. Similar tests of S/N vs. operating temperature on the sky have been done. Weather did not however permit study of this dependence to be measured completely "noise-free". For the moment it appears, that 6 K for the imager is a "good" compromise.

Methods to establish and verify the calibration of the monochromator in the calibration unit were implemented, based on a combination of checking the reproducibility of the zeroth-order spectrum and using VISIR itself as a spectrograph. The originally-delivered VISIR-internal calibrators (plastic foils with characteristic absorption spectra) were found not to be useful for this purpose.

When switching from "thru-the-slit imaging" to spectroscopy, a strong remanence is found. For a DIT of 30 ms, detector ghost images were visible for up to ~ 100s; reducing the DIT by a factor of 2 also reduced the time of ghost visibility to

~ 50s. This suggests that the remanence decay depends on the number of reads and not so much on time. This finding will be applied to the templates by adding fast dummy read-outs. The templates to measure filter curves (imager and spectrometer) have been tested and they basically work; regular tests of the filters thus will now become part of the operations of VISIR.

New templates for burst-mode observations were tested allowing the storage of thousands of single DIT frames in a data cube. However the telescope chopping secondary (M2) status cannot be identified from the frames yet. Thus the automatic reduction of the data via pipeline recipes is not yet possible. The overheads for burst mode were originally very large (up to a factor of five too long) and could be reduced by changing the outdated network link to a state-of-the-art device.

Science Verification

To test the new Silicate filter set on sky, a few hours were used to observe two regions of star formation with dust-embedded young stellar objects (YSOs): M17, UC1 and IRS5; and NGC 3603, IRS9. In Figure 3 we show results of this observation for M17 in comparison to previous data obtained with TIMMI 2 in imaging and long-slit mode (c.f. Nielbock et al. 2007). While the VISIR photometry nicely reproduces the TIMMI 2 results, it allows us in the future to search systematically for YSOs embedded in silicate

Figure 3: **Top:** Sequence of VISIR images of the M17 UC 1/IRS 5 region using the new set of Barr filters: B 8.7, B 9.7, B 10.7, B 11.7 and B 12.4 centred at 8.92, 9.82, 10.65, 11.52 and 12.47 μm, respectively. The frames have provisionally been normalised such that IRS 5 has approximately the same brightness in all filters. Each panel displays a field of view of 7.6 × 7.6 arcsec², corresponding to about 17 000 × 17 000 AU² at the distance of the M17 region. **Bottom:** Overall SED of M17 UC 1 (from Nielbock et al. 2007), with blue asterisks marking the fluxes measured with the new silicate filters manufactured by Barr Associates.
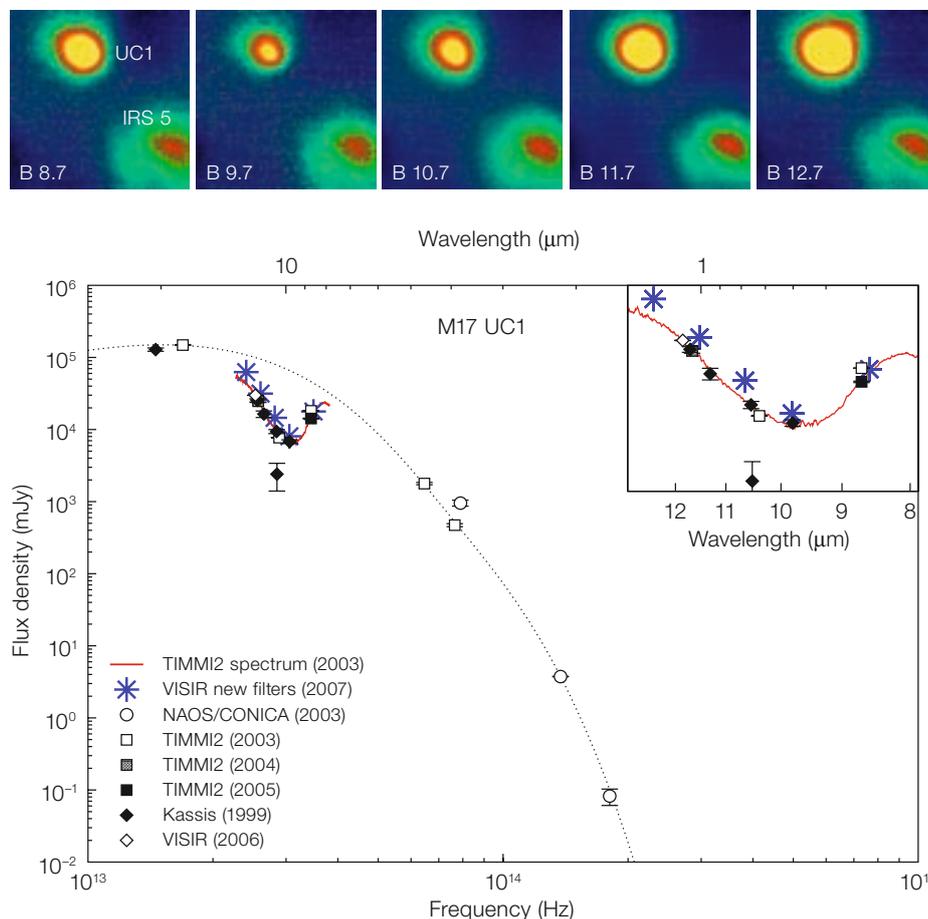
[2] The present VISIR detectors show a variety of artifacts which can be mitigated to a certain extent by choosing the right operating temperature.

[3] Neodymium is a relatively reactive material, and hence machining it is beyond the scope of the ESO workshop. Lead, which is much easier to handle, was chosen for a first try as this had solved the corresponding problem in TIMMI2.
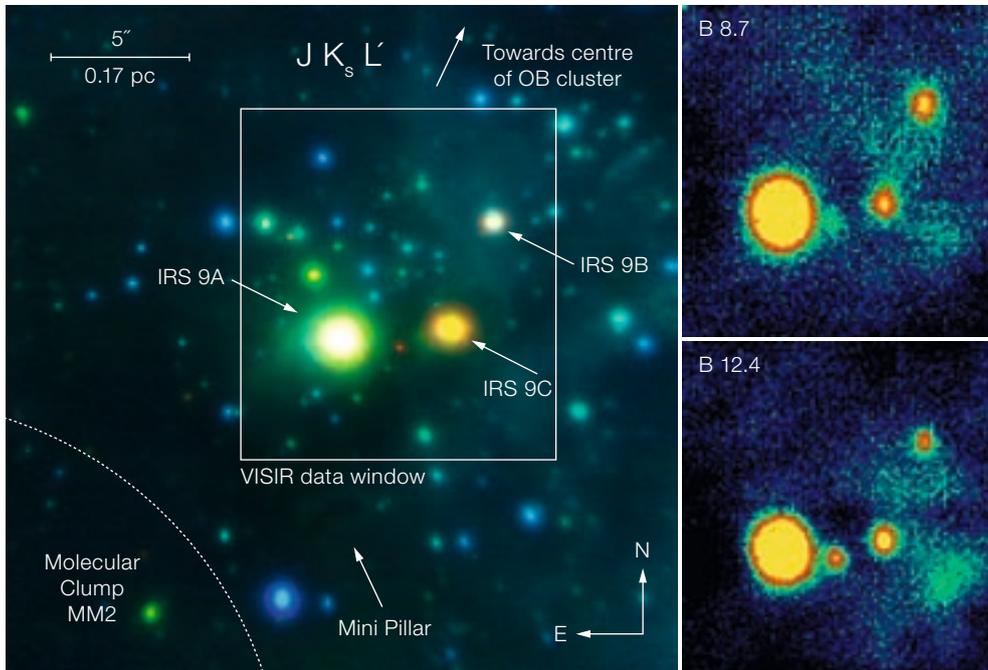
Figure 4: Left: (Nürnberger et al. 2008, in preparation) shows a composite near-infrared image of the IRS9 region, part of the massive star-formation region in NGC 3603. The images were taken in three colours (J, Ks and L') with VLT-UT4 and the adaptive optics instrument NACO. The object of particular interest is the faint red dot between IRS 9A and IRS 9C. This object is so deeply embedded in dust that it could only be detected in the L'-filter ($\lambda \sim 3.8$ µm). A white frame indicates the location of the window for the VISIR images which are shown on the right. Right: The region around IRS 9A–C is shown with two of the new VISIR filters. In the B 8.7 filter, centred at $\lambda \sim 8.7$ µm right in the middle of the silicate absorption band, the object appears faint (upper); in the B 12.4 filter image ($\lambda \sim 12.4$ µm), well outside the absorption feature, the object is bright (lower).

dust. It is also obvious, that the five filter photometry, yielding an effective spectral resolution $\lambda/\Delta\lambda \sim 10$, is perfectly suited to this problem. In many cases the dust is arranged in a circumstellar disk, and VISIR will allow characterisation of such disks with a spatial resolution of 0.3 arcsec, approximately 10 times better than the Spitzer Space Observatory. In Figure 4 we show a similar data set, but for the IRS 9 complex in NGC 3603. This is an extremely rich cluster of young stars with ongoing star formation. The source situated between IRS9A and C is nearly extincted in the B 8.7 filter (upper panel in Figure 4 right), thus it is obvious that the circumstellar dust around this YSO contains silicates. The nature of the extended emission in the VISIR frames ~ 2 arcsec south-west of IRS 9C, which is brighter in the continuum filter, (B 12.4) still needs to be established. In this example it is very obvious how the combination of high spatial resolution, that only ground-based 8 m-class telescopes can currently provide, and the new silicate filter set allows for the identification of objects of yet unknown properties, or even completely unknown so far.

Outlook

For the immediate future another small upgrade to VISIR is anticipated. This will encompass a further improvement of the thermal regulation and add more and better specialised filters for the VISIR high-resolution Echelle mode. This upgrade will in particular enable observers to follow the [NeII]-line at 12.8 µm to a redshift of a few percent – sensitivity permitting. Implementation of the burst mode with full support by pipeline recipes will be implemented on the fly. As to the scientific potential of this mode, reference is made to very recent work on NGC 1068 (Poncelet et al. 2007). At present ESO is also preparing a fundamental upgrade of VISIR which will at least provide for next-generation detectors (most likely 1024 × 1024 pixel As:Si BIB detectors) to overcome the excess noise of the present detectors and to exploit the full field of VISIR of ~ 50 × 50 arcsec² in imaging. Similarly, in spectroscopy, the new detector will allow to take full advantage of the cross-dispersed echelle mode, presently hardly used due to various operational handicaps. Similarly, the new detector format will allow implementation of a new, very high-efficiency, low-resolution mode covering the N-band in one single exposure.

The power and maturity of thermal infrared spectro-photometric imaging has lately been demonstrated in a rather impressive way by Müller et al. (2007). For the near-Earth asteroid Itokawa, which was later visited by the Japanese spacecraft Hayabusa, the careful inversion of optical and thermal infrared light curves (using the VISIR precursor TIMMI2 at ESO's 3.6-m telescope on La Silla) has allowed for the construction of a shape model of this asteroid with a precision of few per cent, including geological characterisation of the surface. This shows not only the potential of ground-based thermal infrared instrumentation, but also that all the basic calibration issues required for precision photometry are now solved.

References

Lagage, P. O. et al. 2004, The Messenger, 117, 12
Müller, T. G. et al. 2007, in IAU Symposium 236.
    Eds G.B. Valsecchi & D. Vokrouhlický. Cambridge
    University Press, 261
Nielbock, M. et al 2007, ApJ, 656, L81
Pantin, E. et al 2005, The Messenger, 119, 25
Poncelet, A., et al 2007, A&A, 472, 823

GROND Commissioned at the 2.2-m MPI Telescope on La Silla

Jochen Greiner[1]
Walter Bornemann[1]
Christian Clemens[1]
Martin Deuter[1]
Günther Hasinger[1]
Mathias Honsberg[1]
Heinrich Huber[1]
Stefan Huber[1]
Markus Krauss[1]
Thomas Krühler[1]
Aybüke Küpcü Yoldas[1]
Hans Mayer-Hasselwander[1]
Benjamin Mican[1]
Natalya Primak[1]
Fritz Schrey[1]
Ingo Steiner[1]
Gyula Szokoly[1]
Christina C. Thöne[1]
Abdullah Yoldas[1]
Sylvio Klose[2]
Uwe Laux[2]
Johannes Winkler[2]

[1] Max-Planck-Institut für extraterrestrische Physik, Garching, Germany
[2] Thüringer Landessternwarte, Tautenburg, Germany

An imaging system capable of operating in seven colours simultaneously, has been designed, built, and recently commissioned at the 2.2-m MPI/ESO telescope on La Silla. This instrument is called GROND, for Gamma-Ray Burst Optical and Near-Infrared Detector. GROND has been designed for rapid observations of gamma-ray burst afterglows. The seven bands from Sloan $gri\tilde{z}$ to near-infrared JHK allow an immediate photometric redshift determination for bursts at $z \geq 3.5$. In addition, the unique capability of simultaneous multi-band imaging allows for many other scientific applications.

Why imaging in more than one band?

Simultaneous imaging in different filterbands is interesting in a variety of astrophysical areas. It primarily aims at measuring the spectral energy distribution, or its variations in variable objects, in order to uncover the underlying emission mechanism. Examples are, among others: (1) monitoring of all kinds of variable stars (flare stars, cataclysmic variables, X-ray binaries) to determine the outburst mechanisms and differentiate between physical-state changes and changes induced by geometrical variations, like eclipses; (2) monitoring of AGN to understand the physical origin of the observed variability; (3) mapping of galaxies to study the stellar population; (4) photometric redshift surveys; (5) observations of extrasolar planets; and (6) mapping of reflectivity inhomogeneities of Solar System bodies as a function of their rotation to map their surface chemical composition.

A new need arose with the observation of a large number of gamma-ray burst (GRB) afterglows with the *Swift* satellite. With its much more sensitive instruments, *Swift* detects GRBs over a very wide redshift range at a rate of about one hundred per year. Since high-resolution spectroscopy to measure the physical conditions of the burst environment is constrained to the first few hours after a GRB explosion, a rapid determination of the redshift becomes important. This is best done with multi-band photometry (until integral field units have grown to several arcmin field of view) and deriving a photometric redshift based on the Lyα break. There are currently few instruments with simultaneous multi-channel imaging, but those combine less than four channels and typically are operated on small telescopes.

Figure 1: The GROND instrument at the 2.2-m telescope. **Left:** View of the 2.2-m telescope with GROND to the lower left, the light baffle on top of M3 in the middle, and the main electronics rack at the rear top. **Right:** Detailed view of the GROND vessel and its various connections.

Instrument Design

GROND was developed for implementation on the MPI-owned 2.2-m telescope, operated by ESO at La Silla. This f/8 Ritchey-Chretien telescope hosts, at its Cassegrain focus, the Wide Field Imager (WFI; *www.ls.eso.org/lasilla/sciops/2p2/E2p2M/WFI/*) and the echelle spectrograph FEROS (*www.ls.eso.org/lasilla/sciops/2p2/E2p2M/FEROS/*). GROND therefore has been placed in a Coudé-like position at the centre piece of the telescope (Figure 1). A special folding mirror was built which can be swept into position within 20 sec and deflects the light into the GROND camera (Figure 2).

The separation of the different photometric bands has been achieved using dichroics (Figure 3), whereby the short wavelength part of the light is always reflected off the dichroic, while the long-wavelength part passes through (see Figure 4 for the wavelength ranges of the seven bands). The dichroics were designed such that the combination of their cut-off wavelengths defines bands as close as possible to the Sloan system, with the exception of the *i*-band. Since in the Sloan system, *riz* the bands overlap at their $\sim 70\%$ transmission values, we decided to compromise the *i*-band in favour of standard width *r* and *z* bands (therefore calling it $\tilde{i}$). For the infrared part, a focal reducer system was devel-
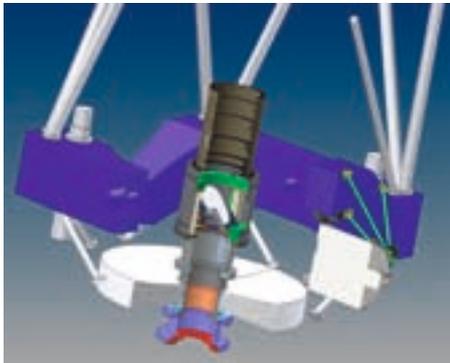
Figure 2: Cutaway view of GROND on the 2.2-m telescope with the new folding mirror M3 within the light baffle (centre).

Figure 3: 3D structure of the optical beam of GROND with most of the components labeled.
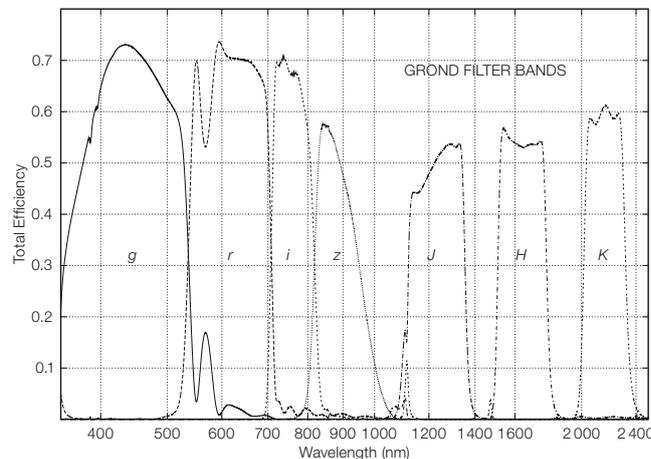
Figure 4: Filter curves of GROND showing the total efficiency of the instrument including the telescope mirrors, GROND-internal optics, and detectors.

oped in order to enlarge the field of view to 10 arcmin, thus ensuring coverage of the full error circles of gamma-ray burst positions provided by the BAT/Swift, SuperAGILE or GLAST/LAT instruments (typically a few arcmin radius). Two stationary folding mirrors are introduced to reduce the overall instrument size. The entire system has been designed for a working temperature of 80 K in vacuum, because deviations from the nominal temperature by more than 20 degrees would already lead to refractive index changes large enough to cause noticeable image quality degradation.

Best possible efficiency was a driver in many decisions during the development of GROND, and included special selection of the four CCDs for maximum sensitivity in their respective wavelength bands (see Table 1), silver (rather than aluminium) coatings for the various mirrors, and very high transmission requirements of the dichroics and anti-reflection coatings. The total efficiency in the visual bands is at the 70% level (except z-band), and still above 50% for the three NIR bands.

Table 1: Detector details of GROND

Optical part:	
Detector	4 × 2048 × 2048 E2V
Field of view	5.3 arcmin
Pixel size	0.″16
Infrared part	
Detector	3 × 1024 × 1024 HAWAII
Field of view	10 arcmin
Pixel size	0.″6

A few noteworthy features of the GROND instrument include:

(1) IR detector focusing motors. Since the depth of focus in the infrared part is only 25 μm (as opposed to 60–120 μm in the visual channels), each IR detector unit involves a focusing stage by an independent stepper motor. Each motor allows relative movements to an accuracy of 0.4 μm over a range of ±2 mm around the nominal focus position

(2) Lens housings. The focal reducer contains five lenses in the collimator, and 6 lenses in each of the camera objectives. In order to keep the lenses properly centred during the cool-down to 80 K, a special spring mount was developed which allows lenses to be held in groups of two to four

(3) K-band dither mirror. Since the readout speed in the optical channels pre-

vents frequent telescope dithering, the K-band channel was equipped with a dither mirror

(4) CCD operation in 80 K environment. Since all channels and detectors are located in the same cryostat, the shutters for the CCDs have to operate at 80 K. Also, the CCD detectors are mounted with special thermal insulation and are kept at their nominal operating temperature of 165 K by 0.2 W counter-heaters.

Software

The GROND Pipeline (GP) system is a software package designed and written specifically for GROND. Its prime objective is to schedule rapid GRB afterglow observations and determine the redshift as quickly as possible. The architecture of the GP is based on an asynchronous

framework to provide speed and the degree of freedom necessary to apply different analysis strategies. The GP mainly consists of two layers, the system layer and the GRB analysis layer (see Table 2). The system layer consists of the processes that receive the GRB alerts, decide whether to follow that burst or not, schedule and reschedule observations and conduct the observations by initiating, continuing, interrupting or ending them. Furthermore, the main system process controls all processes including the analysis processes, and coordinates the interprocess communication. The GRB analysis layer contains pre-processing of the images, photometric analysis, identifying the GRB afterglow, spectral energy distribution (SED) analysis and photometric redshift determination.

First light

GROND was mounted at the 2.2-m telescope in April 2007, and saw first sky light on April 30. During the following months most of the commissioning steps have been successfully conducted, including the derivation of zero points for all seven bands, checks for vignetting, determination of the focus formula, verification of the effect of the K-band dither mirror, and tuning of the exposure and read-out timings in the different channels. Also, the Rapid-Response Mode (*http://www.eso.org/observing/p2pp/rrm.html*) has been implemented in order to allow rapid (few minutes) start of observations after a GRB or transient alert.

All of the various checks have proven the full functionality of the instrument. Two examples of science demonstration results are shown in Figures 5 and 6, each based on just 3-min and 4-min exposure time in the visual and infrared channels respectively!

Figure 5: First-light result from April 30, 2007: green crosses are the GROND camera photometric estimates as derived from a 4-min observation block of the quasar PKS 1251-407 at a redshift of $z = 4.46$. The red line is the composite quasar spectrum.

Figure 6: A science demonstration image taken in early May 2007, showing a *JHK* colour composite of the Omega nebula M17. The colour-coding has been chosen to mimic what the human eye sees; namely, hot and massive stars appear bluish-white, while dust reddens the light. The thick dust lanes at the North (top) and West (right) rims absorb even the 2.4 μm wavelengths. The image is 10 arcmin across, and has an effective exposure time of 4 min (twenty-four 60-sec images in each of the three bands).

Fine-tuning of the operations strategy as well as scheduling and analysis software is expected to bring GROND into complete operational conditions, thus allowing to start full science operations. We are looking forward to an exciting time not only for GRB follow-up observations, but also to many other applications of this unique instrument.

The instrument is operated by the Max-Planck Institute for Extraterrestrial Physics, Garching, under a mutual agreement with ESO, and available to astronomers from the Max-Planck Society. More details about the instrument can be found in Greiner et al 2008.

References

Greiner J. et al. 2008, PASP (in press)

Table 2: The duties of the software system and the GRB analysis layers of the GROND Pipeline

System – Observation Control Layer	GRB Analysis Layer
Receiving GRB alerts	Pre-processing the images
Deciding whether to observe the target	Photometric analysis of 7-band data
Calculating visibility of the target	Constructing the SED of the objects
Scheduling of the observations	Identifying the GRB afterglow
Triggering/continuing/stopping observations	Determining the photometric redshift
Providing web-interface for user interaction	Evaluating the accuracy of the redshift

Status of the ALMA Antenna Production

Stefano Stanghellini (ESO)

The design of the ALMA antennas began in 1999 with a prototyping phase. Two antenna prototypes were built, extensively tested at the VLA site in New Mexico and evaluated in 2003. It was decided to proceed to procurement with two parallel calls for tenders based on the two prototypes. In 2005 contracts were placed with the US VertexRSI and the European AEM Consortium for 25 antennas each. An update on the two designs and the production progress is presented. The Japanese antennas (both 7 and 12 m) are being built by Mitsubishi, which also built an additional antenna prototype. The first antennas have recently arrived at the integration facility at the ALMA Operations Support Facility (OSF).

As reported in previous editions of The Messenger (e.g. Haupt and Rykaczewski, The Messenger, 128, 25, 2007), the ALMA observatory will be equipped with fifty-four 12-m dish antennas and twelve 7-m dish antennas. Of the 12-m antennas, 25 will be provided by North America through Associated Universities Incorporated (AUI) and 25 will be provided by Europe through ESO. Four 12-m antennas, as well as all the 7-m antennas, will be provided by Japan through the National Astronomical Observatory of Japan (NAOJ). The process leading to the procurement of the antennas started in 1999 when the decision was taken to prove the feasibility of the science-driven antenna specifications by prototyping. This occurred shortly after Europe and the U.S., until that time pursuing separately the Large Southern Array (LSA) and the Millimiter Array (MMA) respectively, had signed a formal agreement on collaboration for the development phase of ALMA. The National Radio Astronomy Observatory (NRAO), operated by AUI under a cooperative agreement with the National Science Foundation, and ESO initiated therefore the procurement of two antenna prototypes, to be installed at the Very Large Array (VLA) premises of the NRAO in New Mexico. It was decided that these two prototypes would be evaluated on an agreed test programme by a joint team of experts, the Antenna Evaluation Group (AEG). The National Astronomical Observatory of Japan (NAOJ) engaged in a project of this kind, the Large Millimetre and Submillimitre Array (LMSA), also decided to procure a 12-m antenna prototype and to test it at the VLA.

Procurement strategy and contracting process

Originally it was envisaged to use the blueprints of one prototype antenna for the serial production, if one of the two designs had been found superior to the other. However, the testing of key performance of these prototype antennas proved to be harder than anticipated, due to the intrinsic limitations at the VLA site and the incomplete debugging of antennas and evaluation equipment (receivers, holography systems, subreflector nutator, optical pointing telescopes), so no clear conclusion could be reached in the anticipated time frame.

To avoid a delay of the project by awaiting the final results of the prototype evaluation, parallel calls for tender to industry were issued in December 2003 by AUI and ESO for the supply of the serial antennas based on revised antenna functional specification. The call for tender was not restricted to a particular design and information on the design of the two prototypes was included as background information to potential industrial bidders. In May 2004 the bids were opened and the evaluation and discussions with the bidders started. The bidders based their proposals on the design of the prototypes. Therefore further test campaigns were launched to integrate the data and the preliminary conclusions were collected by the Antenna Evaluation Group. The tests of the prototypes, performed by panels of specialists including ESO personnel, involved verification methods different from those adopted by the AEG (photogrammetry, quadrant detector, out of focus measurements) and included 100 000 cycles of fast switching to stress-test the antenna and the primary reflectors. The tests were concluded in April 2005, with the final conclusion that antennas based on both prototype designs are expected to be able to fulfil the ALMA specification. This result brought a campaign of tests, spanning over two years, to its end. Testing these state-of-the-art antennas had involved a great deal of effort from the persons involved in preparing the test equipment, those collecting the data and finally, from the various groups interpreting the data with analysis and simulation.

Shortly after the completion of the tests, in July 2005, AUI concluded negotiations with VertexRSI, a subsidiary of General Dynamics, and signed a contract for the supply of up to 25 antennas with options for up to 32 antennas. ESO followed in December 2005 with the signature of the contract for 25 antennas, also with options for up to 32 antennas, with the AEM Consortium (Alcatel Alenia Space, European Industrial Engineering and MT-Aerospace[1]). These two contracts are to date the largest contracts for ground-based astronomy projects.

Both contracts, based on identical technical specification and statement of work, foresee an initial design phase terminated by a design review. The design phase allows the antenna vendors to incorporate in the design of the serial antennas modifications demanded by the new ALMA specification, and, equally important, improvements consequent on the findings discovered during testing and operating the antennas. The vendors are asked to perform qualification activities in the technological areas sensibly differing from those validated on the prototype antennas.

In a separate process NAOJ ordered four 12-m antennas from Mitsubishi Electric Corporation on the basis of an almost identical specification to that of the bilateral project. Minor differences are related to the fact that the four Japanese antennas will perform total power measurement and are equipped with individual nutating subreflectors.

[1] After signature of the contract Alcatel Alenia Space was absorbed by Thales to form the company Thales Alenia. Similarly the obligations of MT-Aerospace have been transferred to MT Mechatronics.

Design update

The ALMA antenna team, consisting of members of the three organisations, have conveyed to the manufacturers the experience accumulated in at least two years of testing and operation. This precious experience extended well beyond the assessment of the science-related peformance of the antennas: much more it was related to the reliability and the maintainability aspects of the designs, recognised to be of fundamental importance for the efficient and economical operation of a large array at 5 000 m altitude. Each design modification required by ALMA, or proposed by the Contractors, was reviewed in depth during the design phase. For all three serial antennas the design phase was terminated by formal Pre-Production Design Reviews (PPDR) which saw the participation of a large reviewer group beyond the antenna team staff. The respective PPDRs for the three suppliers were held between November 2005 and February 2007.

The design of the North American antenna was jointly performed by Vertex Antennentechnik (VA) in Duisburg, Germany, and VertexRSI in Kilgore, Texas. VA is also the designer of the APEX Telescope. The Vertex antenna is equipped with a rim pinion drive system with double motors on both axes and a control system based on absolute encoders. The Carbon Fibre Reinforced Plastic (CFRP) Backup Structure (BUS) is joined to a steel cabin by means of a large Invar support cone. This cone decouples the effect of thermal expansion of the steel cabin from the thermally stable BUS, which is manufactured from CFRP. It is significant that the ALMA antennas operate in an outdoor environment and will be subjected to strong temperature variations and gradients. Any thermal stresses in the structure would affect the main specifications like the surface accuracy (25 µm RMS), the pointing accuracy (2 arcsec RMS absolute pointing, 0.6 arcsec RMS differential pointing) and the path length stability (15 µm over a 3-minute period).

The main reflector panels are lightweight, machined from aluminium and supported in a quasi-isostatic way by means of 8

Figure 1: Two views of the linear azimuth motor of the AEM antenna inside the qualification test bench. (Courtesy of EIE/AEM Consortium/ Phase Motion Control).

Invar adjusters. To allow the antenna to perform solar pointing, a scattering effect is implemented on the primary reflector panel with a proprietary chemical etching process. Design changes from the prototype which should be mentioned are: the new architecture of the control system, now based on a single Antenna Control Unit taking care of the antenna control and of the interface to the ALMA common software; the implementation of an automatic greasing system for the rim pinion drives; and a simplification of the temperature control system of the receiver cabin.

Both the Mitsubishi and AEM antennas have undergone major design changes. The cylindrical pedestal of the prototypes was substituted by a conical base, a shape more in conformity with the geometry of the new triple-point attachment interface to the antenna stations. Mitsubishi introduced a major change by adopting linear drives for both azimuth and elevation axes, produced internally by Mitsubishi Electric Corporation.

The AEM antenna has changed visibly in many areas from the AEC prototype design on which it is based. The azimuth axis is the one with the most changes and it now employs: a three-roller bearing, a tape encoder with eight reading heads in azimuth; a more compact cable wrap, providing more space for access and maintenance in the base; and finally a completely new azimuth motor design. This azimuth linear motor design, produced by Phase Motion Control, incorporates various features of existing linear motors for industrial machines, such as a distributed drive system, and an epoxy resin encapsulation for environmental protection (see Figure 1). The linear motor segments are now located outside the base, produce a larger torque and can be easily accessed for maintenance.

The CFRP truss structure used on the prototype was found not to be optimal in terms of the first eigenfrequency, and excitations were recorded sporadically during the test period. This has led to

Static Pressure (Pa)

Air velocity (m/s)
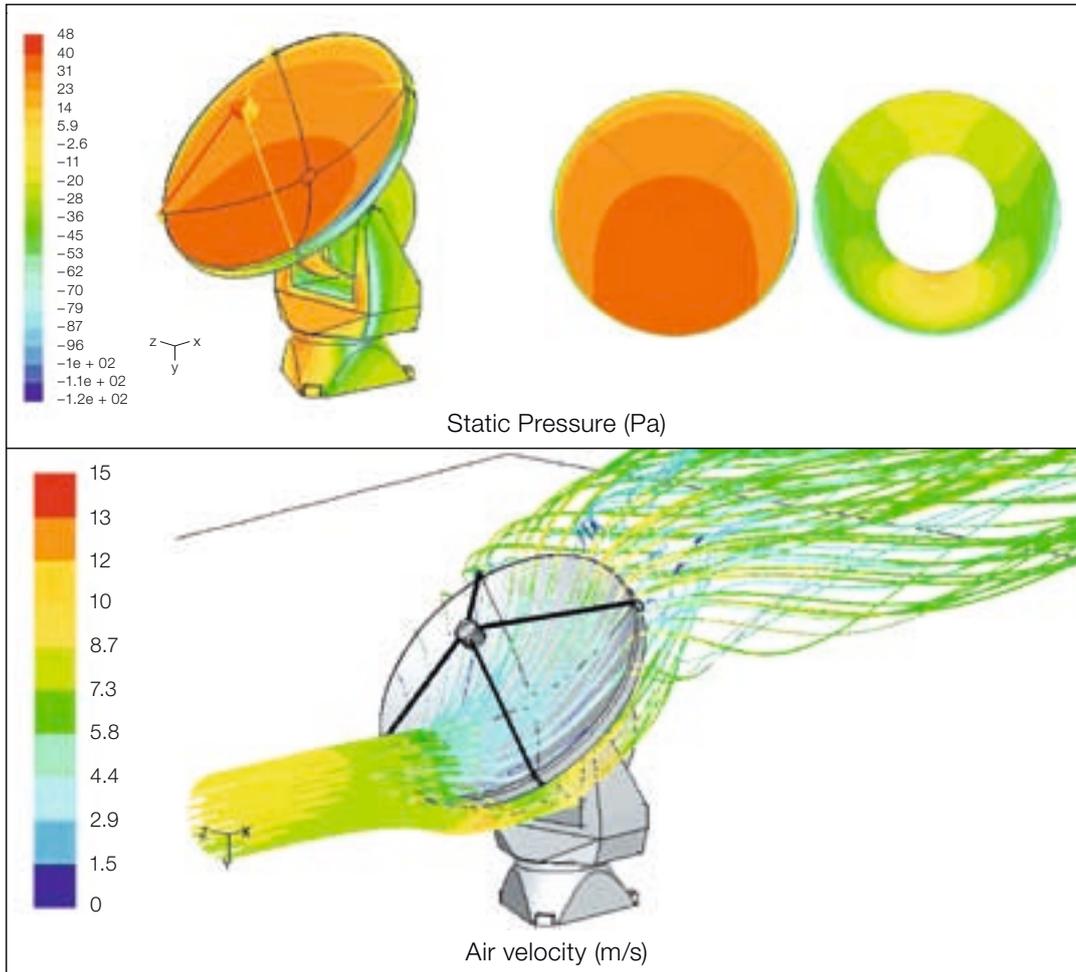
Figure 2: Computational Fluid Dynamics simulation of the wind impingement on the AEM antenna and determination of the static pressure fields. (Courtesy of the AEM Consortium).

a new, simplified single beam design of increased cross section. This, together with a lighter subreflector mechanism, now based on a customised, industrial hexapod, has contributed to significantly increase the first eigenfrequency. The complete antenna has been the subject of detailed fluid dynamical studies to assess the deformation of the main dish and of the quadripod structure to assess the effect on the surface accuracy and the pointing performance (see Figure 2). The fluid dynamical simulation has also been used to validate the heat exchange coefficient, for computing the gradients of temperature in the steel structure, and hence derive effects on path length and pointing accuracy.

Finally, all three antenna manufacturers revised the design of their respective metrology systems. The metrology system of the antennas is used to measure internal deflection caused by temperature and wind, in order to compute, at micrometric level, the path length difference and to keep the pointing accuracy to sub-arcsec level despite temperature changes, sun irradiation and possible strong wind at Chajnantor. Such a system poses a considerable challenge both to the designers and to the people who will later be in charge of commissioning it in the field. At the time of the evaluation testing of the antenna prototypes, the metrology systems had not been sufficiently investigated by the vendors and

their ability to achieve the demanded accuracy could not be demonstrated. Proceeding to the serial production phase without additional experiments would have represented a considerable risk. Consequently the vendors elected to perform dedicated missions for checking the metrology of the prototypes in New Mexico prior to freezing their designs. The results of the test campaigns were presented to the ALMA teams in charge of following the design and the proposed modifications were discussed.

The metrology of the VertexRSI and Mitsubishi antennas is now based on a stable internal reference structure, complemented by a number of thermal

Figure 3 (left): The pedestal of the VertexRSI Antenna #2 in assembly at the OSF (Courtesy NRAO/VertexRSI).

Figure 4 (top): The Backup Structure (BUS) and quadripod of the VertexRSI antenna #2 awaiting assembly on the pedestal (Courtesy NRAO/VertexRSI).

sensors. The AEM antenna uses distributed thermal sensors and a proprietary developed inclinometer. Unlike commercial systems, the AEM inclinometer combines sub-arcsec accuracy with fast response, making its use possible also during fast switching and scanning.

Production Status

The production schedule and status of the three vendors differs significantly, with both Mitsubishi and VertexRSI being sensibly more advanced than the AEM Consortium. AEM was the last to be contracted for serial antenna production and has a relatively long design phase in their project plan, due to the extensive amount of redesign since the prototype. Further, the production techniques employed with the AEM prototype for the CFRP parts were not optimised for serial production and they have now been revisited in view of sustaining a production rate of about one antenna per month after the delivery of the initial units.

The production of the North American antennas is carried out at the VertexRSI

manufacturing facilities of Mexia and Kilgore, Texas. These two facilities are in charge of the complete steel structures, including the base, the yoke, the cabin and the large Invar cone connecting the cabin to the Backup Structure. The individual antennas are partially pre-assembled at the factory with the integration of the base, the azimuth bearing, the yoke, the cabin and the Invar cone. The manufacture of the Backup Structure in CFRP has been awarded to the company Airborne Composites B.V. in The Hague, the Netherlands. Specific tests of stiffness were performed with the first unit to cross-check deflection with the results provided by Finite Element Analysis. Part of the delivery of the antenna is carried out by Vertex Antennentechnik in Duisburg, which is responsible, amongst others, for the control system, including hardware and software. The panels are manufactured by Zrinski in Germany, the same manufacturer selected for the prototype. The production process is well established and the panels for the fourth antenna are currently in production.

As concerns the European antenna, the go-ahead to produce was given to the

various suppliers by the AEM Consortium shortly after the Pre-Production Design Review concluded at the beginning of February 2007. Production of antenna assemblies is spread among various countries. The steel structure is manufactured by Asturfeito in Northern Spain, close to a harbour which can serve for the transport to Chile. A new assembly hall is being dedicated to handle volume production after the first unit. Presently, the first base and yoke are approaching completion with finishing and painting. AEM has accepted the first azimuth bearing and shipped it to Asturfeito, where a pre-assembly phase is taking place (see Figure 5).

The cabin is manufactured by Jallais and their subcontractor Multiplast in Northern France. Multiplast is well established in the field of sailing boats, having manufactured up to 120-ft boats engaged in setting records in round-the-world races. They have experience in large CFRP moulds and the use of high-strength mono-directional fibres such as those used for the cabin. The cabin is manufactured and assembled out of three CFRP moulds at Multiplast. After assembly and

installation of stiffeners, it is shipped to Jallais in Nantes where all the metallic interfaces are assembled and machined on special jigs. The internal walls of the receiver room will be protected by flame-sprayed aluminium for electromagnetic compatibility, and the cabin will be equipped with cabin floor, air conditioning heat exchanger, lights and various other fixtures. At the time of writing the first cabin is being equipped with linear motor interfaces (as shown in Figure 6), the floor and other installations, prior to transport to Asturfeito for mounting on the steel structure. Manufacturing of the second and third units has started.

The BUS of the AEM antenna is manufactured by Duqueine Composite in France. The first slices have been produced and the integration of the BUS has started (see Figure 7). Special tools have been developed from those originally used for assembling the prototype BUS, demanding less manual adjustment to reach the defined precision level. Once assembled, the BUS will be equipped with the panel adjusters, produced by RUAG in Switzerland. A pre-assembly of the panels and the apex structure is planned in Europe. The BUS will then be separated in two halves and prepared for transport. The production of the nickel-deposited replicated panel is proceeding at full speed, clearly profiting from the fact that the design remains unchanged from the prototype design. The Italian-based supplier, Media Lario Technologies, has increased its manufacturing facilities to be able to serve the demanded delivery schedule. The panels for the third antenna are now in production.

Finally, the remaining equipment is being produced by various suppliers, with control system and metrology delivered by Microgate, the linear motors by Phase Motion Control in Italy and the quadripod legs manufactured in Germany by Xperion. The equipment is first internally accepted by AEM, in a process which is closely monitored by ESO, prior to integration into the antenna.

Figure 5: AEM base (upper) and yoke (lower) in manufacturing (Courtesy of AEM Consortium/Astrurfeito).

Figure 6: Mounting of the elevation linear motor on the AEM antenna cabin (Courtesy of AEM Consortium/Jallais).

The Mitsubishi 12-m antennas are currently the most advanced. Three antennas have been produced so far, almost completely assembled at the Osaka factory, and then shipped to Chile where they arrived in July 2007. The fourth antenna is in production and is close to being shipped.

On-site assembly

A large work area at the OSF was put at the disposal of the three contractors by ALMA to perform their integration activities. ALMA has reviewed the design of the respective work areas, levelled the surface and installed a number of antenna pads, identical to those to be constructed at the high site, for performing erection work and final acceptance. In each of the work areas, more than one antenna station can be used for the testing and acceptance of the antennas. In particular, the front antenna pad(s) can be illuminated with the holography transmitter mounted on the holography tower for setting the surface accuracy prior
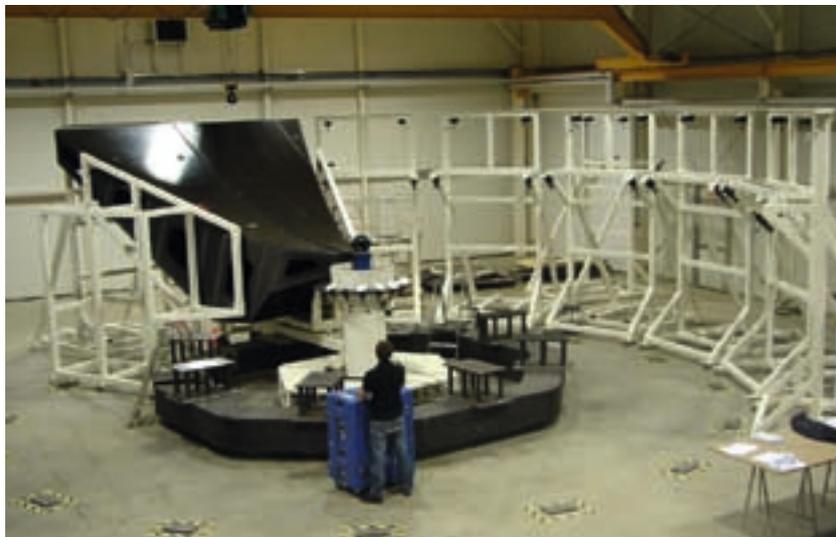
Figure 7: Assembly of the BUS of the first AEM antenna. (Courtesy of AEM Consortium/Duqueine Composites).

Figure 8: Mitsubishi Antennas in testing at the OSF (Courtesy NAOJ/Mitsubishi Electric Corporation).

to delivery. VertexRSI and AEM choose to build temporary facilities at the work area to support their integration activities. VertexRSI installed a full assembly hall, while AEM will build a reduced, thermally controlled facility for the assembly and adjustment of the BUS and panels prior to installation on the antenna. The assembly hall of VertexRSI is already supporting integration work on the antennas (Figures 3 and 4), while the facility of the AEM Consortium will be built shortly. In the design of the work area, attention has been given to the access for the antenna transporter. The antennas, once accepted from the contractors will be handed over to the Assembly Integration and Verification (AIV) group for integration of Front-End and Back-End equipment.

Schedule

By the end of October 2007 three 12-m antennas of Mitsubishi are on site and are undergoing final integration, with internal testing having already started on the first unit (see Figure 8). The antennas are scheduled to have acceptance testing completed before the end of 2007. The fourth 12-m antenna is in advanced construction and is scheduled to arrive at the OSF at the end of the year for testing and delivery a few months later. The first VertexRSI antenna is in an advanced state of integration at the OSF (Figure 9). The primary reflector and the panels are mounted and pre-aligned before the final adjustment. This antenna is scheduled to be delivered to ALMA at the beginning of 2008. The second unit arrived at the OSF at the beginning of October and is being assembled inside the assembly hall. Testing and delivery to ALMA is scheduled for spring 2008. The delivery of the first AEM antenna is scheduled for the fourth quarter 2008, with the second unit scheduled for spring 2009. Both AEM and VertexRSI have a very tight subsequent delivery schedule and delivery of all antennas is expected to be completed at the end of 2011 for both suppliers.

The contract for design and production of the 7-m antennas has been awarded to Mitsubishi Electric Corporation and the design phase is underway. The schedule foresees delivery of the first unit in 2009 and the last in 2011.

Figure 9: VertexRSI Antenna #1 in advanced integration at the OSF (Courtesy of NRAO).

As a concluding remark, we can say that after the initial period of redesign and production of the first units, necessary to move from prototype design to industrially sound scientific machines, the procurement of the ALMA antennas has now acquired considerable momentum. The antenna vendors are making a considerable industrial effort to support the ALMA-demanded delivery. A substantial, parallel effort will have to be made by ALMA in order to be able to smoothly accept the antennas, commission them and deliver them for science operation at the required pace.

Near-infrared image of the Tarantula
nebula (30 Doradus,NGC 2070) in
the Large Magellanic Cloud taken by
HAWK-I during commissioning.
The colour composite is composed
of three exposures in the filters J, K
and Brackett-γ. Image taken by
the HAWK-I team and processed by
Hans Hermann Heyer (ESO)

First Thermal IR Images of Neptune: Evidence for Southern Polar Heating and Methane Escape

Thérèse Encrenaz[1]
Glenn S. Orton[2]
Cédric Leyrat[2]
Richard C. Puetter[3]
Andrew J. Friedson[2]
Eric Pantin[4]

[1] Laboratoire d'Etudes Spatiales et d'Instrumentation pour l'Astrophysique (LESIA), Observatoire de Paris, Meudon, France
[2] Jet Propulsion Laboratory (JPL), California Institute of Technology, USA
[3] Center for Astrophysics and Space Sciences (CASS), University of San Diego, California, USA
[4] Service d'Astrophysique (SAp), Département d'Astrophysique, de Physique Nucléaire, de Physique des Particules et d'Instrumentation Associée (DAPNIA), Commissariat à l'Energie Atomique (CEA), Gif-sur-Yvette, France

Images of Neptune have been obtained in the thermal range, in filters between 8 and 19 µm, using the VISIR mid-infrared imaging spectrometer at the VLT-UT3 (Melipal). They allow, for the first time, mapping of atmospheric temperatures at different altitude levels, ranging from the tropopause to the stratosphere. It was found that the south pole of Neptune, at the level of the tropopause, appears to be warmer than the rest of the planet by 6 to 8 K. This southern polar warming can be explained by its constant solar illumination over the past 40 years, as the southern summer solstice occurred in July 2005. The other unexpected discovery is the evidence for a stratospheric hot spot located at 65–70°S which rotates with the planet at the atmospheric rotation rate of about 12 hours.

Neptune: a very active planet

In spite of its large heliocentric distance, Neptune is known to be dynamically very active. The first evidence came from Voyager 2 visible images at the time of the spacecraft's flyby in 1989 (Smith et al. 1989). Subsequent images and spectra taken in the near-infrared showed a strong variability of Neptune's cloud structure. In addition, high zonal winds have been measured, and IRIS/Voyager infrared measurements have shown that the stratosphere is surprisingly warm. The active meteorology of Neptune is likely to be linked to its internal source of energy, which is 1.6 times the solar energy absorbed.

Other evidence for Neptune's high vertical circulation is the supersaturation of methane, which was discovered some twenty years ago from ground-based and space infrared spectroscopy. As for all the Giant Planets, the thermal profile of Neptune is characterised by a troposphere, where the temperature decreases with pressure, superimposed by a stratosphere where the temperature increases with the altitude. Between the two regions, the tropopause is the level of minimum temperature. Taking into account the low temperatures measured by Voyager at the tropopause of Neptune (typically 55 K at mid-latitudes), methane should be trapped at the tropopause and the CH_4 mixing ratio should be 3–10 ×

Figure 1: Thermal images of Neptune, with North at the top and the south pole visible at the bottom of each image. Images of nearby calibration stars (HD25025 for A, HD216032 for B, HD200914 for C, HD200514 for D and F) are also shown. Images C and E are separated by 6.83 hours in time; images D and F are separated by 2.25 hours.

10^{-4}. In contrast, values several times higher were reported, which implied the existence of strong vertical motions; the mechanism of such circulation, however, was not understood.

Observations with VISIR

The mid-infrared camera/spectrometer VISIR, at the VLT-UT3 (Melipal) enabled us to map Neptune's atmospheric temperatures at all latitudes including the south pole, something Voyager had not been able to achieve during the spacecraft's flyby. The VISIR instrument (Lagage et al. 2004) operated in two modes, imaging and spectroscopy, between 7 and 25 µm. We selected different filters which allowed us to probe different levels of Neptune's troposphere and stratosphere. Observations were obtained on 1 and 2 September 2006. Two images of Neptune were obtained at 17.6 and 18.7 µm (see Figure 1). In this wavelength range, the spectrum of Neptune is sensitive to the collision-induced absorption (CIA) spectrum of hydrogen, due to H_2-H_2 and H_2-He collisions, which is the major source of opacity. Because hydrogen is the major atmospheric constituent in Neptune's atmosphere, this measurement can be directly translated into an atmospheric temperature. At 18 µm, Neptune's radiation mostly comes

from the tropopause, at a pressure about 100 mbars, where the temperature is minimum on all giant planets.

Other images were taken at 8.6 µm and 12.3 µm (Figure 1). At 8.6 µm the opacity is dominated by a CH_3D band (with some contribution from the wing of the strong CH_4 ν_4 band centred at 7.7 µm) and the radiation mostly comes from the stratosphere at 0.1 mbar. At 12.3 µm, the main absorber is C_2H_6 and the radiation also peaks at a level close to 0.1 bar. Ethane, like acetylene C_2H_2 and other hydrocarbons, is a photodissociation product of methane in the stratospheres of all giant planets. Two 8.6-µm images were taken, separated by 6.83 hours in time, and two 12.3-µm images were taken, separated by 2.25 hours (see Figure 1). Figure 2 shows the contribution functions at 8.6, 12.3, 17.6 and 18.7 µm. The two plots at 17.6 and 18.7 µm show a double structure; this is because they probe the tropopause and the lower stratosphere where the temperature increases sharply with altitude. The contribution function, which is the product of the opacity and the Planck function, thus exhibits two maxima.

Temperature increase at the south pole

Both images A and B of Figure 1 (at 17.6 and 18.7 µm respectively) show a strong maximum at the south pole of the planet. In addition, a local minimum appears at mid-southern latitudes and a weak increase is also visible in the equatorial region.

We processed the images using the ESO pipeline (Lagage et al. 2006) and we deconvolved them using the Pixon approach (Puetter and Yahil 1999). After deconvolution, it appeared that the southern bright spot exactly fits the position of the south pole (Figure 3). In order to retrieve the temperature at the tropopause as a function of latitude, we started from a mean thermal profile consistent with previous ground-based and Voyager measurements (Orton et al. 1992; Conrath et al. 1998) and we allowed for a translation by a few degrees to get the best fit. The result is shown in Figure 4, for both deconvolved images A and B. Voyager results (Conrath et al. 1998), ob-

tained between 20°N and 80°S by the IRIS infrared spectrometer, are also shown for comparison. Both images A and B lead to a strong increase of the temperature at the south pole, by about 10 K relative to 60°S latitude, and by about 7 K relative to the equator. The agreement with Voyager data is satisfactory at mid-latitudes, but the Voyager values tend to be weaker at 80°S; no information is available from Voyager at higher southern latitudes.

What can be the explanation of such a phenomenon? Most likely, the temperature increase at the south pole of Neptune results from its constant illumination over the past forty years. Neptune's sidereal period around the Sun is 164 years, and the last southern summer solstice occurred in July 2005. We can expect the opposite phenomenon in the future several decades, after the northern spring equinox, when the north pole of Neptune becomes illuminated. We also note that a similar effect was observed on Saturn (Orton and Yanamandra-Fisher 2005).

Methane escape in Neptune's stratosphere

The temperature excess at the south pole has an important consequence. If we consider the averaged temperature profile of Neptune, as derived from previous observations (Figure 4), methane, the most abundant minor atmospheric constituent (at the per cent level, far below hydrogen and helium), should be trapped at the tropopause in the form of ice. In the stratosphere, its mixing ratio should be constrained by the saturation low at the tropopause. Taking a temperature of 55 +/– 2 K at the tropopause, the mixing ratio should be $3–10\times10^{-4}$. In contrast, much higher values ($0.75–1.5\times10^{-3}$) were measured by infrared spectroscopy, from the ground (Orton et al. 1992) or from the ISO Earth-orbiting satellite (Bézard et al. 1999). Recent measurements by Spitzer have also confirmed this result. It was then proposed that the atmosphere of Neptune had an active vertical circulation, able to transport the tropospheric methane from the troposphere up to stratospheric levels. However, as all these results were obtained on the integrated disc of Neptune, no information could be

obtained on its precise mechanism.

The VISIR images allow us to find an explanation to the circulation process. At the south pole of Neptune, the temperature of 63 K allows a methane mixing ratio of 8×10^{-3}, i.e. about eight times higher than the average observed value. North of 60°S latitude, the CH_4 mixing ratio allowed by the mean temperature of 55 +/– 2 K is, as mentioned above, about two times lower than the mean observed value. It is quite plausible that the active circulation of Neptune transports stratospheric methane from the south pole toward mid-latitudes where it condenses again as it falls down toward the tropopause.

If this explanation is correct, we would expect to find enhanced emissions of acetylene (C_2H_2) and ethane (C_2H_6) around the south pole. These molecules have strong infrared spectral signatures, at 13.7 µm and 12.5 µm respectively, which have been observed at high resolution from the ground and from ISO over the averaged disc of Neptune (Bézard et al. 2000). High-resolution imaging spectroscopy should be able to detect an asymmetry in their latitudinal profiles.

A hot spot in the stratosphere

Another surprise came from the VISIR images. The two 8.6-µm images C and E (Figure 1) clearly show a hot spot at about 65–70°S latitude, which appears at two different positions relative to the central meridian. Assuming it is the same spot on both images, we can calculate its rotation period. Both images are separated by 6.83 hours in time. After deconvolution, the inferred rotation period at 65–70°S latitude is about 12.4 +/– 1.3 hours. We note that this value is slightly different from the value of 13.8 hours quoted in the article where the present results are reported (Orton et al. 2007). The difference comes from a more precise treatment of the images. We believe that our last value is more reliable. It is, by the way, fully consistent with the value of 12.5 hours reported by Limaye and Sromovsky (1991) from cloud motion measurements at this latitude. It is definitely incompatible with the magnetic rotation period of 16.1 hours (Zarka et al.

1995), which implies that the observed spot is not associated with auroral processes. This interpretation would have been most unlikely anyway, as the magnetic pole of Neptune is tilted by 47° with respect to its rotational axis; thus any feature connected to the magnetic field would be expected to appear, 6.8 hours later, at a different latitude.

The two 12.3-µm images D and F (Figure 1), separated by 2.25 hours in time, also show a hot spot at about the same position, in latitude and longitude, as the 8.6-µm images. They also show a significant limb-brightening all around the planet, which probably results from a sharp increase of the temperature in the stratospheric region probed by the C_2H_6 emission (Figure 2).

What could be the origin of the observed hot spot? It is the signature of a localised atmospheric heating, at a pressure level of about 0.1 mbar. We could think of a cometary or asteroidal impact, comparable in nature with the SL9-Jupiter collision, but weaker. Since the discovery of oxygen-bearing compounds (CO, CO_2, H_2O) in Neptune's stratosphere, it has been suggested that the oxygen flux might originate from cometary impacts (Lellouch et al. 2005). However, there is no evidence from any other observation of Neptune, in the visible, infrared or millimetre range, that a cometary impact took place over the past years.

Another more plausible explanation might be that the observed feature has a dynamical origin. The tropopause region is known to exhibit a strong variability of the cloud structure, especially near the pole. The warm polar temperature at the tropopause could be the tracer of a polar vortex which could extend into the stratosphere and generate localised stratospheric enhancements; however this assumption remains to be validated.

How to proceed further?

The next step of this work will consist in measuring the stratospheric mixing ratio of methane as a function of latitude. In the emission bands of hydrocarbons, at 8.6 and 12.3 µm, the outgoing flux depends upon two parameters: the mixing
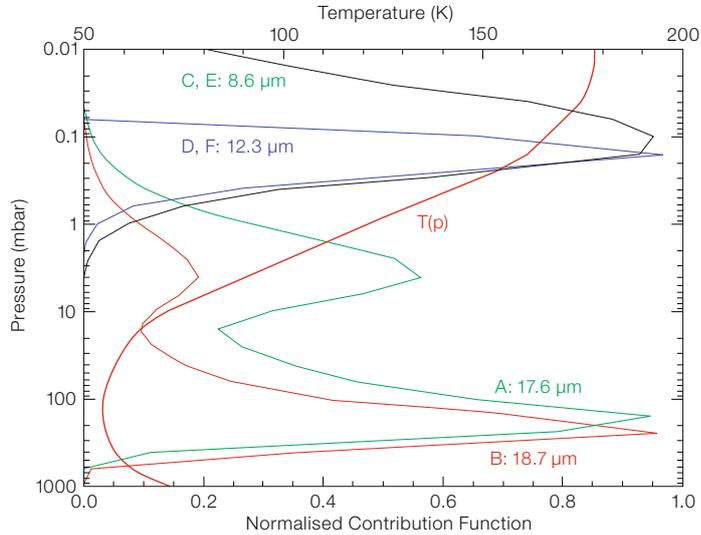
Figure 2: Contribution functions showing the origin of the outgoing radiance in the four filters used at 8.6, 12.3, 17.6 and 18.7 µm. For the 17.6 and 18.7-µm filters, the weighting function peaks just below the tropopause, and the upper maximum is the result of the sharp temperature increase in the lower stratosphere.
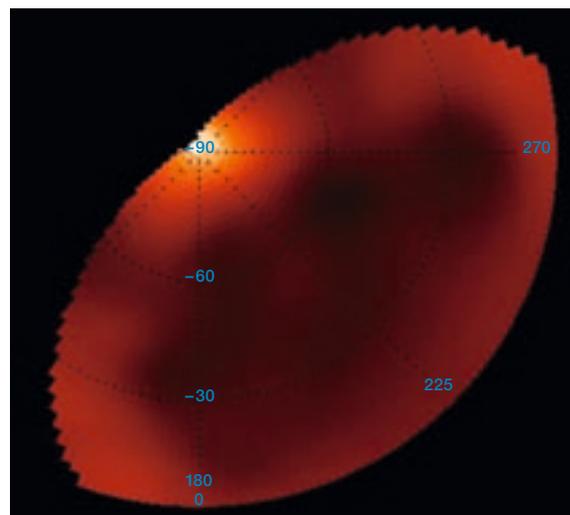
Figure 3: Polar projection of the deconvolved 17.6-µm image of Neptune. It can be seen that the centre of the hot spot exactly coincides with the south pole.
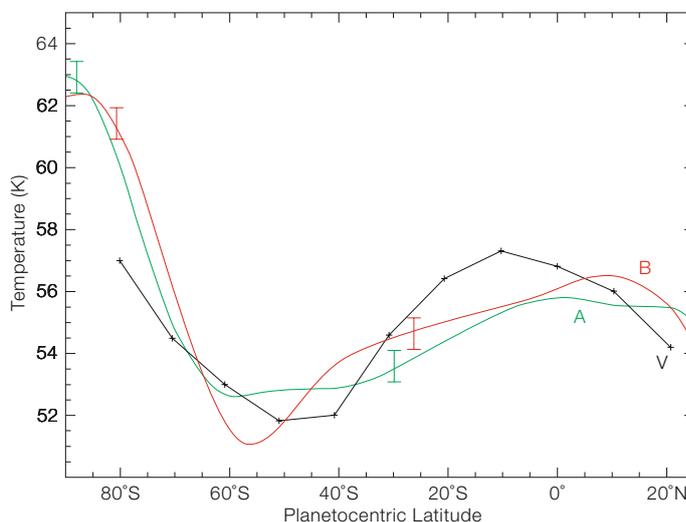
Figure 4: Latitudinal variations of the zonal mean temperature at the tropopause level (at a pressure level of 100 mbar). The green curve corresponds to Image A (in Figure 1); the red curve to Image B; and the black curve to Voyager results (Conrath et al. 1998).

ratio of the hydrocarbon and the temperature. It is thus necessary to determine independently the stratospheric temperature as a function of latitude. This can be done by high-resolution imaging spectroscopy of the S(1) quadrupole line of H_2 at 17.1 μm. Such a measurement was achieved on 3 September 2006, using the spectroscopic mode of VISIR, and is presently under reduction and analysis. Another important measurement would be high-resolution imaging spectroscopy of the most intense hydrocarbon emissions in specific individual lines (C_2H_2 at 13.7 μm, C_2H_6 around 12.5 μm). These emissions, much stronger than CH_4 at 7.7 μm, are very good tracers of stratospheric methane and can be used, through photochemical models, to infer the CH_4 mixing ratio.

Why are Uranus and Neptune so different?

In conclusion, it is interesting to note how different Uranus and Neptune are. In spite of their common status as "icy giants", and their similarities in global atmospheric composition and tropospheric temperature structure, they differ from each other in many ways. First Neptune, as mentioned above, has an internal source of energy, while none has been detected on Uranus. Second, Neptune has a very efficient dynamical circulation, while Uranus has no sign of one. Third, in contrast with Uranus, CO and HCN are very abundant in Neptune's stratosphere. To account for all these differences, it has been suggested that both planets might have different internal structures. In Neptune, the heat (originating from the cooling of the planet since its formation) is transported from the interior by convection. Uranus, closer to the Sun, receives more solar flux than Neptune, which already hampers the escape of internal heat. In addition, the interior of Uranus might have a different stratification, so that convection might be inhibited, which would prevent the upward transport of internal energy. This hypothesis however remains to be tested.

References

Bézard B. et al. 1999, ESA SP-427, 153
Conrath B. J. et al. 1998, Icarus 135, 501
Lagage P. O. et al. 2004, The Messenger 117, 12
Lagage P. O. 2006, Proc. SPIE 6269, 626913
Lellouch E. et al. 2005, A&A 430, L37
Limaye S. S. and Sromovsky L. A. 1991, Nature 354, 380
Orton G. S. et al. 1992, Icarus 100, 541
Orton G. S. et al. 2007, A&A 473, L5
Orton G. S. and Yanamandra-Fisher P. 2005, Science 307, 696
Puetter R. C. and Yahil A. 1999, ASPCS 172, 307
Sromovsky L. A. et al. 1993, Icarus 105, 140
Zarka P. et al. 1995, in "Neptune and Titan", University of Arizona Press, 341

Photo: H. H. Heyer, ESO

An aerial view of the ESO Headquarters in Garching taken in summer 2007. For the required expansion of the ESO Headquarters building, an extension is being planned, for which an architect competition is in progress. The new building will be sited in the ploughed field to the south of the existing complex.

Polarimetry of Solar System Gaseous Planets

Franco Joos, Hans Martin Schmid
(Institute of Astronomy, ETH Zurich, Switzerland)

With the ESO 3.6-m telescope and EFOSC2 we have observed Solar System planets to investigate limb polarisation in detail. Our observations were successful and we can report the detection of limb polarisation in Uranus and Neptune. In addition spatially resolved long-slit spectropolarimetry was obtained for the first time for all the gaseous planets. The observations reveal a decrease of limb polarisation with increasing wavelength and an enhanced polarisation in the methane bands against the adjacent continuum. We describe our measurements and also discuss the diagnostic potential of such data for the investigation of the atmospheric structure of giant planets and the properties of their scattering particles.

Science motivation

Light reflected from planets is polarised. This basic property provides the opportunity to investigate planetary atmospheres by means of polarimetry. Many previous studies of Solar System planets demonstrate that polarimetry is a very powerful tool for the investigation of the atmospheric structure and the characterisation of the scattering particles. Well-known examples are the studies of the polarisation of Venus (e.g. Dollfus and Coffeen 1970), which permitted the determination of the droplet size and composition in the reflecting clouds. Other famous examples are the highly polarised poles of Jupiter which were first described by Lyot in 1929 (Lyot 1929). The polarisation at the poles is high because the radiation is reflected by Rayleigh scattering particles, while it is low at the equatorial limbs since there the light is reflected by clouds (see Figure 1). These examples illustrate well the diagnostic potential of polarimetry.

Polarimetry is also a very attractive technique for the search and investigation of extrasolar planets for three main reasons: firstly, the expected polarisation signal of the reflected light from a planet is high, on the order 5 to 50 % for phase
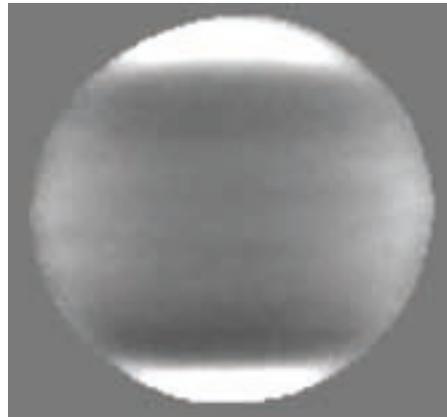
Figure 1: Imaging polarimetry of Jupiter. **Left:** the polarised Stokes Q flux, with white indicating positive (vertically) and black negative (horizontally) polarised light. **Right:** the polarised Stokes U flux (polarisation direction is rotated by 45˚ in a counter-clockwise direction compared with Q). Data taken with the Zurich imaging polarimeter system (ZIMPOL) at the McMath-Pierce solar telescope at Kitt Peak in a methane filter centred at 730 nm.

angles near 90˚ ; secondly, the reflected (= polarised) light can be distinguished from the unpolarised radiation from the central star; thirdly, the amount of polarisation provides information on the scattering particles and the atmospheric structure of the planet (see Schmid et al. 2006). Therefore, the future VLT planet finder instrument SPHERE (Spectro-Polarimetric High-contrast Exoplanet REsearch) will have a polarimetric mode in order to search for polarisation signals of extrasolar planets (Beuzit et al. 2006).

From the Earth all the giant planets are observed near zero phase angle (maximum phase angles are ≈ 11˚ for Jupiter or ≈ 2˚ for Neptune, for example) and essentially no polarisation is expected in integrated light. But if the planetary disc is resolved, then one can expect a limb polarisation, which arises due to a well-known second-order effect for reflecting atmospheres where Rayleigh type scattering processes are dominant (see e.g. van de Hulst 1980).

In order to understand the limb polarisation, one has to consider a back-scattering situation at the limb of a gas-rich planet, where there is locally a configuration of grazing incidence and grazing emergence for the incoming and the back-scattered photons, respectively.
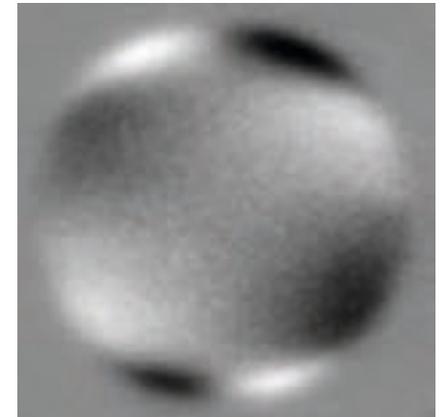
Light reflected after one scattering is unpolarised, because the scattering angle is 180˚. Photons undergoing two scatterings travel, after the first scattering, predominantly parallel to the surface before being reflected towards the observer by the second scattering process. The reason is that photons travelling outwards from the planet will mostly escape without a second scattering, while photons travelling inward have a low probability of being reflected towards the observer after the second scattering, but a high probability to be absorbed or to undergo multiple scatterings. Since the polarisation angle induced by a single dipole-type scattering process, like Rayleigh scattering, is perpendicular to the propagation direction of the incoming photon (which in this case is parallel to the limb), polarisation perpendicular to the limb is produced.

Limb polarisation of the giant planets has up to now hardly been investigated. Although there exist several studies based on filter polarimetry for Jupiter, and a few for Saturn, we have found no previous polarimetric observations which resolved the limb of Uranus and Neptune, nor disc-resolved spectropolarimetric measurements indicating limb polarisation. For this reason we proposed such observations with EFOSC2 at the ESO 3.6-m telescope.

Polarimetry with EFOSC2

The EFOSC2 instrument is a multi-mode Cassegrain imager and grism spectrograph which can be equipped with a Wollaston prism and a rotatable super-achromatic half-wave plate for linear im-

aging polarimetry and spectropolarimetry. For linear polarimetry one measures the Stokes parameters Q and U, which are the differential intensity signals between two orthogonal linear polarisation directions according to $Q = I_0 - I_{90}$ and $U = I_{45} - I_{135}$ (where 0,90, … signify the polarisation direction on the sky). In EFOSC2 a Wollaston prism splits the light into the $I_\perp$ and $I_\parallel$ polarisation directions (relative to the orientation of the prism). The two images, called the ordinary and the extraordinary beams, are separated on the CCD by 10″ or 20″, respectively (see Figure 2). The two beams from the Wollaston do not overlap thanks to a special aperture mask in the focal plane with a series of open stripes (or slitlets for spectropolarimetry), whose width and separation correspond to the image separation introduced by the Wollaston beam splitter. Combining the polarimetric components with normal EFOSC2 filters or grisms then yields imaging polarimetry or spectropolarimetry, respectively (Figure 2).

It is important for a high polarimetric precision that the two polarisation directions $I_\perp$ and $I_\parallel$ are measured simultaneously in order to avoid errors due to atmospheric seeing and transmission variations. Rotating the half-wave plate between two exposures, e.g. from 0° to 45° for Stokes Q, allows the two polarisation images to be swapped on the detector, so that differential effects in the two Wollaston beams cancel out in the polarisation signal (including the individual pixel efficiencies of the CCD). Thus, two frames taken with different retarder plate orientations yield one normalised Stokes parameter: Q/I with the half-wave plate orientations 0° and 45°; and U/I with the orientations 22.5° and 67.5° (cf. Tinbergen 1996).

The instrumental set-up for imaging polarimetry and spectropolarimetry for our planet observations is summarised in Table 1.

Figures 3 and 4 show examples of the raw frames for Uranus, taken in imaging polarimetry mode and spectropolarimetric mode, respectively. In imaging mode the ordinary and the extraordinary beams are separated by 10″ in spectropolarimetric mode the separation is 20″. The 20″ long slit was oriented North-South over the disc of Uranus, approxi-

Figure 2: Schematic concept for spectropolarimetry (upper) and imaging polarimetry (lower).

Imaging polarimetry	Spectropolarimetry
Wollaston 10″ stripe mask	Spectropolarimetric 20″ slitlets
Half-wave plate	Half-wave plate
Broad- and narrowband filters	Wollaston prism 20″
Wollaston prism 10″	Grism ESO#5
CCD	CCD

Table 1: Set-ups for EFOSC2 imaging polarimetry and spectropolarimetry.

Figure 3: Raw data for an exposure of Uranus in imaging polarimetry mode. The ordinary and the extraordinary images are separated by 10″. The two images are not perfectly round because Uranus showed a bright south pole and darker northern latitudes.
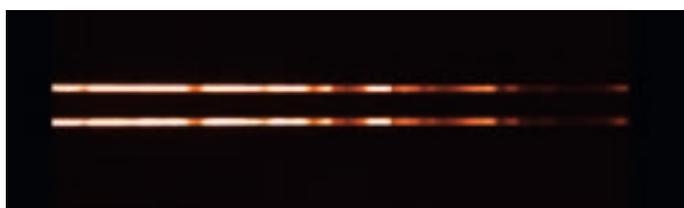
Figure 4: Raw data for an exposure of Uranus in spectropolarimetric mode. The deep methane absorption bands at longer wavelengths are clearly visible to the right.

mately along the planetary equator. This configuration yields long-slit spectropolarimetry, providing a centre to limb profile in intensity and polarisation for each wavelength covered by the grism.

EFOSC2 at the 3.6-m telescope is an ideal polarimetric instrument because it is attached to the Cassegrain focus and there are no strongly inclined optical components in the beam. The whole optical set-up is rotationally symmetric, so that the instrumental polarisation from the telescope and the instrument are essentially zero, at least near the optical axis. One problem of our observations was that the surface brightness of Jupiter and Saturn was too high for imaging polarimetry, even in narrowband filters. For this reason we inserted, together with some narrowband filters, an opaque mask near the pupil of EFOSC2. The mask was a self-made black plate with 28 small holes which blocked about 99 % of the telescope light.

Imaging polarimetry of Uranus and Neptune

During two nights in visitor mode we were fortunate to often have subarcsec seeing conditions at the 3.6-m telescope. This allowed us to well resolve the discs of Uranus (diameter 3.5″) and Neptune (2.2″) and to detect the limb polarisation. The measured normalised polarisation was in the range 0.5 to 1.5 % for both planets. Observations with R (644 nm), i (803 nm) and z (890 nm) band filters were taken for these two targets. The resulting i-band polarimetry is shown in Figures 5 and 6. The position of the limb, the equator and the south pole are indicated.

The Stokes Q and U images for Uranus both show a very characteristic quadrant pattern. $Q = I_0 - I_{90}$ is positive (white in the figures) or vertical at the equatorial limbs, negative (black in the figures) or horizontal at the polar limbs, and essentially zero in the centre of the planetary disc. For U the same pattern is apparent but rotated by 45°. Neptune shows qualitatively the same pattern. In order to obtain these Q and U maps one has to carefully align the images from the ordinary and extraordinary beam. The precision has to be better than a tenth of a
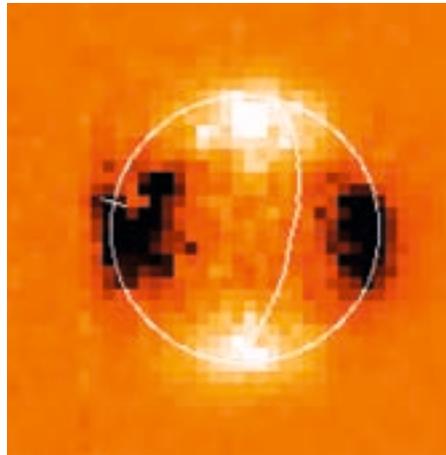
Figure 5 (above): Imaging polarimetry of Uranus in i-band; white corresponds to positive and black to negative polarisation. The limb is indicated by the circle, the equator by an arc and the south pole by the tick mark. Left: the polarised flux in the Q-direction with positive vertical and negative horizontal. Right: the polarised flux in the U-direction. The polarisation pattern is rotated by 45° in a counter-clockwise direction.
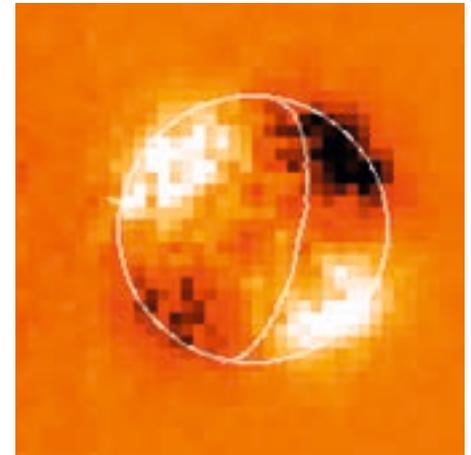
Figure 6 (below): Radial polarisation of Uranus and Neptune constructed from the Q and U images. White denotes radial polarisation and black would denote tangential polarisation, with orange as intermediate values. Left: Uranus in the i-band. Right: Neptune in the R-band.
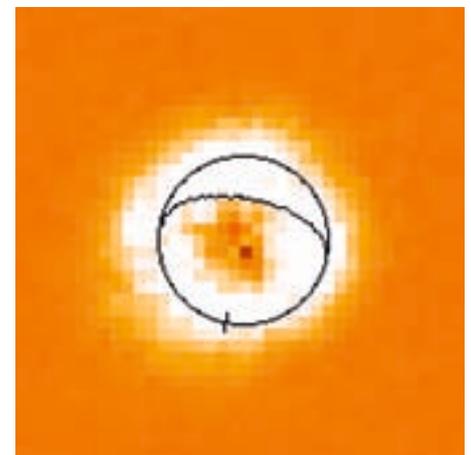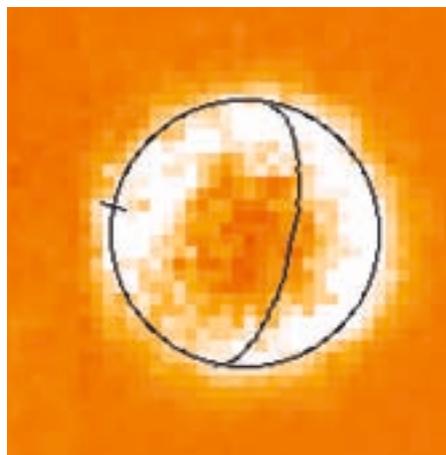
pixel (1 pixel = 0.157″). A misalignment of one image would create a spurious positive polarisation signal at one limb and at the same time a spurious negative signal at the opposite limb.

The observed Q and U images indicate that the polarisation is high at the limb and low in the disc centre. The position angle of polarisation is perpendicular to the limb everywhere. This pattern can be better illustrated with a transformation to radial Stokes parameters Q_r and U_r, which are defined relative to the radial direction on the planetary disc. Positive Q_r indicates a radial polarisation and neg-

ative Q_r a tangential polarisation, while $\pm U_r$ are the polarisations at $\pm 45°$ orientation relative to the radial direction. The resulting Q_r images for Uranus and Neptune are shown in Figure 6. In both cases the limb polarisation is clearly visible as a bright ring with positive Q_r polarisation. The U_r images are essentially zero as there is no polarisation with a tilted orientation relative to the limb. The figures also suggest that the polarisation has a constant strength along the entire limb. This situation is unlike Jupiter (see Figure 1) or Saturn where significant limb polarisation is only observed at the poles.

For a quantitative analysis we have to take into account that the seeing-limited spatial resolution of our observations causes a degradation and cancellation in the polarisation. Our imaging polarimetry reveals that the limb polarisation decreases for both planets from the *R*- to *i*- to *z*-bands. From the Q_r maps it is also possible to derive the disc-integrated limb polarisation, which is a good parameter for comparing observations with model calculations. Unfortunately, there exists a severe lack of model calculations for limb polarisation. For this reason we compared our results with analytic calculations for Rayleigh scattering atmospheres from the 1970's and earlier, going back to the classical work of Chandrasekhar in 1950. Consulting these simple models indicates that the Rayleigh scattering layers in Uranus and Neptune have an optical depth of about $\tau = 0.2$ in the *R*-band continuum and lower for longer wavelengths. This dependence is expected as the Rayleigh scattering cross section behaves like $\sigma \propto 1/\lambda^4$. The polarisation is therefore higher for short wavelengths.

Spectropolarimetry

During the same observing run we also performed long-slit spectropolarimetry of the four giant gaseous planets. The spectropolarimetric mask consisted of a series of 20″ long by 0.5″ wide slitlets, aligned along a line and separated by 20″ (corresponding to the beam separation of the Wollaston used for spectropolarimetry). We chose the grism ESO#5 which covers the spectral region 530 to 930 nm, providing a spectral resolution of 1.3 nm for a 1″ wide slit. In this wavelength range the giant planets show a rich spectrum of weak and strong methane absorption bands. For Jupiter and Uranus we present in Figure 7 the extracted intensity (arbitrary scale) and polarisation spectrum for the limb.

For the observation of Uranus, the slit was oriented along the celestial N-S direction, covering the entire equatorial region from limb to limb. The intensity and polarisation signal were then extracted and averaged from the N and S limb regions with their high polarisation. For Jupiter the slit was aligned along the central meridian covering the northern parts
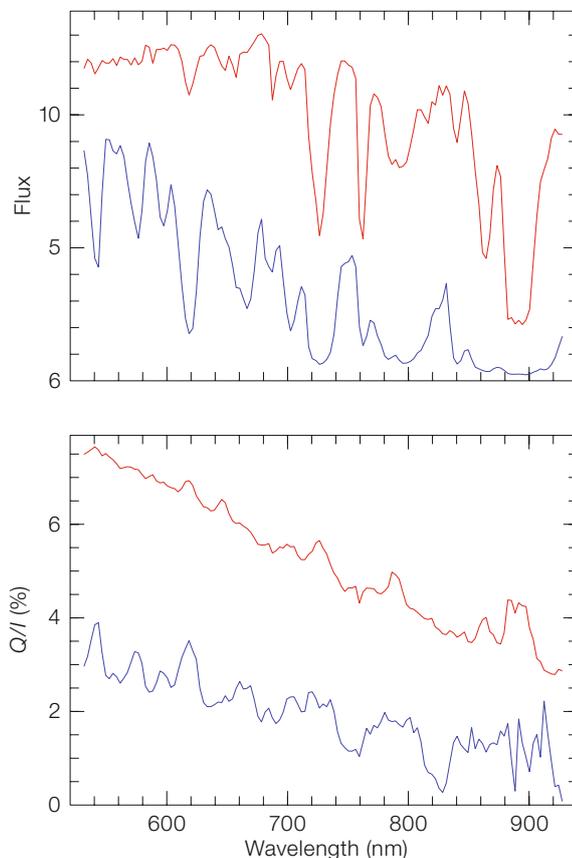
Figure 7: Spectropolarimetry for the limbs of Jupiter (red) and Uranus (blue). Top: flux in arbitrary units. Bottom: Stokes *Q/I* in per cent for both planets. For Uranus the polarisation signal is corrected for the degradation due to the seeing-limited resolution.

of the planet from about the centre to the limb. The diameter of Jupiter in the polar direction was 33.6″. The Jupiter data in Figure 7 represent the high polarisation region at the northern limb. Further observations with different slit orientations were obtained for Jupiter and Uranus. Also Neptune and Saturn were observed in a similar way.

The data reduction turned out to be very demanding because the Wollaston introduces some dispersion perpendicular to the grism dispersion. This dispersion differs between the ordinary and extraordinary beams. Therefore, we had to align the two bent long-slit spectra to a precision of about a tenth of a pixel in the spatial direction in order to avoid spurious polarisation features due to misalignment. In the end we obtained two-dimensional long-slit spectropolarimetry providing for each wavelength disc profiles or centre-to-limb profiles for the intensity and polarisation.

First, we consider the spectropolarimetric signal of the limb. There are two general features which are present in all limb polarisation measurements of the giant planets (see Figure 7): the polarisation at the limb decreases to longer wavelengths; the polarisation is enhanced in the strong methane absorptions when compared to the adjacent higher flux regions. The overall decrease is due to the wavelength dependence of Rayleigh scattering, as already pointed out above. The enhanced polarisation in the methane bands can be explained with a two-layer model. An optically thin Rayleigh scattering layer producing the limb polarisation is located above a diffusely reflecting atmosphere or cloud layer, which reflects predominantly unpolarised light. Enhanced absorption in molecular bands efficiently reduces the unpolarised reflection of the lower layers resulting in a higher normalised polarisation for spectral regions with a low albedo.

There are significant quantitative differences in the polarisation properties of the

two planets. For example, the polarisation is very high at the poles of Jupiter, reaching values up to 9 % in the *V*-band and the maxima in the normalised polarisation spectrum are quite narrow, due to narrow methane absorption bands. For Uranus the limb polarisation is lower, and accordingly, the polarisation maxima associated with the broad absorption bands are broader. Nevertheless, the relative polarisation enhancements in the methane bands are much more pronounced in Uranus.

Our long-slit spectropolarimetry also provides the centre-to-limb profile for the intensity and polarisation for each wavelength covered by the spectrum. For example, for Uranus we see in the strong absorption bands that the enhanced limb polarisation correlates with a limb brightening of the reflected intensity (cf. Joos and Schmid 2007). Both limb brightening and limb polarisation probe the uppermost layers of the reflecting atmospheres. Long-slit spectropolarimetry seems to be an ideal tool to investigate the structure and particle properties for these layers.

Prospects

Our polarimetric observations of the giant planets with EFOSC2 at the 3.6-m telescope demonstrate that detailed observational studies of the limb polarisation effect are possible. We have shown that a rich palette of observational parameters can be deduced from such observations and they can be used to constrain the atmospheric structure and particle properties. Additional investigations, including the still-pending analysis of our Saturn data, will further clarify the diagnostic potential of limb polarisation. Currently, an important stumbling block is the lack of detailed model calculations of the limb polarisation for realistic planetary atmospheres. Although computer codes for such model calculations exist (e.g. Braak et al. 2002), they need to be run for simulations of Earth-bound limb polarisation measurements, as presented in this article. Without such calculations we can at present only extract qualitative properties from our observations. Model calculations could significantly improve this situation.

The comparison of our data with simple (analytic) models of Rayleigh scattering atmospheres indicates that the detected limb polarisation is compatible with expectations. In general, the limb polarisation is due to Rayleigh scattering particles. They are located high in the planetary atmosphere, above layers of diffusely reflecting gas or clouds. The limb polarisation is high if the Rayleigh scattering layer is optically thick or if the penetrating radiation is strongly absorbed in deeper layers, e.g. by methane.

For Uranus and Neptune, for which no polarimetry at large phase angles exist from space missions, we can extrapolate from the limb polarisation and estimate the expected disc integrated polarisation for phase angles near 90 degrees. We find that the polarisation must be high ($p > 20$ %) in the *R*-band. Such estimates are of interest for the interpretation of future polarimetric detections of extrasolar planets with the SPHERE VLT Planet Finder.

References

Beuzit J. L. et al. 2006, The Messenger 125, 29
Braak C. J. et al. 2002, Icarus 157, 401
Dollfus A. and Coffeen D. L. 1970, A&A 8, 251
Joos F. and Schmid H. M. 2007, A&A 463, 1201
Lyot B. 1929, Ann. Observ. Meudon 8
Schempp W. V. and Smith W. H. 1984, Icarus 77, 228
Schmid H. M. et al. 2006, IAU Coll 200, 165
Tinbergen J. 1996, Astronomical polarimetry, Cambridge University Press, 100
van de Hulst H. C. 1980, Multiple light scattering 2, Academic Press

In August 2007 the Uranus ring system was almost exactly edge-on to Earth, an event which only occurs every 42 years. The two images show the Uranus system in November 2002, with the rings well displayed, and in August 2007 when the rings were edge-on and no longer visible. The image of 2002 was taken with ISAAC on the VLT while the one of 2007 was taken with NACO and made use of adaptive optics, explaining the higher resolution. The NACO image is a false colour composite based on images taken at wavelengths of 1.2 and 1.6 microns. See ESO PR 37/07 for more details.

η Carinae 2009.0: One of the Most Remarkable Stars in the Sky

Christiaan Sterken[1]
Arnout van Genderen[2]
Gerd Weigelt[3]
Andreas Kaufer[4]

[1] Vrije Universiteit Brussel, Brussels, Belgium
[2] Leiden University Observatory, Leiden, the Netherlands
[3] Max-Planck-Institut für Radioastronomie, Bonn, Germany
[4] ESO

η Carinae is one of the most luminous and massive stars in the Galaxy. The star underwent a major eruption in 1838, followed by a second maximum a few decades later and a low-gradient brightening to the present. The central source of η Car is a highly-eccentric binary with a period of 5.54 years. The photometric and interferometric monitoring programmes with ESO telescopes are summarised. On the occasion of the forthcoming periastron passage in 2009.0, the star will be the target of intensive photometric, spectroscopic and interferometric monitoring from Chile and other southern observatories.

η Car: an extreme LBV

S Doradus variables – commonly known as Luminous Blue Variables (LBVs) – are evolved massive stars that undergo four major types of intrinsic photometric variability: microvariations, S Doradus phases, stochastic variability, and eruptions. For a detailed discussion of these types of variabilities, and for a very complete review of the state of affairs at the end of the second millennium, we refer to van Genderen (2001). These stars were labelled S Dor variables in the General Catalogue of Variable Stars on the basis of their behavioural similarities with the prototype star S Doradus. The Armagh 2000 definition (see ASP Conference Series 233, page 288) states: "S Doradus variables are hot, luminous stars that show photometric and/or spectroscopic variations like S Doradus and which have undergone – or possibly will undergo – an η Carinae or P Cygni-type outburst."
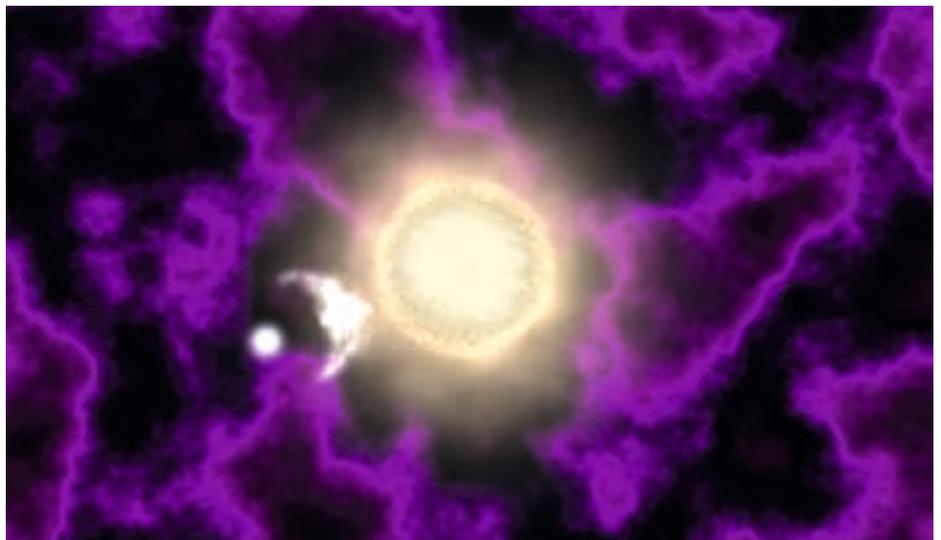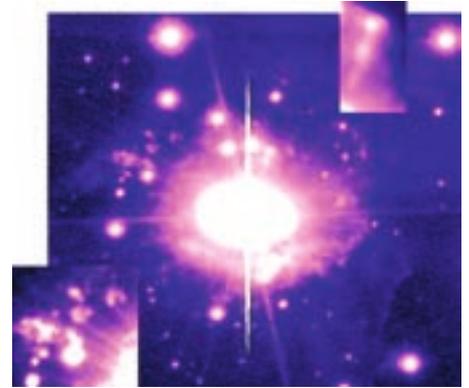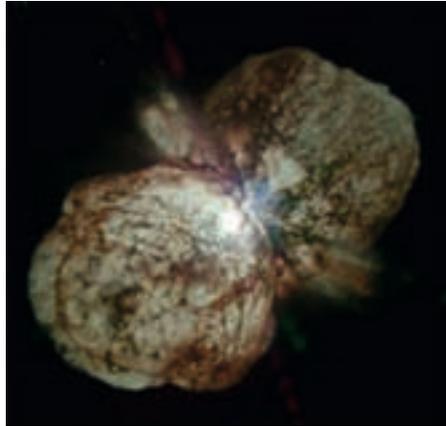
Figure 1: Images of η Carinae: HST image from Morse et al. (1998) (top left); VLT/UT1 First Light Photo No. 5, (top right); artist's impression of the binary configuration, courtesy S. Ivarsson (bottom).

P Cygni and η Carinae (Figure 1) are the historically best-documented cases of eruptive behaviour of S Dor stars. P Cygni was discovered by the Dutch chartmaker Willem Adriaensz Blaeu in 1600. The star faded, becoming invisible to the naked eye until 1658, when it flared again to a secondary maximum, followed by another return to oblivion and a subsequent very weak increase during a centuries-long brightening phase. η Carinae was observed in a similar eruption by John Herschel at the Cape in 1838, and the historical light curve (Figure 2) illustrates a pattern very similar to the light history of P Cygni: a major eruption (also called the Great Eruption), followed by a second maximum a few decades later, and then a steady low-gradient brightening during more than a century.

It became obvious that the central star of η Car is a true S Dor variable: the star migrates in the Hertzsprung-Russell diagram (at constant luminosity) so that brightness increases are accompanied by redder colours, and vice versa (see Figure 3 for a partial light curve and colour curve between 1992 and 2000). Such a migration cycle is called an S Doradus phase.

η Carinae is one of the most luminous and massive stars in the Galaxy, with a luminosity of $L \sim 5 \times 10^6 \, L_\odot$ and a mass of $M \sim 100 \, M_\odot$, a mass loss rate of $\dot{M} \sim 10^{-3.3} \, M_\odot$ for a distance of d = 2.3 kpc. The system consists of a bright hollow bipolar nebula, called the Homunculus, and an apparently much fainter (currently 2.4 mag) central star. In reality,
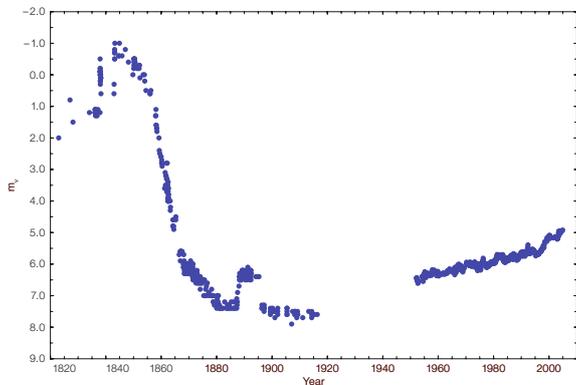
Figure 2: Visual light curve of η Carinae. The Great Eruption extended from 1837 to about 1856. Source: Frew (2004).
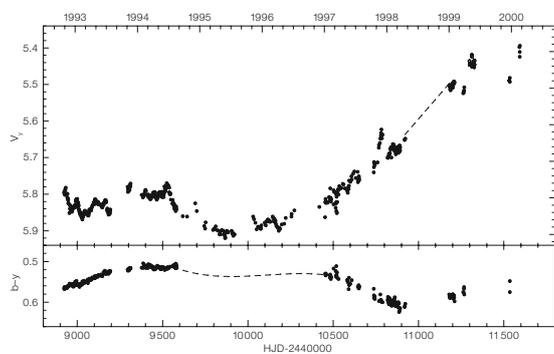
Figure 3: V_y (•, based on Geneva V and Strömgren y) light curve (left Y-axis) and b–y colour index of η Car, with an **approximate** indication of visual magnitude on the Johnson V-scale (right Y-axis). The dashed line in the light curve is based on broadband visual estimates and CCD photometry and fills in the seasonal gap in 1998; the dashed line in the colour curve is based on broadband colour data. ○ represent measurements through a V-filter. The narrow peak at HJD-24410800 coincides with the time of the 1997.9 event. Source: Sterken et al. (2000).

this central star is much brighter, but appears fainter due to nebular extinction. The Homunculus is now 16 arcsec across, which corresponds to 0.2 pc. During the S Dor-eruption phase in the 1840s, one peak reached an exceptional brightness of $M_{bol} \sim -14$ (van Genderen and Thé 1984).

η Car, a highly-eccentric binary

A variety of observations have suggested that the central source of η Car is a highly eccentric binary. Augusto Damineli first noticed the 5.5-year periodicity in the spectroscopic changes of this object (see Damineli et al. 2000 and Whitelock et al. 2004). The periastron separation is only ~ 2 AU, whereas at apastron the separation is ~ 20 AU, corresponding to ~ 9 milliarcseconds. Smith et al. (2004), on the basis of Hubble Telescope images, removed most doubts on the existence of a hot companion. Iping et al. (2005) state that the companion star was seen in the far-UV spectrum shortly before the 2003.5 event. The orbital parameters however are still a matter of debate. Figure 4 is a schematic drawing of the bi-

nary configuration (for the 2003.5 periastron passage, based on orientation B of Akashi et al. 2006).

Photometric monitoring at ESO

Photometric monitoring of the integrated brightness of η Car at ESO La Silla was started in 1979 when the 90-cm tele-

scope of the Leiden Southern Station (South Africa) was moved to Chile, where it became known as the Dutch Telescope. The telescope, equipped with the Walraven VBLUW system, was decommissioned in 1999. Between 1983 and 2000 the observations were then continued with the ESO 50-cm and Danish SAT telescopes in other photometric systems, mainly as part of the Long-Term Photometry of Variables (LTPV) Group (see The Messenger 33, 10), between 1994 and 1998 with the 70-cm Swiss Telescope, and later on with the Danish 1.54-m. The combination of the data, obtained over such a long time base of an extended emission-line object measured with different detectors and photometric systems, is a real challenge.

Between 1992 and 1994, when η Car was observed very intensively in the optical, microvariations typical for S Dor variables were identified with a quasi-period of 58.6 days. Note that oscillation periods of this order of magnitude are often present during the low-brightness stages of S Dor variables. Peculiar UV colour-variations indicate that part of the light variations must be due to non-stellar causes. For example, the flux of the relatively strong Balmer continuum glow (coming from the equatorial disc) shows a modulation of 0.1 mag in concert with the 5.5-year binary revolution, but is asymmetric with respect to the periastron passages. However, it is not unlikely that short-cycle oscillations in the Balmer-continuum radiation (200–400 days) are, in fact, caused
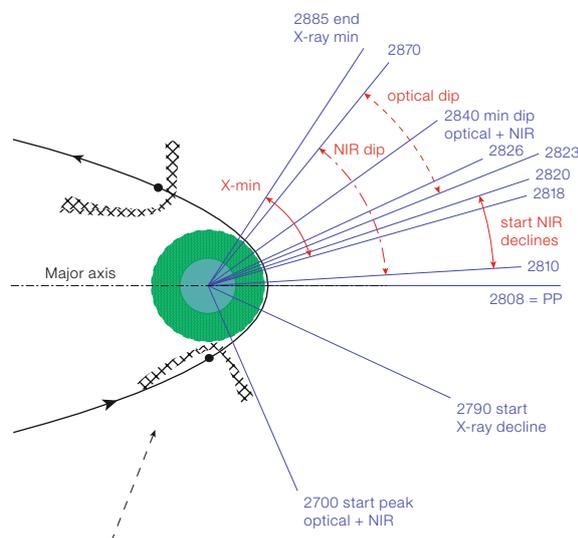
Figure 4: A schematic drawing of the binary system (for the 2003.5 periastron passage and e = 0.9, seen pole-on and not to scale, viewing angle ~ 45°) based on orientation B described by Akashi et al. (2006). Central circle and small dot: the primary and secondary, respectively. Large circle (dashed): the wind envelope of the primary. Hatched area: the shocked secondary wind. A number of features are indicated by time marks (JD-2450000).

by stellar oscillations. Some starlight va-
riability seems to be induced by tidal
forces of the secondary acting on the pri-
mary and its extended envelope, like the
long timescale optical and near-IR light
maxima coinciding with the periastron
passages and the shorter light peaks (van
Genderen et al. 2006, and references
therein).

All the observed variations are super-
imposed on a slow 'secular brightening'
(documented since 1935), partly due
to a decrease of self-extinction of the ex-
panding lobes. Note that in 1935 the
Homunculus was only 60% of its present
size. The near-IR also shows a secular
brightening, but it seems that a gradual
enhancement of circumstellar free-free
emission could be the major cause of the
brightening in the *JHK* bands (Whitelock
et al. 2004).

As the lobes of the Homunculus are near-
ly pure reflection nebulae, and have large
dimensions, the important question was
raised whether the observed variations
are in fact a mix of genuine variations of
the core and time-delayed reflected and
scattered light (against the inner and
outer walls of the lobes), and of time-de-
layed ionisation and recombination proc-
esses in the equatorial plane. Such light-
time effects can amount to weeks and
months. Consequently, if these time-de-
lay effects would be quantitatively sub-
stantial, one would inevitably obtain false
timescales and amplitudes for the ob-
served variations. The much steeper
brightening of the central star as seen by
the HST in 1998 and 1999 compared to
that of the Homunculus (Figure 5), noted
by the HST Treasury Program Team, led
them to conclude that serious smearing-
out effects do exist. Consequently, there
arose the general feeling that ground-
based integrated optical photometry of
the Homunculus is an unreliable means
for studying the variability of the central
star, and that the only valid photometry
is photometry from space-borne tele-
scopes. Figure 5 shows the combination
of schematic light curves from the ground
and HST data obtained between 1998
and 2003. Apart from the above-men-
tioned steeper brightening of the central
star in 1998 and 1999, due to decreas-
ing extinction in front of the core (with an
anomalous extinction law R ~ 5.3; van
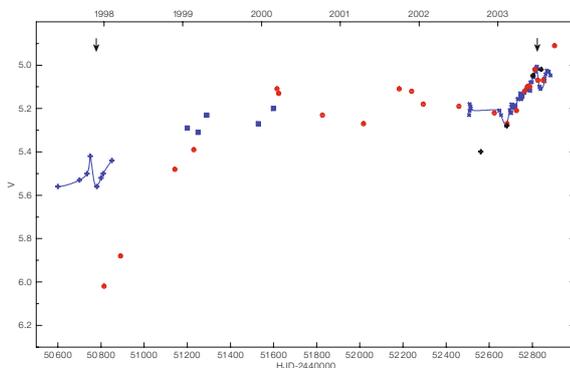
Figure 5: Schematic light curves be-
tween 1997 and 2004. The *V* scale
is close to the *UBV* system. The arrows
at the top indicate the computed
events (or periastron passages). The
short full curves on the left and right
and the blue squares are for the whole
Homunculus (van Genderen et al.
2006). For the central region, points
refer to HST data (aperture 0.1″): red
symbols are the broadband *V* daily av-
erages, +'s are the narrowband *V* daily
averages from Martin et al. (2004),
shifted in magnitude for a good match
between their 2002.8–2003.6 curve
and the short full curve to the right.

Genderen et al. 2006), most data points
of the central star fit the light curve
and show that the Homunculus mimics
the light variations originating in the core
quite well. Thus, light-time effects and
any other smearing effects are negligible,
although substantial time delay effects
exist between parts of the Homunculus
and individual clouds inside the Homun-
culus and the central region.

Interferometric monitoring at ESO

One of the keys to understanding η Cari-
nae is to resolve its central region using
ESO's Very Large Telescope Interferom-
eter (VLTI). The AMBER instrument (As-
tronomical Multi-BEam Recombiner) at
the VLTI combines the near-infrared light
collected by three VLT Unit Telescopes
to attain an angular resolution 16 times
higher than the resolution of each of the
8.2-m telescopes alone (Malbet et al.
2007). Therefore, VLTI/AMBER measure-
ments can unveil details about the out-
flowing stellar wind in the innermost stel-
lar environment. Using AMBER, it was
possible, for the first time, to study η Car
with the fascinating spatial resolution
of 5 milliarcseconds (11 AU) *and the high
spectral resolution of 12 000* (Weigelt et
al. 2007). In η Car's innermost region, the
observations are dominated by the ex-
tremely dense stellar wind, which totally
obscures the central star. It was possible
to resolve η Car's optically thick wind re-
gion and to measure its diameter of 4.0 ±
0.2 milliarcseconds (Gaussian FWHM, fit
range 28–89 m baseline length), in good
agreement with previous VLTI/VINCI ob-
servations.

The AMBER observations are also in
good agreement with the NLTE radiative

transfer model from Hillier et al. (2001). In
the continuum, an elongation of the wind
zone along a position angle of 120 ± 15
degrees and with a projected axis ratio of
1.18 ± 0.10 was found. The AMBER ob-
servations show that the extensions of
the regions where the continuum radia-
tion, the Brγ 2.166 μm and HeI 2.059 μm
line emission originate are remarkably
different. While the size of the dense stel-
lar wind in the continuum is only 10 AU,
AMBER measured an extension that
is twice as large for the line-emitting re-
gions. The non-zero differential and clo-
sure phases measured within the Brγ line
can be explained by a simple geometric
model of an inclined, latitude-dependent
wind zone (see Figure 6). The AMBER
observations support theoretical models
of anisotropic winds from fast-rotating,
luminous hot stars with enhanced high-
velocity mass loss near the polar regions.

HST STIS observations show that the
HeI lines are strongly variable and blue-
shifted throughout most of the 5.54-year
variability period. These observations
cannot be explained in the context of a
single-star wind model. It now appears
likely that a large fraction of the HeI line
emission originates in a wind-wind inter-
action zone in the binary system. The
blue-shift of the HeI emission line can be
explained if this line is produced in the
portion of the primary wind which is flow-
ing towards the observer. Furthermore,
our AMBER observations show that there
is an obvious difference between the
observed HeI visibility profiles and the
model predictions. This discrepancy can
also be explained by additional HeI emis-
sion from the wind-wind interaction zone
between the binary components and by
the primary's ionised wind zone caused
by the secondary's UV light. If this model
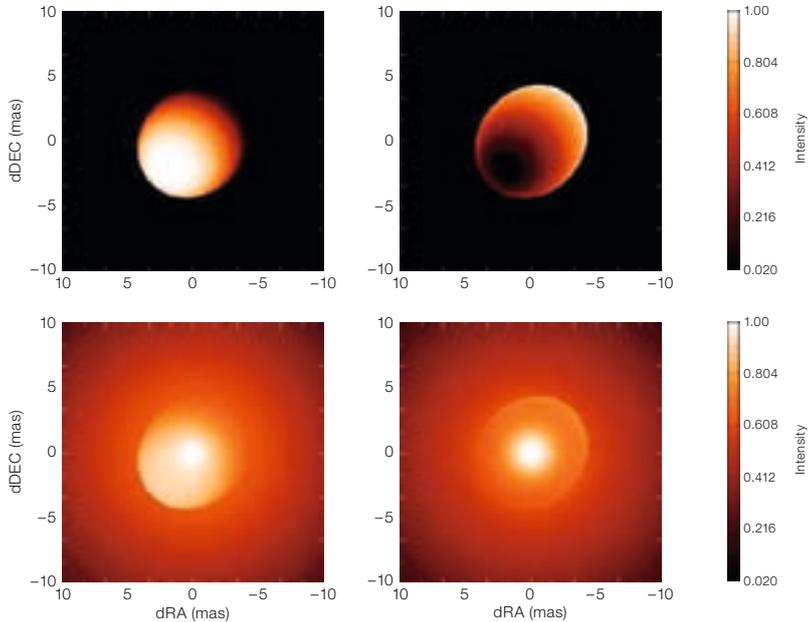
Figure 6: The upper row shows the brightness distribution of the modelled aspheric wind component of η Car in the blue- and red-shifted wings of the Doppler-broadened Brγ line. In the blue-shifted line wing, the south pole region of the wind zone is dominant, whereas in the red-shifted wing, the light near the north pole is dominant (the north pole itself is not visible since it is turned away from us). The pair of figures below show the total brightness distribution after adding the contributions from the two spherical constituents of the model derived from VLTI/AMBER observations (Weigelt et al. 2007).

is correct, the two-dimensional, asymmetrical intensity distribution of the orbiting HeI emission region will be strongly variable during the 5.5-year orbital period and offset from the primary star by a few milliarcseconds. The detection of this moving HeI zone is one of the goals of our future AMBER observations. Finally, this binary model can also explain the periodic variation of the three ejected speckle objects at separations between 0.1 and 0.3 arcsec from the central object. The UV flux of a hot companion is necessary to explain the excitation of the speckle objects at most orbital phases. However, during periastron passage of the hot companion, its ionising UV radiation is blocked by the dense primary wind for a few months.

The upcoming 2009.0 event

Numerous theories and explanations for the η Car phenomena were put forward, rejected and replaced by others. The outstanding problems of this extremely massive eccentric binary system raised in the course of the many observing campaigns covering the complete electromagnetic spectrum from X-ray to radio wavelengths, have still resulted in too few concrete solutions that lead to a full understanding of its nature. All these riddles are prime motives for continuing the photometric monitoring from La Silla as well

as the interferometric and spectroscopic observing campaigns with the VLT telescopes.

η Car will be a prime target during its forthcoming periastron passage in 2009.0, where it will be important to monitor the peculiar optical features, viz. the light-peak event preceding the periastron passage, the following asymmetric eclipse-like dip, and subsequently the recovery of the brightness – perhaps surpassing the previous peak. Repeated near-infrared spectro-interferometric observations will allow us to monitor morphological changes over η Car's spectroscopic 5.5-year period, possibly revealing the motion and structural variation of the orbiting wind-wind collision zone, as predicted by the η Car binary model. Furthermore, future AMBER observations with higher accuracy might be sensitive enough to directly detect the hot companion.

Afterword

η Carinae is a most important object for study (as also summarised by Richichi and Paresce 2003) and can really be considered as the Rosetta stone in studies of
– the formation and evolution of extremely massive stars

– dynamical and chemical interactions with the environment
– stellar instabilities in the outer envelopes of single stars
– periodic tidal forcing by a companion and the formation of asymmetric nebulosity
– the relation of extremely massive stars to peculiar supernovae and hypernovae.

Ground-based monitoring has proven to be as useful as space-borne observations, but possesses the unmistakable advantage of providing data over a long time-baseline at modest cost. As such, the ESO Observatories in Chile will play a key role during the coming periastron passage in 2009.0 in the sense that the subsequent event to occur in July 2014.5 will be poorly observable. By the time the next optimally observable periastron passage occurs in 2020.0, the base line of observational technology will have completely changed, and we should have full use of the the ELT giant facility that will then be operational.

References

Akashi M. et al. 2006, MNRAS 368, 1706
Damineli A. et al. 2000, ApJ 528, L101
Frew D. J. 2004, JAD 10, 6
Hillier D. J. et al. 2006, ApJ 642, 1098
Iping R. C. et al. 2005, ApJ 633, L37
Malbet F. et al. 2007, The Messenger 127, 33
Martin J. C. et al. 2004, AJ 127, 2352
Morse J. A. et al. 1998, AJ 116, 2443
Richichi A. and Paresce F. 2003,
    The Messenger 114, 26
Smith N. et al. 2004, ApJ 610, L105
Sterken C. et al. 2000, in "A Decade of HST
    Science", 89
van Genderen A. M. and Thé P. S. 1984,
    Space Sc. Rev. 39, 317
van Genderen A. M. 2001, A&A 366, 508
van Genderen A. M. et al. 2006, JAD 12, 3
Weigelt G. et al. 2007, A&A 464, 87
Whitelock P. A. et al. 2004, MNRAS 352, 447

The Monitor Project: Tracking the Evolution of Low-Mass and Pre-Main-Sequence Stars

Suzanne Aigrain[1]
Jonathan Irwin[2]
Leslie Hebb[3]
Simon Hodgkin[4]
Adam Miller[5]
Estelle Moraux[6]
Keivan Stassun[7]

[1] School of Physics, University of Exeter, United Kingdom
[2] Harvard-Smithsonian Center for Astrophysics, Cambridge, Massachusetts, USA
[3] School of Physics and Astronomy, University of St Andrews, United Kingdom
[4] Institute of Astronomy, University of Cambridge, United Kingdom
[5] Astronomy Department, University of California at Berkeley, California, USA
[6] Laboratoire d'Astrophysique de Grenoble, France
[7] Department of Physics and Astronomy, Vanderbilt University, Nashville, Tennessee, USA

The Monitor project is a large-scale programme of photometric and spectroscopic monitoring of young open clusters using telescopes at ESO and other observatories. Its primary goal is to detect and characterise new low-mass eclipsing binaries, and the first three detected systems are discussed here. We derive the masses and radii of the components of each system directly from the light and radial velocity curves, and compare them to the predictions of commonly used theoretical evolutionary models of low-mass stars.

Eclipsing binaries as calibrators of stellar evolution

Well-observed detached eclipsing binaries (EBs) are extremely valuable systems, because it is possible to derive accurate (to a few per cent) model-independent estimates of the individual masses and radii, the temperature ratio directly from the light curve and radial velocity (RV) curves of each component. This is particularly true in open clusters, where the age and chemical composition of the stars is well known, and even more so in young clusters and star-forming regions, where

one probes: (1) one probes a phase of rapid stellar evolution, as highlighted by Figure 1 in the mass-radius plane, and (2) low-mass systems, which are of particular interest because the physics and chemistry of their convective interiors and cool atmospheres are complex to model, are still relatively bright. Yet, pre-2004, there were no sub-solar pre-main-sequence EBs known, and very few on the main sequence.

This was the principal motivation for starting the Monitor project[1], a systematic survey for low-mass EBs in nine young (less than 200 Myr), rich and relatively nearby star-forming regions and open clusters. The survey proceeds in two phases, starting with intensive *I*-band photometric monitoring to detect candidate eclipsing systems, followed by multi-epoch spectroscopic observations to measure radial velocities, and hence derive component masses and determine if the systems belong to the clusters or are older field objects. A strong additional motivation was the possibility of detecting young transiting planets, which would give important insights into planet formation timescales and the initial conditions for giant planet evolution.

Cluster photometry

The full target list and detail of the photometric observations are given in Aigrain et al. (2007). For this part of the project, we use 2–4-m telescopes equipped with wide-field optical imagers. This enables us to efficiently monitor large fractions of

[1] http://www.ast.cam.ac.uk/research/monitor/

each cluster, while ensuring both the photometric precision and the time sampling necessary to detect eclipses down to mid-M spectral types. Typically, each cluster must be observed for about 100 hours in total. A major component of the photometric observations was carried out as part of an ESO Large Programme[2] using the Wide Field Imager (WFI) on the 2.2-m ESO/MPI telescope between June 2005 and May 2006.

All the Monitor photometric data are reduced automatically using a uniform procedure, described in detail in Irwin et al. (2007a). Briefly, we first carry out all the standard CCD data reduction steps and astrometric and photometric calibration using the Cambridge Astronomical Survey Unit (CASU) pipeline. We then perform simple aperture photometry to generate light curves, but with a number of precautions designed to maximise photometric precision and minimise correlated systematic effects, often termed red noise, which are known to have a major impact on the yield of planetary transit surveys (Pont et al. 2006), and, by extension, mixed eclipse and transit surveys such as Monitor. The resulting precision is illustrated in Figure 2 for the WFI observations of NGC 2547. We achieve sub-per cent relative photometry over four magnitudes or more from the saturation limit for all Monitor clusters. The noise level over a typical eclipse timescale of 2.5 hours varies between 1.5 and 3 mmag (depending on the instrument

[2] Advanced data products (reduced images and source catalogues) from the first run of this programme (LP 175.C-0685) have recently been made available via the ESO archive.
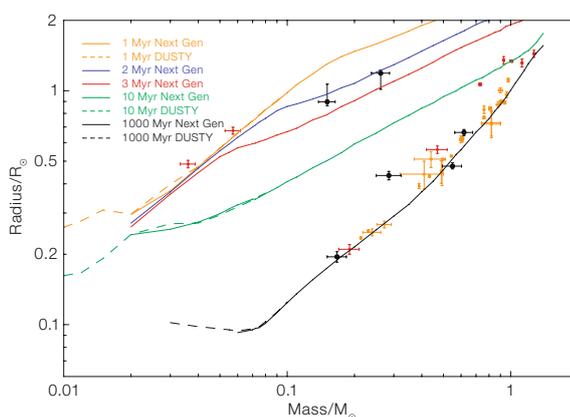
Figure 1: Age-mass-radius relation for low-mass stars and brown dwarfs in eclipsing binaries. Yellow and red symbols represent field and pre-main-sequence systems from the literature, respectively (see Irwin et al. 2007b for a full reference list). The stellar components of the three new systems detected by Monitor are shown in black. The solid and dashed lines show the NextGen and DUSTY isochrones of the Lyon group for 1, 2, 3, 10 and 1000 Myr (yellow, blue, red, green and black respectively). The black isochrone essentially corresponds to the main-sequence relation.
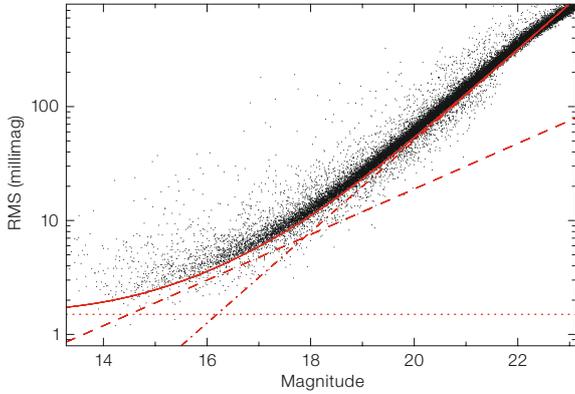
Figure 2: Photometric precision *versus I*-band magnitude for the WFI observations of NGC 2547 (100 h in service mode spanning eight months from October 2005 to May 2006). The dashed, dotted, dash-dot and solid lines represent the source photon noise, sky photon noise, a 1.5 mmag constant added to account for systematics, and the final expected precision (quadrature sum of the other three lines) respectively.

and observing conditions) for the brightest objects in each cluster.

For each cluster, we also take long *V*-band exposures which, combined with a stacked selection of the best *I*-band images, enables us to construct a deep colour-magnitude diagram (CMD). We identify likely members of the cluster as those lying close to an empirically defined cluster sequence on this CMD, allowing for the fact that cluster binaries are overluminous for their colour, and for the increased uncertainties towards the faint end. This selection results in candidate membership lists with a global estimated level of contamination by field stars varying between 30 and 80 %, depending on whether the cluster lies in the Galactic plane.

The light curves of candidate members are then systematically searched for eclipses, using a combination of visual examination and an automatic procedure (Miller et al. submitted) involving a pre-filtering step to remove the significant spot-induced variability of our young, active targets where possible, followed by an automated box-shaped eclipse search algorithm. In this fashion, we have so far identified 48 high quality EB candidates, ~ 15 % of which have depths compatible with a planetary companion.

Table 1: Derived primary mass (M$_1$), secondary mass (M$_2$), primary radius (R$_1$), secondary radius (R$_2$) and period (P) for three newly-discovered eclipsing binaries.

Spectroscopic follow-up

Once EB candidates have been identified, multi-epoch medium- to high-resolution spectroscopy is needed to determine RV orbits for both components, and thus derive their masses and determine (by comparing the systemic velocity to that of the cluster) whether the detected systems are really cluster members or older field systems projected onto the cluster. The latter can still be of interest, as our CMD cut typically implies they are low-mass systems.

Initially, we opted for a two-step, risk-minimising strategy, starting with medium-resolution (R ~ 10 000) spectroscopy on 4-m-class telescopes, including EMMI on the NTT and ISIS on the William Herschel Telescope (WHT), to weed out obvious non-members and derive orbits for the systems with higher RV amplitudes and a more favourable flux contrast between primary and secondary. For the remaining systems, we then used higher-resolution (R ~ 20 000 to 50 000) observations on 8-m-class telescopes, including FLAMES on the VLT and Phoenix on Gemini-South, to resolve the two components and/or detect lower amplitude RV variations. Since virtually all of the candidates we have followed-up so far with sufficient precision have turned out to be binaries, in future we will concentrate on VLT/FLAMES observations for all candidates, the multiplex capability of FLAMES allowing us to exploit optimally the spatial concentration of our candidates. In all cases, RVs are derived by cross-correlation with simultaneously observed RV standards or model spectra of appropriate spectral type.

Three new low-mass eclipsing binary systems

The spectroscopic follow-up to date has enabled us to derive partial orbits for over a dozen systems in six different cluster fields, and full solutions for three previously unknown systems. JW380 (Irwin et al. 2007b) is a member of the ~ 1 Myr old Orion Nebula Cluster (ONC). The other two are likely field systems (as indicated by their systemic velocities and confirmed by the relatively compact radii derived for their components) projected onto the fields of NGC 2362 and NGC 2547 respectively, and are the subject of publications in preparation. For simplicity, they are referred to, from now on, as EB2 and EB3.

The RV data for each system were modelled assuming Keplerian orbits (see Figure 3). The period and phase were fixed at the values determined from the light curve. The best-fit eccentricities are zero within the uncertainties; the fits shown therefore assume circular orbits. These fits were used to derive mass ratios and a minimum total mass (the RV data alone does not yield the inclination of the orbit). The *I*-band light curves were modelled separately (see Figure 4) using the JKTE-BOP[3] code after manual removal of most of the out-of-eclipse variability (assigned to surface spots) to derive inclinations and individual radii. Estimates of the main system parameters are summarised in Table 1, but the reader is referred to the relevant individual publications for more details.

When these systems are placed on a mass-radius diagram (Figure 1) and compared with other known systems and theoretical isochrones, it becomes apparent that each probes a distinct, but so far ill-constrained mass range. JW380 is one of only a handful of sub-solar pre-main-sequence systems, and one of the two youngest (both are in the ONC). At M$_1$ =

[3] *http://www.astro.keele.ac.uk/~jkt/codes/jktebop.html*

Object	M$_1$ (M$_\odot$)	M$_2$ (M$_\odot$)	R$_1$ (R$_\odot$)	R$_2$ (R$_\odot$)	P (d)
JW 380	0.262 ± 0.025	0.151 ± 0.013	1.189 $^{+0.039}_{-0.175}$	0.897 $^{+0.170}_{-0.034}$	5.29918
EB2	0.285 ± 0.038	0.167 ± 0.017	0.434 ± 0.018	0.195 ± 0.010	0.71362
EB3	0.618 ± 0.018	0.549 ± 0.054	0.663 ± 0.020	0.476 ± 0.016	0.58530

0.26 $M_\odot$ and $M_2 = 0.15$ $M_\odot$, it is also one of the lowest-mass EBs known. The 2 and 3 Myr NextGen isochrones of the Lyon group are in reasonable agreement with the measured parameters of its components (although the canonical age for the ONC is 1 Myr, a significant age spread is thought to be present in the region, so an age of 2 or 3 Myr is not inconceivable for JW 380). More photometric and spectroscopic observations of this system are planned to better constrain the component masses, attempt to derive their temperatures, and refine the radii by sampling the out-of-eclipse variations more tightly.

EB2 and EB3, with component masses of 0.29 $M_\odot$ and 0.17 $M_\odot$, and 0.62 $M_\odot$ and 0.25 $M_\odot$ respectively, fill gaps in the existing empirical main-sequence relation. Given our preliminary radius estimates, the main-sequence isochrone fits the secondaries of both field systems well, but the primaries appear significantly larger than expected. In other words, for a given luminosity, these primaries appear too cool for their mass and age. This phenomenon has already been seen in other systems, and the young eclipsing binary brown dwarf 2MASS J05352184-0546085 (Stassun et al. 2006), whose primary is cooler than the secondary, may be an extreme example. It is not yet clear what causes this effect, but it could be a consequence of the high magnetic fields expected in the rapidly rotating components of close binaries (Chabrier et al. 2007). These fields might inhibit convection in the interior, and hence heat transport to the surface of the star, and do so more strongly for the more massive of the two stars. Additional photometric observations are planned for EB2 and EB3 to refine the radius determinations.

Additional science from Monitor

High-cadence, high-precision time-series photometry of large samples of young stars of known age allows for a wealth of ancillary science going far beyond the sole search for eclipsing binary systems. In particular, we have so far used Monitor data in four of our target clusters (M34, NGC 2516, NGC 2547 and NGC 2362) to identify over 1500 new photometric rotation periods for low-mass stars. Com-
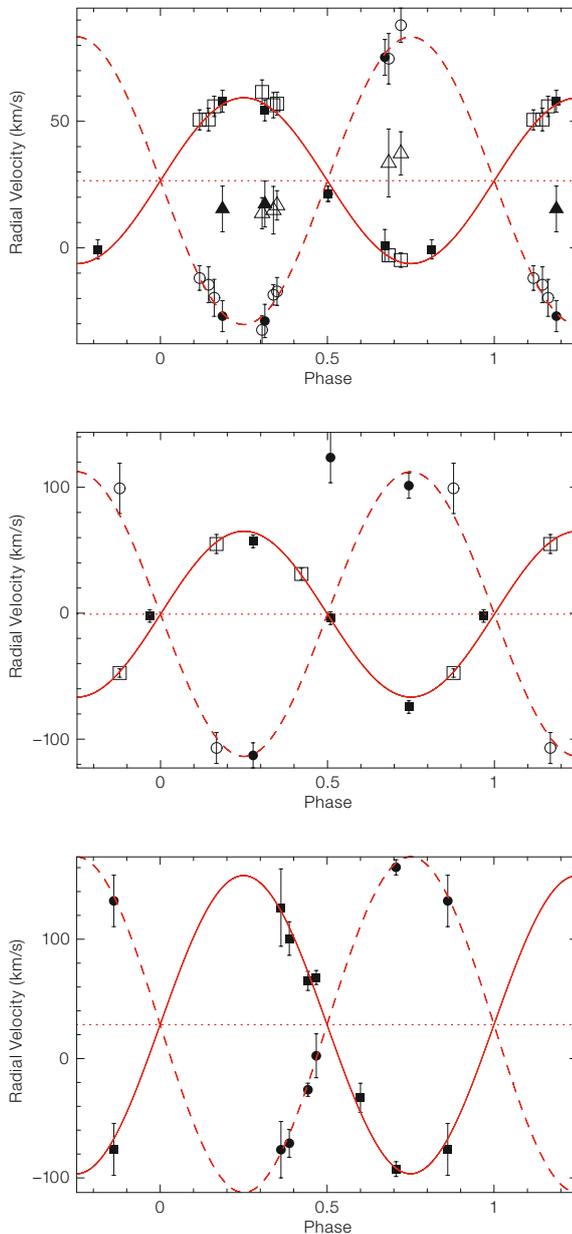
Figure 3: RV data and best-fit model for the three new Monitor eclipsing binaries. Filled symbols represent VLT/FLAMES data for JW 380 (top), NTT/EMMI data for EB2 (centre) and EB3 (bottom); hollow symbols data from Gemini/Phoenix and ISIS/WHT respectively. Velocities for the primary, secondary and (if present) tertiary of the systems are shown as squares, circles and triangles respectively. The solid, dashed and dotted red lines show the best-fit orbits for the primary and secondary and the systemic velocity respectively.

bined with existing data from the literature in other clusters, these data now constitute a well-populated age sequence, from the birth-line to the start of main-sequence evolution. They have detailed implications for models of the angular-momentum evolution of low-mass stars, which is intrinsically linked to the evolution of their internal structure and, in the initial evolutionary phases, coupling with their circumstellar discs (for a review of the Monitor rotation results, see Bouvier 2007 and references therein).

Because of the favourable radius ratio for low-mass primaries, it is also possible that some of our remaining candidate eclipsing systems have secondaries in the planetary mass range. If so, they would provide the first radius measurement(s) for young, close-in giant planet(s). Already, we have used observations of NGC 2362 to derive statistically significant upper limits on the incidence of such planets at 5 Myr (Miller et al. in prep.).

Future prospects

The follow-up of our candidates is ongoing, with upcoming FLAMES observations of the ONC and three other clusters. We are also using these observations to carry out systematic spectroscopic binary searches in the clusters, in order to measure (near-)primordial close binary fractions and mass ratio distributions for low-mass stars, and to investigate the connection between rotation, accretion and binarity.

References

Aigrain S. et al. 2007, MNRAS 375, 29
Chabrier G., Gallardo J. and Baraffe I. 2007, A&A 472, L17
Bouvier J. 2007, in IAUS 243: Star-Disk interaction in young stars, eds. J. B. and L. Appenzeller, 231
Irwin J. et al. 2007a, MNRAS 375, 1449
Irwin J. et al. 2007b, MNRAS 380, 541
Pont F., Zucker S. and Mazeh T. 2006, MNRAS 373, 231
Stassun K. G., Mathieu R. D. and Valenti J. A. 2007, ApJ 664, 1154
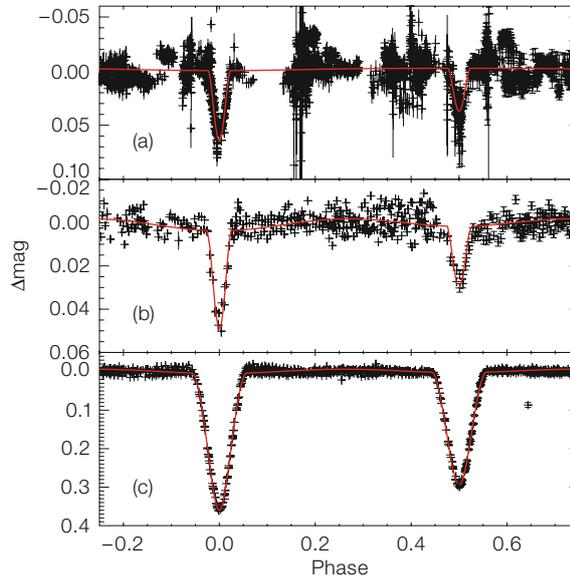
Figure 4: I-band relative light curve and JKTEBOP best-fit model for the three new eclipsing binary systems: (a) JW 380 (ONC) I = 13.82, data from the Wide Field Camera on the 2.4-m Isaac Newton telescope; (b) eclipsing binary in the field of NGC 2362, I = 15.6, data from MosaicII on the CTIO Blanco 4-m telescope; (c) eclipsing binary in the field of NGC 2547, I = 15.5, data from WFI on the ESO/MPI 2.2-m telescope.

Colour-composite image of the spiral galaxy NGC 1288 in which the recent Type Ia supernova SN 2006dr was discovered. The image is based on exposures with the FORS1 instrument through five filters (B, V, R, I and H-alpha) for a total exposure time of 5 minutes, taken in July 2006. The supernova is the bright object visible to the left of the centre of the galaxy. The image size is 6.0 × 5.7 arcmin and north is up, east to the left. Image processing by Henri Boffin (ESO).

Star-Forming Nuclear Rings in Spiral Galaxies

Jesús Falcón-Barroso[1]
Torsten Böker[1]
Eva Schinnerer[2]
Johan H. Knapen[3]
Stuart Ryder[4]

[1] European Space Agency, Noordwijk, the Netherlands,
[2] Max-Planck-Institut für Astronomie, Heidelberg, Germany
[3] Instituto de Astrofísica de Canarias, Tenerife, Spain
[4] Anglo-Australian Observatory, Epping, Australia

The study of gas transport to the inner regions of galaxies is a fundamental aspect in our understanding of the way galaxies evolve. In this context, star-forming nuclear rings are key features as they contain large amounts of gas and are the sites where a significant fraction of the current star formation is taking place in their host galaxies. Here we present some results from a study of how star formation progresses along nuclear star-forming rings in five spiral galaxies, based on near-infrared SIN-FONI integral-field observations at the VLT.

Nuclear Rings

The basic picture of how nuclear rings form is well established, both from a theoretical and an observational perspective (see Buta and Combes 1996 for a review). They are usually associated with the interplay between bar-driven gas inflow and the bar resonances. Perturbations in the gravitational potential, nearly always due to the presence of a stellar bar or oval distortion, causes the gas to loose angular momentum and spiral in towards the nucleus. Because of its dissipative nature, gas accumulates at the radii where the stellar orbits experience dynamical resonances with the rotating bar potential. In the case of the nuclear rings discussed here, this gas accumulation typically happens at the so-called Inner Lindblad resonance. When observed in more detail, the gas is found to enter the ring via two tightly wound spiral arms or dust lanes. At the contact points between the dust lanes and the ring, the gas be-

comes less turbulent, and enters almost circular orbits, which delineate the ring. While it is clear that there is abundant (molecular) gas throughout the ring, there has been an on-going debate about how and where star formation occurs.

Integral-field observations of nuclear rings

Integral-field spectroscopy allows the simultaneous measurement of a large number of spectra over a two-dimensional field of view. We used SINFONI H- and K-band spectroscopy to study the two-dimensional morphology and kinematics of star-forming nuclear rings in five spiral galaxies drawn from a large sample of galaxies observed in Hα by Knapen et al. (2006). In Figure 1 we show a colour-composite image of one of the galaxies in our sample (NGC 613), highlighting the main structural features and in particular the nuclear ring discussed in the following.

Figure 2 shows the intensity and velocity maps for some of the most prominent spectral features in NGC 613. The Brγ emission shows a clearly defined ring structure, composed of seven almost regularly spaced bright clumps that are the sites of current massive star formation. These 'hot spots' are brightest along the southern half of the ring, while the northern half shows a well-defined 'gap' at PA 30° which is also evident in the [Fe II] emission map. This direction agrees

well with that of the radio jet found by Hummel et al. (1987). It thus appears that a mechanical outflow from the central active black hole has disturbed the ring morphology.

H_2 emission is also apparent in the nuclear ring, but is strongest in the nucleus. The H_2 in the ring is not composed of distinct hot spots like the Brγ emission, but is more smoothly distributed. There are two emission peaks, found on opposite sides of the ring, at approximate PAs of 90° and 270°. If the H_2 emission in the ring of NGC 613 were caused purely by UV radiation, one might expect a spatial correspondence between H_2 and the ionised gas traced by Brγ and/or He I. However, many of the Brγ hot spots are not bright in H_2. Therefore, the H_2 emission probably contains a non-negligible contribution from shock-heated molecular gas.

The nuclear spectrum shown in the bottom panel of Figure 2 highlights the presence of molecular emission (H_2) and the complete absence of hydrogen recombination lines (e.g. Brγ). In contrast, the nuclear spectra of the remaining galaxies in our sample (not shown here) appear rather quiescent, i.e. their spectra are devoid of any line emission. This is not unexpected in a scenario in which gas accumulates at the nucleus over time until a critical density is reached. Star formation is then triggered, but can continue only until the gas supply is consumed or the energetic outflow from supernova explo-

Bar | **Nuclear Ring**

Spiral Arms
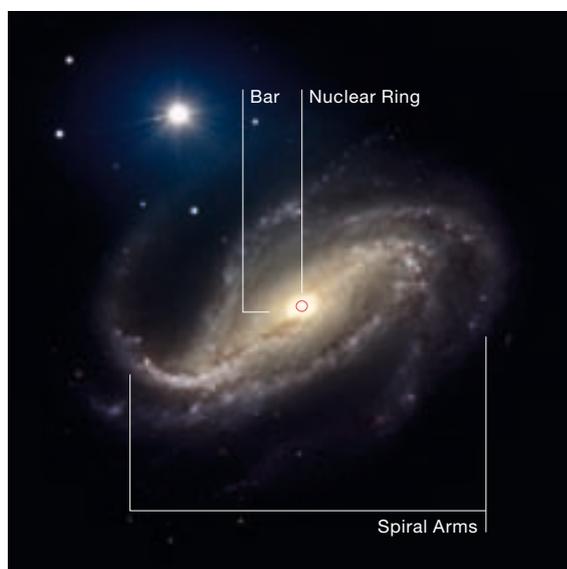
Figure 1: Colour-composite image of NGC 613 taken with FORS1 and FORS2 instruments (ESO Press Photo 33a/03). Labels highlight some of the main morphological features.
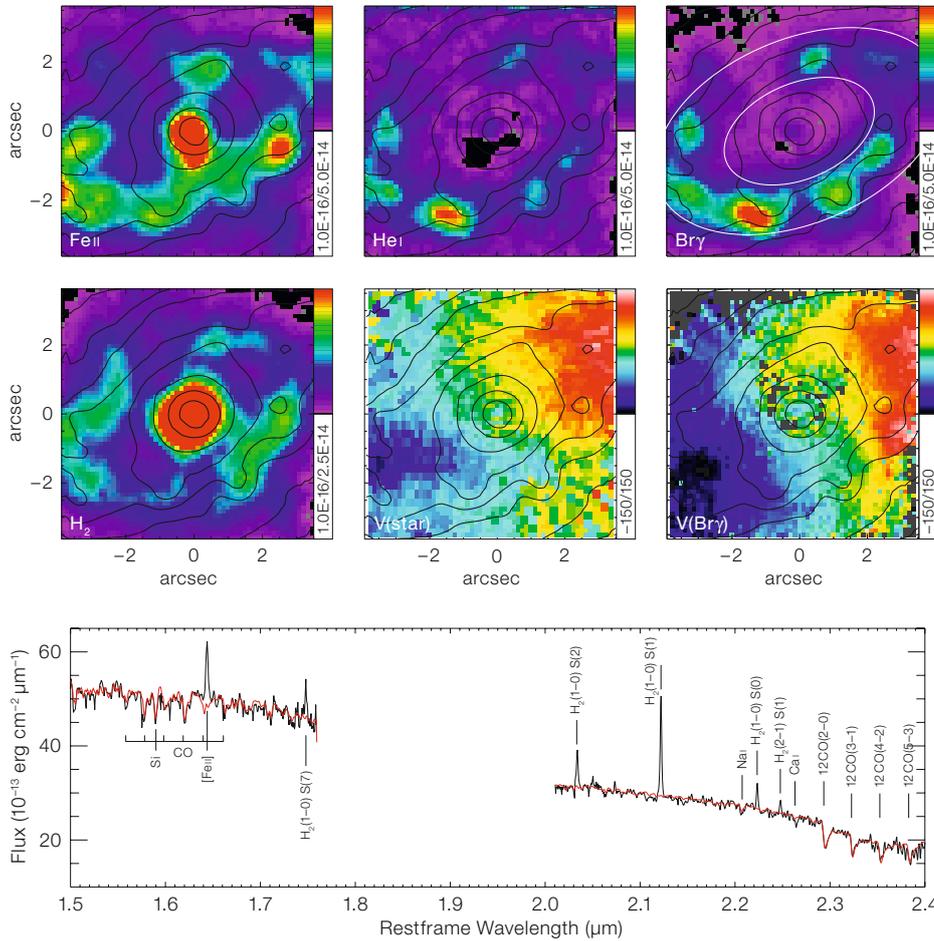
Figure 2: SINFONI near-infrared integral-field spectroscopy of NGC 613. Top row shows the morphology in the [FeII], HeI and Brackett-γ emission; lower row the H_2 emission morphology, the stellar kinematics (V(star)) and the Brackett-γ kinematics (V(Brγ)) of the nuclear ring in this galaxy. The black contours delineate the K-band light measured from the SINFONI observations while ellipses in the Brγ map delimit the extension of the ring. Bottom panel shows the nuclear spectrum of NGC 613 with the main spectral features highlighted.

sions disrupts and/or expels the gas, thus 'quenching' the star formation. This scenario is entirely consistent with observations, at least for late-type spirals: only about 10 % of nuclear star clusters currently show emission lines, although most of them harbour a young stellar population of less than 100 Myr old (Rossa et al. 2006). This can naturally be explained if star formation in galactic nuclei is episodic in nature, with a duty cycle of about 10 %.

In Figure 2 we also show the stellar and ionised-gas kinematics for NGC 613. The stellar velocity field appears rather regular, despite the intense star formation within the nuclear ring. Because Brγ is generally the most prominent emission line in our data, we used it to make an estimate of the ionised gas kinematics. In all galaxies of our sample, the velocity gradients within the nuclear rings are smooth and the ionised gas has the same sense of rotation as the stars.

The ages of the stellar clusters

Measuring the relative ages of the different stellar clusters (i.e. hot spots) along the ring is a difficult task. The orbital time-scales in the ring are short (e.g. a few tens of Myr). In order to perform the age dating, it is therefore imperative that one uses tracers that are sensitive to these time-scales. The most widely used diagnostic for this purpose is the Hα emission line. There are several reasons why this line is a popular choice. First, it is an optical emission line that can easily be measured. Second, its equivalent width (EW) decreases almost monotonically with time for an instantaneous burst allowing one to determine the evolutionary stage of a cluster from the EW value alone. The use of this emission line, however, is limited to clusters in the age range between 3 and 10 Myr, and therefore any inferred age differences have to be small (few Myr). Below 3 Myr, the EW of the Hα is almost constant, and above 10 Myr the

value is well below typical detection limits (~ 1 Å).

An alternative approach is to make use of several spectral lines, whose emission peaks at different cluster ages. In our case, we use the flux of three emission lines that are prominent in the NIR spectra of the star-forming regions in our sample of galaxies: HeI, Brγ, and [FeII]. Under the assumption that the underlying bulge/disc can be considered quiescent, and that most of the emission is produced in the ring itself, line fluxes are a better probe than the EWs. The reason is that EWs require an accurate knowledge of the continuum emission, not only for the hot spot itself, but also for the underlying bulge and/or disc, which is very hard to measure. The HeI and Brγ lines are both produced by photoionisation in the vicinity of hot O- or B-type stars. Given that the ionisation energy for the HeI line is higher than that of Brγ, it requires the presence of hotter and more massive stars, and hence its brightness falls off more rapidly after an instantaneous burst than that of the Brγ line. The time range covered by these two lines is from 0 to 10 Myr. Larger ages can be probed with the [FeII] line (a tracer of fast shocks produced in supernova remnants) whose contribution is almost constant from 3 to 35 Myr, and decreases sharply after that. Using the relative strength of those three lines, we are therefore able to probe ages in the range between 0 and 35 Myr, which represents a good match to the expected travel time of gas and star clusters along the nuclear ring.

Star formation along the rings

Figure 3 illustrates two plausible mechanisms that describe how star formation could proceed along the circumnuclear rings. In the first scenario, the popcorn model, gas enters the ring and accumu-

Figure 3: Two possible scenarios describing how star formation progresses along a nuclear ring. **Left:** the *popcorn* model, where star formation occurs randomly along the ring. **Right:** the *pearls on a string* scenario, where the ages of the stellar cluster define two sequences of increasing age along the ring. (Courtesy of J. Paillet, ESA)

Figure 4: Evidence in support of the *pearls on a string scenario* in NGC 613. **Left:** *HST F666W* image. **Right:** Heɪ-Brγ-Feɪɪ (blue-green-red) composite image of NGC 613 nuclear ring. Solid ellipse lines mark the location of the ring, star symbols the positions of the over-dense regions (ODRs), and arrows the sense of rotation of the stars and gas in the galaxy.

lates around it with no preferred location. Once a critical density is reached, the gas becomes unstable to gravitational collapse and star formation is triggered. In this model, individual hot spots collapse at random times and locations within the ring, and therefore there is no systematic age sequence. In the figure (left plot) the different starbursts are denoted by the star symbols and the different colours indicate different ages of the hot spots. In the second scenario (right), gas enters the ring at the intersection between the bar major axis and the inner Lindblad resonance. Downstream from this location, at the so-called over-density region (ODR), the gas density becomes sufficiently high to ignite star formation in a short-lived burst. A young cluster formed there will continue its orbit around the ring, but star formation will cease as soon as the first supernova explosions expel the gas. A series of starbursts triggered in the ODR will then produce a sequence of star clusters that

enter the ring like *pearls on a string*. In this scenario, the star clusters should show a bipolar age gradient along the ring, with the youngest clusters found close to the ODR, and increasingly older cluster ages in the direction of rotation, up to the opposite ODR. This is shown in the figure, where the colour sequence blue-green-red denotes clusters with increasing age.

In Figure 4 we put these two models to the test by showing the observations for NGC 613. In the left panel we display an *F666W HST* image of the nuclear regions. The ring is outlined with an ellipse, and two star symbols mark roughly the positions of the ODRs (based on the regions with highest dust extinction in the ring). In the right panel we present a false-colour image constructed from the SINFONI emission line maps of Heɪ, Brγ, and [Feɪɪ] assigned to the blue, green, and red colour channels, respectively. The bottom half of the ring shows the trends ex-

pected under the pearls on a string picture: an age sequence (blue-green-red) in the different hot spots. The sequence is less obvious in the top part of the ring due to the strong interaction between the ring and the radio jet. In the full sample, not shown here, three out of five galaxies show some evidence for an age gradient of hot spots along the ring, while the remaining two galaxies have incomplete information and thus are consistent with either model.

A more detailed account of the results presented here can be found in Böker et al. (2007).

References

Böker T. et al. 2007, AJ, in press
Buta R. and Combes F. 1996, Fund. Cosmic Physics 17, 95
Hummel E. et al. 1987, A&A 172, 51
Knapen J. et al. 2006, A&A 448, 489
Rossa J. et al. 2006, AJ 132, 1074

Gamma-Ray Bursts as Cosmological Probes: from Concept to Reality

Johan Fynbo[1]
Paul Vreeswijk[1]
Páll Jakobsson[2]
Andreas Jaunsen[3]
Cédric Ledoux[4]
Daniele Malesani[1]
Christina Thöne[1]
Sara Ellison[5]
Javier Gorosabel[6]
Jens Hjorth[1]
Brian Jensen[1]
Chryssa Kouveliotou[7]
Andrew Levan[8]
Palle Møller[4]
Evert Rol[9]
Alain Smette[4]
Jesper Sollerman[1,10]
Rhaana Starling[9]
Nial Tanvir[9]
Darach Watson[1]
Klaas Wiersema[11]
Ralph Wijers[11]
Dong Xu[1]

[1] Dark Cosmology Centre, Niels Bohr Institute, University of Copenhagen, Denmark
[2] Centre for Astrophysics Research, University of Hertfordshire, United Kingdom
[3] Institute of Theoretical Astrophysics, University of Oslo, Norway
[4] ESO
[5] Department Physics and Astronomy, University of Victoria, Canada
[6] Instituto de Astrofísica de Andalucía, Granada, Spain
[7] ASA Marshall Space Flight Center, Huntsville, Alabama, USA
[8] Department of Physics, University of Warwick, United Kingdom
[9] Department of Physics and Astronomy, University of Leicester, United Kingdom
[10] Stockholm Observatory, University of Stockholm, Sweden
[11] Astronomical Institute, University of Amsterdam, the Netherlands

We describe the current status and recent results from our ongoing programme at the VLT aimed at performing target-of-opportunity follow-up spectroscopy of gamma-ray burst (GRB) afterglows. Our primary goal is to secure redshifts for a complete sample of GRBs, thereby allowing the use of GRBs as probes of the cosmic star-formation history, chemical evolution and the luminosity functions of the GRBs themselves as well as their host galaxies. Contrary to earlier expectations, most optical afterglows are already faint a few hours after the bursts and 8–10-m telescopes are therefore crucial to determine redshifts for most GRBs.

GRBs as unique probes at all redshifts

It is fundamental to know the distance to an astronomical object. The majority of physical parameters depend on it, such as the luminosity and the size. The same holds true for γ-ray bursts and their afterglows. About ten years ago it was still controversial whether these brief flashes of γ-rays detected by satellites were located in our own Galaxy, or at cosmological distances. It was only after the first distance determination, or redshift, in 1997 that this debate was settled in favour of GRBs originating from the very distant Universe, implying that their energy output is enormous. We here describe our efforts to determine redshifts for a complete sample of GRBs.

One of the most interesting aspects of GRB research is that it sheds new light on a very broad range of astrophysics – from stellar evolution and the formation of compact objects, through ISM studies, dust formation, extinction curves, chemical evolution, intervening absorption systems, high-z galaxies at the faint end of the luminosity function, and all the way to probing the reionisation epoch. During the last ten years GRB research has seen enormous progress thanks to intensive global campaigns to identify and follow-up GRB afterglows and their host galaxies. Hence, while GRB research is challenging in using target-of-opportunity time at very large telescopes, it is an investment that certainly pays off. This is reflected in the high citation rates for GRB papers – a consequence of the broad range of astrophysics on which GRB results have implications. However, the full potential for advances based on GRB observations in all of these fields has not yet been exploited.

The idea to use GRBs as probes goes back to the beginning of the so-called afterglow era (e.g. Wijers et al. 1998). So far the main obstacle to using GRBs as probes of the luminosity function of star-forming galaxies, the cosmic star-formation history and the fraction of obscured star formation (to mention just three examples) has been the very incomplete and heterogeneous nature of the small sample of GRBs with measured redshifts. The currently operating *Swift* satellite (Gehrels et al. 2004) is changing this. *Swift* was specifically designed for GRB studies and offers a unique chance to build a sample of GRBs that is sufficiently large and complete to address very fundamental questions that cannot adequately be addressed in other ways. This is a golden opportunity that we simply cannot afford to miss.

Our complete sample of *Swift* GRBs

The *Swift* satellite has been operating for about three years and is far superior to previous GRB missions. The reason for this is the combination of several factors: (1) it detects GRBs at a *rate* of about two bursts per week – about an order of magnitude larger than the previous successful BeppoSAX and HETE-2 missions; (2) with its X-ray Telescope (XRT) it *localises* the bursts with a precision of about 5 arcsec – also orders of magnitude better than previous missions; (3) it has a much shorter *reaction time*, allowing the study of the evolution of the afterglows literally seconds after the burst, sometimes during the prompt γ-ray emission itself. The *Swift* mission is funded at least until 2010. Our primary objective is to secure a large sample, as complete as possible, of GRB afterglows while *Swift* is still operating. More concretely, rather than including all *Swift* detected GRBs, our group is concentrating on those GRB afterglows with favourable observing conditions, which fulfil the following criteria:
(1) XRT afterglow detected within 12 hr
(2) Small foreground Galactic extinction: $A_V < 0.5$ mag
(3) Favourable declination: $-70° < dec < 70°$
(4) Sun distance larger than 55°.

By introducing these constraints, we are not biasing the sample towards optically bright afterglows, but we select a sample for which useful follow-up observations are likely to be secured. About 50 % of all

Swift GRBs do not fulfil these criteria, primarily because *Swift*, for technical reasons, has to point close to the Sun a significant fraction of the time. For bursts fulfilling the above criteria, we make every possible effort to detect optical and near-infrared afterglows and to measure their redshifts.

As shown below, we have been very successful in this effort, using the ESO VLT. Redshifts, or more generally spectroscopic observations, are crucial for almost all GRB-related science. The most important science cases for which spectroscopy is critical are listed below:
(1) Determining the luminosity function for GRBs (prompt emission as well as afterglows)
(2) Determining the redshift distribution of GRBs and using GRBs as tracers for the cosmic star-formation history (Jakobsson et al. 2006; Fiore et al. 2007)
(3) Studying the host galaxies, in particular those faint, high-redshift galaxies that are unlikely to be found and studied with other methods (e.g. Vreeswijk et al. 2003)
(4) Studying GRB-selected absorption-line systems (e.g. Prochter et al. 2006)
(5) Characterising the dust extinction curves of high-z galaxies (see Figure 5 for example)
(6) Spotting very high redshift GRBs (e.g. Kawai et al. 2006; see also Figure 2)
(7) Probing cosmic chemical evolution wth GRBs (e.g. Fynbo et al. 2006; see also Figure 4)
(8) Studying if GRBs can be used for cosmography (e.g. Ghirlanda et al. 2004).

The need for 8–10-m telescopes

Since the launch of *Swift*, we have had programmes running at the VLT with the aim of securing redshifts for *Swift* GRBs (PIs Fynbo and Vreeswijk). The status at the time of writing is that 109 *Swift* GRBs fulfilled our selection criteria. For 57 of these a redshift measurement has been secured (see Figure 1). The VLT has been the dominant single contributor in all GRB redshift measurements, providing around 40 % of the secure redshifts to date. The second highest redshift was also measured by our group with the VLT (Figure 2). The redshift of the most distant
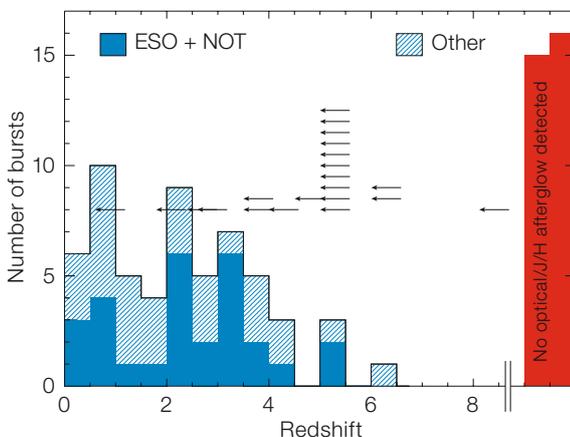
Figure 1: Redshift distribution (up to October 2007) of 109 long *Swift* GRBs localised with the X-ray telescope and with low foreground extinction $A_V \leq 0.5$. Of the 58 measured redshifts, our group has measured nearly half (25, shown in blue). As shown, the VLT is the dominant source of redshifts in the Swift era (four of the blue bursts in the histogram are also from the Nordic Optical Telescope). Bursts, for which only an upper limit on the redshift could be established so far, are indicated by arrows. Note that it is also difficult to secure redshifts for GRBs in the desert between $z = 1$ and $z = 2$. The red histogram at the right indicates the 27 bursts for which no optical/J/H afterglow was detected and hence no redshift constraint could be inferred (see Ruiz-Velasco et al. 2007 for a full discussion).

known GRB 050904 at $z = 6.295$ was measured with the SUBARU telescope (Kawai et al. 2006). Most of the other redshifts have been measured using other 6–10-m telescopes (Keck, GEMINI, SUBARU, Magellan). This is contrary to the expectations prior to the launch of *Swift*, where it was suspected that *Swift* itself, or at least 2–4-m telescopes, would be able to measure most of the redshifts. However, optical afterglows turned out to be much fainter at early times than anticipated. As we show in Figure 3, the majority of the afterglows are fainter than R = 20 when a slit can be placed on them. R = 20 is, in our experience, the limit for spectroscopic redshift determination using 2–4-m telescopes (typically, no more than 1–2-hr exposure time is available for observing GRB afterglows). Several optical afterglows are already fainter than R = 22 a few hours after the

burst. Hence, 6–10-m telescopes are crucial for securing redshifts for the majority of *Swift* GRBs.

The fact that, in particular, the VLT, but also other 6–10-m telescopes, have made tremendous efforts to secure redshifts means that we now have a much higher redshift completion than for pre-*Swift* samples. But it is clear that we will not get redshifts for all bursts from spectroscopy of the afterglows for multiple reasons. In about 20–30 % of the triggers we are not able to measure the redshift, either due to lack of lines (probably bursts at redshifts between 1 and 2 – see Figure 1), bad weather or because the afterglow has faded too much before it is observable from Paranal. For these bursts our only chance of measuring the redshift is via spectroscopy of the host galaxy. We have also pursued this route ex-
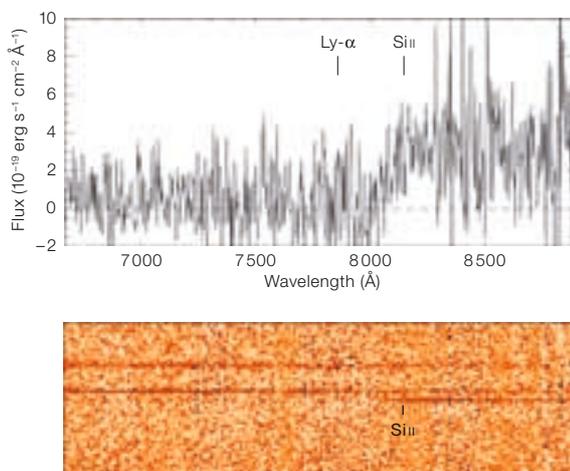
Figure 2: The spectrum of GRB 060927 obtained with FORS2 about 12.5 hr after the burst (from Ruiz-Velasco et al. 2007). A clear cutoff in the afterglow trace is observed at $\lambda = 8100$ Å, due to the onset of the Lyα forest at $z \approx 5.5$, making this the second most distant *Swift* GRB so far for which the redshift has been measured. The probable Si II line (shown more clear in the 2-dimensional spectrum below) allows a precise redshift determination of $z = 5.47$.
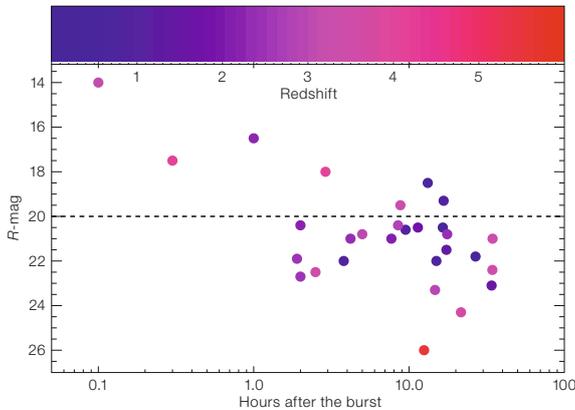
Figure 3: The *R*-band magnitude of the optical afterglows as a function of the time after the burst at which the spectroscopic observations were obtained. Only included are *Swift* bursts for which we have measured the redshift (using primarily the VLT, but also NOT, WHT and GEMINI). The colour bar at the top indicates the colour code for the measured redshifts. The dashed line marks a magnitude of R = 20 which is roughly the spectroscopic limit for 2–4-m telescopes for detecting absorption lines. As seen, most afterglows are fainter than this limit when observable.

tensively in an ESO large programme (PI Hjorth). This is a challenging task due to the faintness of these systems, and the analysis of these data is still ongoing, but we have already determined a number of redshifts (included in Figure 1).

The redshift distribution of *Swift* GRBs: current status

The first conclusion from Figure 1 is that *Swift* GRBs are very distant. *Swift* GRBs are more distant than GRBs from previous missions due to its higher sensitivity to the lower energies prevalent in the more distant events (Fiore et al. 2007). The median and mean redshift are now both 2.3, while for previous missions it was closer to 1 (Jakobsson et al. 2006). The record holder is $z = 6.295$ (Kawai et al. 2006) compared to the former $z = 4.50$ measured at the VLT. It is striking how events at redshifts as large as 6 can be detected within such a small sample. For comparison, only a few QSOs are detected at similar distances out of a sample of a hundred thousand QSOs. Remarkably, the redshift distribution, measured for just over 50 % of all bursts, is consistent with the redshift distribution predicted if GRBs are unbiased tracers of star formation (see e.g. Jakobsson et al. 2006 and *http://www.dark-cosmology. dk/~pallja/GRBsample.html* for a regularly updated analysis).

Additional science derived from afterglow spectroscopy

It is currently debated if and how GRBs may be biased towards a special sub-

set of massive stars, in particular those with low metallicity. This issue is not resolved, but there is evidence that, if it exists, such bias cannot be strong. Afterglow spectroscopy often allows us to measure the metallicity of the line of sight in the host galaxy. In Figure 4 we plot the metallicities along GRB sightlines together with metallicities derived from QSO absorbers and emission-selected galaxies. Here it can be seen that GRBs are more metal-rich than QSO-DLAs at similar redshifts and almost as metal rich as the Lyman-break galaxies. The shift in metallicity relative to QSO-DLAs can be understood from the different selection functions of the (star-formation selected) GRB-DLAs and the (H I cross-section selected) QSO-DLAs (Fynbo et al., in preparation). Hence, most likely, GRBs will be unbiased tracers of star-forming galaxies, at least at $z > 2$ (Fynbo et al. 2006). This further adds to the value of GRB afterglow spectra: they provide red-

shifts and information on ISM properties such as metallicity and kinematics of the inner, intensively star-forming regions of distant starbursts.

In addition to H I column densities, metal and molecular abundances and kinematics, the afterglow spectra also provide information on the extinction curves. The intrinsic spectrum of the afterglow from theory is predicted to be a power law and therefore any curvature or other broad features in the spectrum can be interpreted as being due to features in the extinction curve. So far, almost all the extinction curves we have derived for GRB host galaxy sightlines have been consistent with an extinction curve similar to that of the SMC. Recently we obtained the clearest detection yet of the 2 175 Å bump, known from the Milky Way extinction curve, in a $z = 2.45$ GRB (Elíasdóttir et al., in preparation and Figure 5). This GRB absorber also has unusually strong metal lines suggesting that the presence of the 2 175 Å extinction bump is related to a high metallicity. However, we have examples of GRBs with nearly solar metallicity for which the bump is not seen so it seems that metallicity is not the only parameter controlling the presence of the 2 175 Å extinction bump.

Finally, the VLT rapid response mode (RRM) has now started to deliver the first very interesting discoveries. The first time that the RRM was used fully automatically, without any human intervention from the *Swift* satellite GRB alert to the preset of the VLT, was when we triggered UVES

Figure 4: The logarithmic abundance with respect to hydrogen, expressed as a fraction of the Solar abundance, is plotted for various probes. Red circles represent the measurements for GRB metallicities (taken from the compilation of Fynbo et al. 2006). The small dots with no error-bars are the measurements for 121 QSO-DLAs taken from Prochaska et al. (2003). For comparison the range of metallicities for bright Lyman-break galaxies (LBGs) found by Pettini et al. (2001) is also shown. It is clear that GRBs in this small sample are more metal-rich than the QSO-DLAs and almost as metal-rich as the LBGs. Whereas the QSO-DLAs are cross-section selected, and the LBGs represent the most luminous (and hence rare) starbursts, the GRB hosts are presumably close to being purely star-formation selected.

Figure 5: The spectrum of the afterglow of GRB0 70802 obtained with FORS2 (from Elíasdóttir et al., in preparation). The flux calibrated spectrum (upper curve) and the observed error spectrum (lower) are shown. From the unusually strong metal lines we derive a redshift of $z = 2.45$. A broad absorption bump peaking around 7500 Å is clearly apparent. The spectrum is well fitted (red line) with a power-law spectrum and an extinction curve containing the 2175 Å extinction bump, known from our Galaxy and the LMC. This is the clearest detection of the 2175 Å extinction bump for any sightline outside the Local Group.

observations of GRB 060418. The afterglow happened to be bright, and the resulting sequence of spectra is truly unique due to the spectacular combination of response time (10 min), spectral resolution (45 000), time resolution (a succession of pairs of exposures with durations of 3, 5, 10, 20, 40 and 80 minutes) and signal-to-noise ratio (10–15 per pixel for each spectrum). This response time of only 10 minutes represented the fastest spectroscopic follow-up of any GRB by an optical facility at that time, let alone at this resolution (this record was later broken by another trigger from our team, for GRB0 60607, which was started a mere 7.5 minutes after the GRB).

The GRB 060418 spectra allowed us to measure the column density variability of various FeII fine-structure levels and metastable levels of FeII as well as NiII (see Figure 6). Both the observed variability and the detection of metastable levels of FeII and NiII had never been seen before in GRB host galaxies. Modelling the time evolution of the excited level population unambiguously shows that UV pumping from afterglow photons is the dominant excitation mechanism, and that the distance from the GRB to the cloud

Figure 6: The UVES spectra of GRB 060418 obtained in RRM (from Vreeswijk et al. 2007). The five epochs of spectra, beginning 10 min after the burst, are plotted with the colours black, red, blue, green and magenta, respectively. In the left panel individual lines are shown: typical resonance lines on the left; the lines arising from the excited levels of FeII and NiII on the right. The latter show evidence for a varying equivalent width as a function of time. To make this variability clearer, we have combined various lines that arise from the same level and constructed apparent column density profiles, smoothed with a boxcar of 5 pixels; these are shown in the right panel.

of excited atoms is unexpectedly large: 1.7 kpc (Vreeswijk et al. 2007). Applying this method to a sample of bursts will provide the radial distribution of neutral gas clouds around GRBs, and therefore around massive star-forming regions in faint distant galaxies.

Prospects

Spectroscopy of GRB afterglows provides redshifts and information on the ISM properties for the population of galaxies possibly responsible for the bulk of the high-redshift star formation. We are currently working on securing this information for a complete sample of *Swift* GRBs. The current sample of 109 GRBs is 53 % complete and we wish to increase both the sample size and the completion. Such a large and complete sample of GRBs constitutes a powerful tool to study the star-formation history of the Universe, complementary to studies based on either deep galaxy surveys or QSO absorbers. The spectra also allow a broad range of additional science, most importantly the study of the ISM of the galaxies hosting the GRBs. As stressed, *Swift* makes it possible to build such a sample. With the VLT we are finally moving GRBs as probes from concept to reality

References

Fiore F. et al. 2007, A&A 470, 515
Fynbo J. P. U. et al. 2006, A&A Letters 451, L47
Gehrels N. et al. 2004, ApJ 611, 1005
Ghirlanda G. et al. 2004, ApJ Letters 613, L13
Jakobsson P. et al. 2006, A&A 447, 987
Kawai N. et al. 2006, Nature 440, 184
Pettini M. et al. 2001, ApJ 554, 981
Prochaska J. X. et al. 2003, ApJ Letters 595, 9
Prochter G. E. et al. 2006, ApJ Letters 648, L93
Ruiz-Velasco et al. 2007, ApJ 669, 1
Vreeswijk P. M. et al. 2003, A&A 419, 927
Vreeswijk P. M. et al. 2007, A&A 468, 83
Wijers R. A. M. J. et al. 1998, MNRAS 294, L13
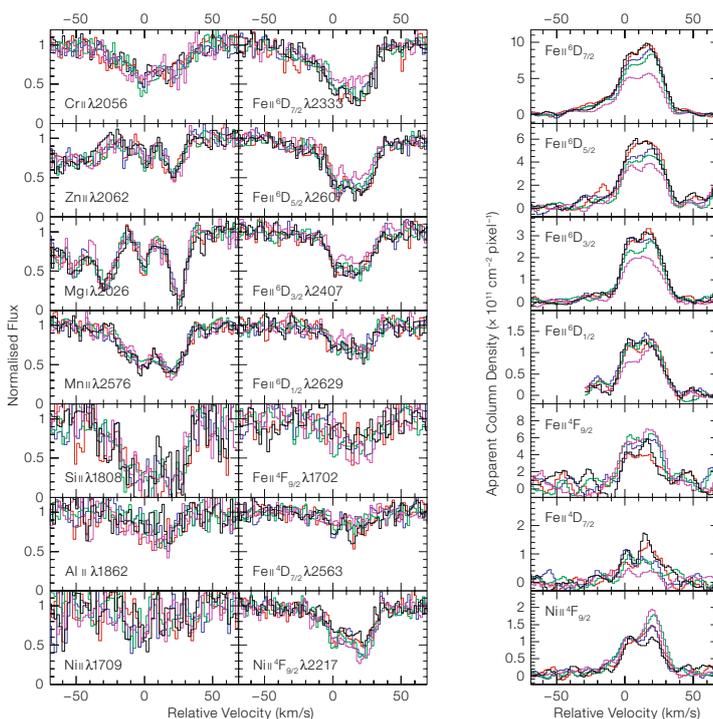
The Long Night of Science outside ESO Headquarters: a group of young people being shown around the constellations by Andreas Wicenec (at left).

The Long Night of Science inside ESO Headquarters: Jochen Liske explaining the ELT to a group of attentive visitors. (See article on page 59.)

Photos: H. H. Heyer, ESO

Report on the Conference

Science with the VLT in the ELT Era

held in Garching, Germany, 8–12 October 2007

Alan Moorwood
(ESO – on behalf of the SOC)

The workshop 'Science with the VLT in the ELT Era' was organised by ESO to provide a forum for its community to debate the likely evolution in the scientific use of the VLT over the next 10–20 years and to propose concepts for new instrumentation. Sessions were devoted to VLT and VLTI science highlights; future science priorities; VLT and VLTI synergy with ELTs, ALMA and JWST; second-generation VLT and VLTI instrumentation; new instrument concepts and VLT/I operating modes. Ample time was also made available for some very lively discussion sessions. This retrospective aims to summarise very briefly what was presented and to convey some feeling of the expectations and wishes of the community raised in the discussion sessions.

This was the latest in a series of Workshops organised primarily to provide the ESO community with a further opportunity to propose ideas and discuss the future of instrumentation at the VLT and VLTI. It was organised by ESO with help and input from its Scientific and Technical Committee (STC). A new slant this time was given by the fact that the timescale for the instrumentation concerned is expected to overlap with the availability of ALMA, JWST and, hopefully, a European Extremely Large Telescope. It was therefore considered important to devote time to discussing to what extent synergy or complementarity between these facilities might influence both the choice of instruments and/or operating modes of the VLT and its interferometric mode, the VLTI. This Workshop also provided the first opportunity to specifically assess the role of VLT and VLTI in the implementation of the recently published ASTRONET Science Vision. In practice, interest in these topics proved to be so high that it proved necessary to relocate the Workshop from ESO to the neighbouring Max-Planck-Institut für Extraterrestrische Physik whose help and hospitality in providing a large enough auditorium is most gratefully acknowledged. About 180 finally participated in the Workshop, some of whom appear in

Figure 1 and most of whom enjoyed the Bavarian style Workshop Reception and Dinner hosted by ESO at the Gasthof Neuwirt in Garching.

The opening welcoming address was given by the Director General, Tim de Zeeuw, who reminded us of ESO's priorities as established by Council, which include continuing to fully exploit the VLT and VLTI and its associated survey telescopes, VST and VISTA, as well as completing ALMA on time and budget and designing and securing funding for construction and operation of an E-ELT. I then made a short introduction to the Workshop, recalling its most recent predecessors in 2001 and 2005, devoted to VLT and VLTI second-generation instruments respectively, and explaining the intention of including 'ELT era' in the title as proxy for the wider context in which VLT/I is expected to be operating around a decade from now.

VLT and VLTI Science

The programme started with sessions on VLT and VLTI Science Highlights with invited (Alvio Renzini, Andrea Cimatti and Guy Perrin) and contributed (Martin Hähnelt, Piercarlo Bonifacio, Valentina D'Odorico, Mattieu Puech, Roberto Maiolino, Natascha Forster-Schreiber, Makato Kishimoto, Norbert Przybilla, Yiannis Tsamis, Giuseppe Bono, Walter Jaffe, Olivier Chesnau, Thorsten Ratzka, Gerd Weigelt, Stefan Kraus and Thomas Driebe) talks presenting scientific results which emphasise the unique science capabilities of the VLT and VLTI. This revealed that perhaps the most striking capability of the VLT so far has been its wide instrumental capability, distributed over 12 focal stations on 4 telescopes, thus allowing large amounts of observing time for each of a wide range of science programmes. This is somewhat in contrast to the original utilisation planned, which foresaw more simultaneous use of multiple instrument copies and the use of both coherent and incoherent combination of all four telescopes. During the discussion there appeared to be some consensus that maybe more consideration should, in fact, be given to exploiting these unique capabilities in the longer-term future.

The next session on Future VLT Science Priorities was the first such discussion on the future of the VLT/I since the appearance of the ASTRONET Science Vision document which was presented at the beginning (by Guy Monnet on behalf of Catherine Turon, chair of the ASTRONET Science Vision working group, who was unfortunately unable to attend). A short report on the Science Vision document can be found on page 2 of this issue. Although this Vision is to some extent directed more to future facilities, it is clear that VLT and VLTI will remain outstanding tools for addressing many of its high-priority science questions. These include a wide variety of capabilities for detecting and characterising exoplanets and the use of interferometry to study the effects of strong gravity e.g. produced by the black hole at the centre of our Milky Way. Jacqueline Bergeron elaborated beyond the Science Vision itself in outlining the many galaxy evolution studies needed. Many other areas were covered by contributions from Bob Nichol, Stephane Udry, Olivier Le Fèvre, Will Sutherland, Luigi Guzzo, Eelco van Kampen, Bram Venemans, Mike Irwin, Steffen Mieske, Grazina Tautvaisene and Klaus Reinsch.

The most lively discussion centred around the use of the VLT for extragalactic studies and, particularly, its suitability to address cosmological/physics questions concerning the origin and nature of dark matter and dark energy. Progressing beyond our current understanding of these mysteries appears to require investigations of massive samples, provided by imaging and redshift surveys, beyond those for which the VLT was designed and instrumented. Nevertheless, the VLT can bring powerful imaging and multi-object spectroscopic survey capabilities to bear on many questions concerning the origin and evolution of galaxies. The main issue to many for the future is field – e.g. could the field at the VLT be increased from its current maximum of 30′ at Nasmyth, to say around 1.5 degrees, by adding a prime focus on at least one of the 8-m Unit Telescopes? This facility could then be devoted to massive imaging and spectroscopic surveys. Although nothing is impossible, later contributed talks indicated that it would at least be technically challenging (weight and space restrictions, new active

Photo: H. H. Heyer, ESO

optics system) and would probably re-quire an expensive rebuilding of the tele-scope, requiring financial and human resources well beyond those foreseen for the 2nd-generation instrumentation plan which triggered this workshop. As stressed later by Mark Casali, it should also not be forgotten that the 4-m VISTA telescope, expected to start operation on Paranal in the near future, will also be the most powerful infrared survey facility world-wide for years to come.

Synergies between Facilities

Possible VLT and VLTI synergy with ELTs was the specific topic of the next session which was kicked off by a series of invited talks by Roberto Gilmozzi, Isobel Hook and Sandro D'Odorico who pro-vided an excellent overview of the European ELT project including its sci-ence goals and growing instrumentation plan. Marijn Franx also gave an invited talk on VLT/ELT synergy but ended up concluding that there might not be as much as commonly assumed. At least the VLT will probably not be needed to generate targets for the ELT which would more likely come from smaller survey telescopes. Contributed talks on various scientific and instrumental aspects were given by Jochen Liske (ESPRESSO to CODEX), Cesare Barbieri (quantum astronomy), Klaus Strassmeier (magnetic fields), Ralf Siebenmorgen (mid-IR imag-ing and spectroscopy), Matthias Tecza (near-IR IFU spectrometer for the ELT),

Luca Labadie (synergy between LBT and ELT) and David Crampton (TMT science and instruments). In the following discus-sion there was indeed a feeling that, while the VLT may be useful for preparatory work in the the pre-ELT era, the VLT and, particularly VLTI, will be most in demand for its complementary and unique scien-tific capabilities; these are therefore probably the ones to enhance through its future instrumentation programme. David Crampton's talk also suggested some possible complementarity between ELT and TMT, since neither project appears likely to have the resources to do every-thing alone.

This session was actually split into two by a dedicated Poster break to allow those interested to discuss with the presenters of a wide range of interesting posters covering: further scientific and technical aspects of ESPRESSO; science demon-strations of VLT/I; possible upgrades e.g. of FORS and FLAMES; science cases for high-resolution infrared spectroscopy and interferometry; etc.

The synergy theme was continued in the following session devoted to ALMA and JWST whose status were reviewed for us by Leonardi Testi and Mark McCaughrean respectively, and supplemented by con-tributions by Massimo Stiavelli and Luis Colina on extragalatic observations with JWST. Again, in the following discussion, the complementarity of these facilities rather than their synergy was stressed, although this may be largely a question of

semantics – obviously many astronomers want to use all of these facilities to tackle their particular science objectives.

Second-Generation Instrumentation

Then came one and a half days devoted specifically to Second-Generation VLT and VLTI Instrumentation. By way of intro-duction I summarised the current status which includes several second-generation instruments already under development for the VLT, plus three VLTI instruments, selected for Phase A studies following the VLTI dedicated workshop in 2005. The studies have just been completed and are awaiting recommendation by the STC in October 2007. I also summarised the ESO resources available to implement one or more of these and also those resources for new VLT instruments, for which a similar amount of money and FTE resources have been earmarked in ESO's Long-Term Perspectives as for the already approved complement of second-generation instruments. Most of this money is foreseen to become available, starting in 2010, for the development of instruments intended to fill the gaps left by the retirement of first-generation instruments due to technical or obsoles-cence reasons, starting around 2015!

Presentations of the recently commis-sioned HAWK-I and the already approved second-generation instruments X-shooter, KMOS, MUSE and SPHERE by Mark Casali, Lex Kaper, Ray Sharples, Roland Bacon (Figure 2) and David Mouillet respectively demonstrated what a power-ful enhancement of the VLT scientific capability they will bring in the period from now to around 2012. HAWK-I and MUSE will also profit from the ground layer and narrow angle adaptive optics corrections provided by the Adaptive Optics Facility (deformable secondary mirror, four laser guide stars and associated wavefront sensors to be installed on UT4 in 2012). Anticipating another topic featuring in this Workshop, that of VLT and VLTI

Figure 2: Roland Bacon presenting the approved second-generation VLT instrument MUSE.

operational modes in the future, it is clear that HAWK-I, KMOS, MUSE and SPHERE have to a large extent been built to conduct specific surveys. With the last three instruments built with large external participation, these surveys will partly be performed by the Consortia themselves in their Guaranteed Observing Time. The community may also, however, increase the demand on survey-mode science, which means probably longer but fewer programmes and perhaps revisiting the large-programme restrictions currently applied by the ESO OPC.

Presentations of the three VLTI instruments VSI, MATISSE and GRAVITY were given by their PI's Fabien Malbet, Bruno Lopez and Frank Eisenhauer respectively. These are all genuine second-generation instruments that will permit combination of 4–6 telescopes, compared with the current 2–3, to enhance the 'imaging' capability, and also employ various fringe tracking and AO techniques to go deeper, thus enlarging the astrophysical areas open to interferometric research.

New Instrument Concepts and Operating Modes

The final session on New Instrument Concepts and VLT/I Operating Modes was kicked off by Colin Cunningham who reviewed some exciting developments in smart focal plane and photonic technologies which may enable radically new types of instrumentation on the longer

term. Some of these and related aspects were returned to by Anthony Horton and Simon Ellis (photonics, IFUs, OH suppression). Wide-field options were presented separately by Stephen Todd and Ian Parry who illustrated the limited weight and space available for installing a prime focus at the VLT and by Roberto Ragazzoni who presented an alternative field-splitting approach being studied in connection with the ELT. Matt Lehnert proposed, alternatively, exploiting the Nasmyth field of nearly 30´ with a super-GIRAFFE equipped with deployable IFUs.

The other extreme of combining all four 8-m telescopes was advocated by Paolo Molaro to tackle extreme science questions such as the possible variability of the fundamental constants. This was actually one of several talks and posters on scientific and technical design aspects of ESPRESSO, a high-resolution visible echelle spectrograph for the incoherent combined focus which was presented by Luca Pasquini on behalf of a large consortium. This instrument developed out of the studies of CODEX for the ELT but, in addition to being a pathfinder for this instrument and some of its new technologies (e.g. the use of a laser comb for wavelength calibration), would be a super HARPS and UVES with a wide science case and could operationally complement 4 UT VLTI by being usable during medium to poor seeing conditions. In the infrared Alistair Glasse and Tino Oliva proposed considering N band spectropolarimetry and near-IR echelle spectroscopy respec-

tively. Thomas Ott argued for the retention of high spatial resolution capability to continue Galactic Centre studies in the post-NACO era and Markus Kissler-Patig presented CASIS, a concept study of one possibility, a wide-field ($1 \times 1´$) MCAO imager to be fed by the AOF at the Cassegrain focus of UT4. This proposal was in partial response both to a request by the STC, at the time of their recommendation of the Adaptive Optics Facility on UT4, to consider an optimised instrumentation of this focus plus the extremely promising results achieved with MAD, the MCAO demonstrator and shown earlier in this meeting by Giuseppe Bono. An interesting feature of the proposed design is that it provides simultaneous imaging in 5 bands between 0.6 and 5 µm.

In the category of operational modes, Craig Mackay urged us to think more about 'lucky imaging' and showed results of sub-0.1´´ images obtained combining this technique with AO in the visible; Andrea Richichi demonstrated the even higher resolution achieved by recording lunar occultations with burst-mode IR photometry; Andreas Seifahrt argued the possibility of squeezing micro-arcsecond astrometry even from existing instruments; Valentin Ivanov promoted more high-time-resolution observations; and Florian Kerber showed how more science could be achieved through the use of physical instrument models and improved calibration.

The last presented word was given to VLTI with a closing session of contributed talks on the VLTI in the ELT era by Markus Schöller, extrasolar science with the VLT/I by Didier Queloz and the next step in AGN research with interferometers by Klaus Meisenheimer.

Closing Discussion

The Workshop was finally closed with a lively discussion centred initially on the instrument proposals but recapitulating also other aspects already discussed earlier. These included the complementarity of VLT/I with other facilities including, but not exclusively, ALMA, JWST and ELT and the potential virtue of playing to unique features of the VLT/I, e.g. the ability to combine up to four 8-m telescopes

at the coherent and incoherent combined focii which have not been exploited so far. On the other hand it was repeated that some vital science goals, particularly related to DM and DE, require wide-field surveys and large amounts of observing time. For imaging at least there seemed to be a concensus that this might be better done by dedicated survey telescopes (including VISTA) on the ground or in space and that priority for supporting these science objectives should be given to more multi-object spectroscopy. Some proponents of this argued that the ideal would be a > 1 deg field, but if this proved too difficult or costly then at least an attempt should be made to exploit better one or more of the 0.5 deg Nasmyth fields, e.g. by adding a near-infrared spectrograph to the FLAMES facility.

Support was also forthcoming for extending the AO imaging capabilities of the VLT using the AO Facility + MCAO, but not necessarily at the expense of other powerful applications including spectroscopy. Questions were also raised as to the availability within the ESO community of the resources needed to realise all these new powerful instruments on the VLT, VLTI and ELT. As yet, there is no definitive answer but an optimistic prognosis based on the increase in the number of ESO member states and instrument groups since the start of the VLT development. Many groups may also be particularly and specifically interested in exploiting VLT/I for its unique scientific capabilities and/or as a testbed for ELT pathfinder instruments or technology.

The talks and posters will be published as both paper and ebooks in the Springer Astronomy and Space Science Proceedings series.

Report on

ALMA Community Days

held at ESO Headquarters, Garching, Germany, 3–4 September 2007

Leonardo Testi
Carlos De Breuck
(ESO)

The third of the ALMA Community Days was held at ESO Garching in September 2007. Prospective ALMA users were updated on the progress of the ALMA project, the plans for operations and for the ALMA Regional Centres (ARCs). The meeting was a lively forum for the discussion of the detailed organisation of the network structure for the European ARC.

The third European ALMA Community Days took place in Garching on September 3 and 4, 2007. The previous ALMA Community Day took place in September 2004 (see Messenger, 118, 67). More than 120 people from the astronomical

community came to learn about the progress of the ALMA construction and the plans for operations, as well as to discuss the organisation of the ALMA Regional Centre in Europe. The meeting was sponsored by Radionet, which provided funding for many of the participants to travel to Garching.

The workshop was opened with a welcome from the new ESO Director General, Prof. Tim de Zeeuw, who reassured the audience of astronomers that one of the top priorities of ESO is to deliver the ALMA observatory on time and on budget, in order to allow timely exploitation of its full scientific potential. Prof. Massimo Tarenghi, ALMA Director, reported on the enormous progress in the construction activities in the last few years. Three years ago, at the time of the last European ALMA Community Day

meeting, ALMA was still mostly a project 'on paper' with only a few of the pieces of prototype equipment being designed and built. In September 2007, most of the site infrastructure at both the Array Operations Site (AOS, Chajnantor Plateau 5 000m) and the Operations Support Facility (OSF, at a more comfortable altitude of 2 900m) is either completed or on track to be completed by the beginning of 2008. Five production antennas are being assembled and tested at the OSF, with more being manufactured in Europe, North America and Japan. The first front- and back-end sets are being integrated and a full quadrant of the correlator has been completely assembled, tested and is being packed for shipment to Chile and installation at the AOS Technical Building.

Alison Peck, ALMA Deputy Project Scientist, illustrated the plans for commissioning and for the initial opening of the

Figure 1: Opening of the ALMA Community Days in the auditorium of the Max-Planck Institut für Plasmaphysik in Garching.

ALMA observatory to users – first through participation in the Science Verification activities and then with the Early Science Call for Proposals, planned for 2010. It was pointed out that there is the possibility for astronomers in the community to be involved even earlier in the Commissioning phase of ALMA by going to Chile for extended periods with ESO support. The points of contact for expression of interest in Europe are the European ALMA Project Scientist (Leonardo Testi), the national representatives in the ALMA European Science Advisory Committee (ESAC) and the representatives of the European ALMA Regional Centre.

The workshop proceeded with a report on the status, scientific results and opportunities provided by the ALMA pathfinders, which are some of the current leading millimetre observatories (APEX, IRAM, JCMT and SMA). A number of interesting scientific results and prospects were highlighted by contributions, mostly from young fellows and postdocs, who form an army of enthusiastic future ALMA users. Neil Nagar illustrated the current developments of the astronomical institutes in Chile. The millimetre community in the ALMA host country is rapidly growing to ensure full and timely use of their share of observing time.

Another important focus of the Community Days was the presentation and

discussion of the current plans for scientific ALMA operations and user support. Lars-Åke Nyman, Head of the ALMA Department of Science Operations, and the three ALMA Regional Centre (ARC) managers, Paola Andreani (ESO), John Hibbard (NRAO), and Ken Tatematsu (NAOJ), illustrated the current operations plan and the proposed implementation. The North American ARC will be located in Charlottesville (USA), but will also collaborate with various institutes in the USA and Canada. The East Asia ARC will be located in Mitaka (Japan), serving the Japanese and Taiwanese astronomical communities.

The status and planning for the European ARC was presented in detail. This will have a network structure with a core node at ESO and at least six nodes in as many European countries. The core node at ESO will be responsible for carrying out all the ARC core functions (all stages of managing observing proposals and projects, data handling and archiving, maintenance of documentation) and to coordinate the overall activities of the European ARC. The ARC nodes will be responsible for many science-enabling functions essential for the astronomical community to take full advantage of the scientific potential of ALMA. Their activities will include face-to-face user support at all stages from proposal preparation to

data reduction and analysis. Each ARC node will specialise in providing advanced support in specific areas (e.g. high-frequency observations, polarisation, mosaicing, surveys, etc.) and their services will be open to all ALMA users. Postdoctoral programmes will be carried out by the whole ARC.

The current status and activities of the European ARC nodes were presented by representatives: Frank Bertoldi (Germany); Jan Brand (Italy); Tom Muxlow (UK); Hans Oloffson (Nordic countries); Karl Schuster (IRAM); Floris van der Tak (the Netherlands). These talks were followed by a discussion session led by José Afonso, Chair of the ALMA European Science Advisory Committee. The response from the community was generally very positive on the proposed support and competence of the various ARC nodes; the possibility for users to access ARC nodes outside their own country to use the services provided by the most experienced groups was highly valued. There was strong support to advance to the next step of ARC organisation by formalising the roles of the ESO ARC core and of the various ARC nodes. This would also help the ARC nodes to secure the required funding from their own national funding agencies and possibly the European Commission.

The programme and presentations from the ALMA Community Days can be found online at: *http://www.eso.org/projects/ alma/science/meetings/gar-sep07/agendas.html.*

We thank Elena Zuffanelli and Jennifer Hewitson for providing the logistical help that made this meeting possible.

Report on the Workshop

Surveys for ALMA

held at ESO Headquarters, Garching, Germany, 5–6 September 2007

Leonardo Testi
Carlos De Breuck
(ESO)

Current plans for surveys with existing, or soon to be operational, space and ground-based facilities relevant for ALMA science were presented and discussed. Special attention was given to the survey plans with the Atacama Pathfinder Experiment (APEX) and early results from pilot surveys were presented. The goal of the meeting was to ensure that optimal use can be made of ALMA as soon as operations begin. The role of surveys and large programmes in the early years of ALMA was also discussed.

Figure 1: 8 × 2 degrees of the Galactic Plane at 870 μm as seen in the APEX/LABOCA ATLASGAL survey (PI: F. Schuller/C.M. Walmsley). Approximately 60% of the sources discovered by ATLASGAL were not previously detected by IRAS or MSX. Surveys at mm wavelengths like this one will provide whole new classes of sources for ALMA follow-up in the coming years.

The 'Surveys for ALMA' workshop was held immediately following the ALMA Community Days. The workshop was partly supported by Radionet. The goals were to review the current plans for surveys relevant to ALMA, either ongoing or about to begin in the coming years, and evaluate whether these were adequate to ensure optimal use of ALMA from the beginning of science operations. The possible role of surveys and large programmes with ALMA during Early Science and the first years of Full Science Operations, and the synergy with other major facilities, were also discussed.

Many contributions reviewed the current plans for surveys from radio through infrared to optical wavelengths. The main facilities discussed were the Spitzer and Herschel Space Observatories, as well as the ESO survey telescopes (APEX at millimetre wavelengths and VST/VISTA in the optical and near-infrared), and other international observatories such as the JCMT, IRAM, NANTEN and ASTE, and the NRAO and ATNF facilities. The discussion that followed these presentations highlighted that there is a comprehensive plan in place for surveys that will provide ample ground for ALMA follow-up during Early Science and the first years of operations. In this phase, considering that ALMA will rapidly expand its capabilities up to Full Science Operations and that commissioning activities will proceed in parallel with science operations, there will probably be little scope for very large programmes with ALMA during these early years.

The general sentiment among the workshop participants was that as soon as the full ALMA capabilities will be available, a number of large projects will become possible and it will be necessary to think of possible schemes to handle this type of programme.

The possible synergies between ALMA and other large future facilities, like JWST, EVLA, CCAT and SKA, were briefly discussed. In the future it may be useful to explore possible ways to optimise programmes that will require the use of ALMA in conjunction with these facilities, in a similar fashion to what is currently done with ESO-VLT and ESA-XMM.

On the afternoon of 6th September, a topical meeting on the coordination of Surveys with APEX was also held in Garching, and was attended by about 50 participants. The three APEX partners (MPIfR, ESO and Sweden) first explained their respective time allocation procedures and provisions for large programmes. As each partner has a limited amount of observing time on this heavily oversubscribed facility, there is a clear desire to collaborate on large projects to increase their scientific impact.

Next, the results from pilot studies for two surveys were highlighted, both using the LABOCA bolometer array: (1) a joint ESO + MPIfR project to map the Extended Chandra Deep Field South. A first map including 100 hours of observing time has already identified more than a dozen new submm sources; (2) the ATLASGAL survey of the Galactic Plane is a joint project between the MPIfR, ESO and Chile exploiting the wide-field capabilities of LABOCA (see Figure 1).

Finally, plans for other surveys were also introduced, including further cosmological surveys with both LABOCA and the APEX SZ camera. Surveys include mapping of galaxy lensing clusters, the SMC and LMC, southern star-forming regions in Chamaeleon and Lupus III, main-sequence stars in nearby moving groups and CO surveys in nearby galaxies. Clearly, there will be no shortage of ideas on how to use APEX in the coming years!

The programme and presentations from the 'Surveys for ALMA' workshop can be found online at *http://www.eso. org/projects/alma/science/meetings/ gar-sep07/agendas.html*.

Announcement of

The Launch of the New ESO User Portal

Lowell E. Tacconi-Garman
(ESO – on behalf of the User Portal
Project Team)

A unified interface connecting ESO with
its community, the User Portal, has
been introduced. The motivation for the
new interface, and its implications for
users, are briefly outlined.

On November 14, a new interface con-
necting ESO and its user community was
launched: the User Portal. Within this
system, account information (username,
password, contact information) for all sci-
ence and observation-related web-based
applications (e.g. WASP, the Web Ap-
plication for Submitting Proposals) and
stand-alone software (P2PP, the Phase 2
Proposal Preparation tool) is unified, and
user-controllable.

This new interface is the result of a large
inter-division collaborative effort, that
has involved all those ESO groups and
departments responsible for providing
operational support to the users via dif-
ferent web-based applications (e.g. pro-
posal submission, preparation of Phase 2
packages, access to the ESO Archive).

The need for such a change was required
by the substantial increase of the
number of users of the science facilities
and services offered by ESO. If we
count those people who have registered
at the ESO Science Archive Facility
and/or have been a Principle Investigator
on an observing proposal, the number
we arrive at is more than 7 000 people.

To aid these users in all aspects of their
scientific interaction with ESO, from
preparing and submitting observing pro-
posals, to configuring Observation
Blocks (at Phase 2 or in preparation of a
Visitor Mode run), to requesting data
from the Science Archive Facility, ESO
provides a number of web-based
routines and standalone software appli-
cations. Examples of the former include
routines for data requests from the
Archive, while perhaps the best-known
example of the latter is P2PP.

To make full use of some of these tools,
users have always had to identify them-
selves by providing a recognised
username and password. For example,
in order to check the Webletter contain-
ing the outcome of the Observing
Programmes Committee (OPC) evaluation
and the scheduling review of their pro-
posals, users were required to enter iden-
tifying credentials.

Prior to last month, those usernames
and/or passwords were imposed by
different groups within ESO, and were
basically unchangeable thereafter. More-
over, since these different groups were
themselves operating with different
user databases, there were no straight-
forward means available to ensure that
the information for any given user agreed
across the board.

The User Portal project was developed
with these issues and drawbacks in mind.
The final goal was to provide our user
community with one single entry point for
all operational services we offer.

As a starting point, ESO made a strong
effort to establish a central list of users,
by combining information in both the
archive and proposal databases. Anyone
who had registered for the Archive or
submitted an observing proposal,
or both, was notified in an e-mail that an
ESO User Portal account had been
created for them. Despite the major effort
that was invested to try and merge users
with multiple usernames (mostly due
to different initials and/or last names on
submitted proposals, different e-mail
addresses, different registrations for
Archive access), some users ended up
receiving more than just one e-mail.
Users were then encouraged to activate
their account and update their contact
information, e.g. their ESO User Portal
profile. Users with unwanted multiple
activated accounts should contact ESO
(*usd-help@eso.org*) to request that
the extra accounts are merged. It is highly
recommended to have only one User
Portal account per user. Otherwise, the
history of any user's interactions with
ESO (e.g. submitted observing proposals,

approved/rejected runs, Phase 2 and pro-
gress report pages) will be split among
the different accounts, depending on
the account that was activated before a
certain interaction.

Clearly, this new interface affects all users
of ESO facilities, not only those that
were already registered. For instance, new
users wishing to submit an observing
proposal will now need to have a User
Portal account in advance of the proposal
submission deadline. Similarly, new users
wishing to retrieve non-proprietary
data from the ESO Archive will also need
to have an active User Portal account
beforehand. To make it easy to create
accounts we provide a simple, three-step
process. This begins by browsing
http://www.eso.org/UserPortal and click-
ing on the "I would like to create a
new account." link. As a second step, the
users are then asked to fill in the details
of their User Portal profile. The final
step is to click on the link provided in the
e-mail that the user will receive from us.
Account activation is crucial if any data
package is expected to be received
from the Archive: this step will not happen
automatically.

After activating their ESO-supplied
or self-created accounts, users have full
control over their usernames and pass-
words, and they are responsible for keep-
ing their contact information up to date.
Affiliation and postal address are, once
again, rather important at the time of data
shipment by the ESO Archive.

The ESO User Portal is intended to
make the use of ESO web applications,
and other software, simpler and more
manageable. For instance, users will now
employ the same username and pass-
word for all applications that require
them. More features will be added in the
near future. In fact, as far as ESO is
concerned, the launch of the User Portal
does not mark the completion of the
project, but we consider it to be only the
achievement of its first milestone.

For more information see *http://www.eso.
org/ESOUserPortal/docs/faq.html*.

Announcement of the ESO workshop on

Star Formation across the Milky Way Galaxy

3–6 March 2008, ESO Chile Headquarters, Santiago de Chile

Star formation in the Milky Way is a ubiquitous phenomenon. It occurs on many different scales and in diverse environments ranging from isolated cores, to small groups and modest associations, up to massive clusters and super star clusters. Our knowledge about the onset, dominant modes and typical outcomes of star formation is, however, in general biased by the limited observational accessibility of star-formation sites at their various distances and locations within the Galaxy.

Current large-scale surveys like GLIMPSE, SCUBA, ATLASGAL and UKIDSS trace gas, dust, and young stellar populations across our Galaxy. They provide new insights into the Galactic distribution of star-forming regions and young clusters, and the spatial and environmental variation of the star-formation history, efficiency and the initial mass function down to substellar masses. A revised picture of Galactic star formation is slowly emerging. This is required in order to understand the physics of young stellar objects, and star formation at large, which are key science topics for future projects like ALMA and E-ELT.

We therefore want to gather an up-to-date and comprehensive view of Galactic star formation by tracing ongoing and recent star formation across the Milky Way. The workshop aims to link communities that usually focus on specific scales and environments, and we will discuss star-formation activity spatially spanning from the Solar Neighbourhood, nearby star-forming regions and OB associations, to spiral arms, the Galactic disk, including the central bar and bulge, towards the Galactic Centre.

Our ultimate goal is to identify similarities, differences and the dominant modes of the star-formation process, and its typical outcomes, across the Milky Way, and beyond.

The workshop will be grouped around highlight talks that progressively cover the Galactic spatial scale, i.e. starting from local star formation towards increasing distance. The spatial coverage of the Milky Way will be complemented by topical sessions that will highlight overarching concepts and observations.

Invited Speakers include:

Fabrice Martins, Garching, Germany
Fred Adams, Michigan, USA
Giovanni Carraro, ESO/Chile
Joao Alves, Granada, Spain
John Bally, Colorado, USA
Nate Bastian, London, UK
Leo Blitz, Berkeley, USA
Bruce Elmegreen, Yorktown Heights, USA
Mark Gieles, ESO/Chile
Preben Grosbøl, ESO/Garching
Phil Lucas, Hertfordshire, UK
Piero Madau, Santa Cruz, USA, TBC
Tom Megeath, Toledo, USA
Jorge Melnick, ESO/Chile
Thierry Montmerle, Grenoble, France
Sergei Nayakshin, Leicester, UK
Livia Origlia, Bologna, Italy
Francesco Palla, Florence, Italy
Fred Schuller, Bonn, Germany
Andrea Stolte, Los Angeles, USA
Hans Zinnecker, AIP Potsdam, Germany

Please see the conference web-site for details, and registration information
http://www.sc.eso.org/santiago/science/MilkyWayStarFormation/

Announcement of

A Practical Workshop on IFU Observations and Data Reduction

19–24 May 2008, Astrophysikalisches Institut Potsdam, Germany

The NEON consortium (Network of European Observatories in the North) announces a workshop on Integral Field Unit observations and data reduction, to be held at AIP-Potsdam, Germany, from Monday to Friday, 19–24 May 2008.

The aim of this workshop is to provide the opportunity for potential IFU users to obtain practical experience in observational techniques, data reduction and analysis. Various types of IFU set-ups will be represented (e.g., fibre instruments, lens arrays, slicers) and participants will have the opportunity to work in small groups on data from instruments of their choice, under the direction of experienced tutors.

The mornings will be devoted to general lectures on various technical aspects, as well as some scientific highlights from actual observations.

The afternoons are reserved for practical work. The presence of experts in the field will offer a unique opportunity to share experience obtained with various IFU instruments; however the school is not primarily intended to respond to specific questions on particular data.

The workshop is open to PhD students or postdocs, and also to more senior astronomers, who would like to gain first-hand experience with IFU data and techniques.

The workshop is sponsored by the European Community, Marie Curie actions, and by Opticon. For PhD students who are nationals of a member state or associated state of the EU, a contribution to their expenses will be provided. Other requests for cost reimbursement will be considered on a case-by-case basis.

Owing to organisational constraints, the number of participants is limited to 30. The application deadline is 24 February 2008.

For details, see: *http://eas.iap.fr/ifu.html*

Announcement of the workshop on

Gas and Stars in Galaxies – a Multi-Wavelength 3D Perspective

10–13 June 2008, ESO Headquarters, Garching, Germany
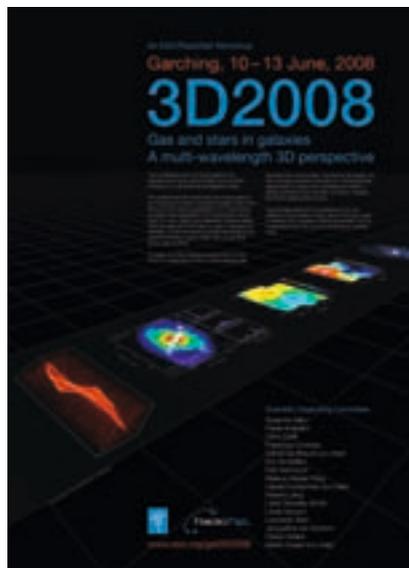
This workshop aims to bring together the optical/near-IR and submm/radio communities working on 3-dimensional extragalactic data. The aim is to have a mainly science-driven conference, centred on both gas and stars in and around galaxies in all stages of their evolution.

The optical/near-IR community now has access to an increasing number of powerful Integral Field Units (IFUs) and the second-generation VLT instruments, as well as the proposed E-ELT instruments, will all have IFU units. Radio and millimetre interferometers have provided 3D information on gas in galaxies for decades. ALMA will – by design – always provide high spatial and spectral resolution data cubes, and so will other future radio facilities.

To foster an active research environment for the future it is important to have a good interchange between the communities. Combining the stellar, hot and cold

gas dynamics provides an unprecedented opportunity to study many processes involved in galaxy formation such as infall, outflows, mergers and AGN-related phenomena.

A secondary goal of this conference is for the different communities to learn about the tools used to analyse and visualise 3-dimensional data, and to understand how they can be combined in the most optimal ways.

We envisage a highly interactive meeting and aim to achieve a balance between the presentation of scientific results based on current technology, and an investigation into the exciting possibilities of future technologies. The workshop is jointly supported by ESO and RadioNet.

For registration and more information, please visit:
http://www.eso.org/gal3D2008.
The registration deadline is 1 March 2008.

Announcement of

ONTHEFRINGE: the Very Large Telescope Interferometer Training Schools

Astrometry and Imaging with the Very Large Telescope Interferometer, 2–13 June 2008, Keszthely, Hungary

Optical interferometry is a new technology enabling observations with an angular resolution an order of magnitude larger than that of the largest single telescopes available at visible and infrared wavelengths. Europe has achieved world leadership with the ESO Very Large Telescope Interferometer (VLTI). This science machine will play a central role in understanding the life cycles of stars in the Milky Way, in the discovery and characterisation of planets orbiting stars in the Solar Neighbourhood, and the understanding of the energy conversion mechanisms in Active Galactic Nuclei (AGN).

ONTHEFRINGE is a set of four schools on optical interferometry and related science financed by the Marie Curie programme. The goal of the schools is to train young astronomers in the use of the

VLTI, therefore optimising the scientific return of the VLTI investment. Two of the schools are on data reduction. The other two deal with scientific topics where the VLTI will bring significant advancements – circumstellar disks/planets and active galactic nuclei.

Three of the schools have already taken place and were very much enjoyed by both students and lecturers! It is now the last chance to be part of one of these stimulating schools. This final school themes are astrometry, imaging and on the exciting science made available by PRIMA. The goals of these schools are to train proficient VLTI users by: (a) teaching interferometry basics in order to prepare successful observational proposals for the VLTI; (b) providing practical ses-

sions on data reduction; (c) presenting advanced techniques, such as astrometry and imaging, with a hands-on approach.

"In addition" all schools have a complementary skills pack dealing with: (a) presentation skills; (b) topics in scientific written communication; (c) professional ethics; (d) career development; and (e) opportunities in FP7 for young researchers.

The schools are open only to 50 students, the vast majority having their participation (travel and living) fully financed by the Marie Curie programme.

For further information, including application deadlines and procedures, refer to the ONTHEFRINGE site at *http://www.vlti.org.*

Announcement of

The NEON Observing Schools

The 7th NEON Observing School, La Palma Observatories, La Palma, Spain, 23 June – 5 July 2008

The 3rd NEON Archive Observing School, ESO Headquarters, Garching, Germany, 27 August – 6 September 2008
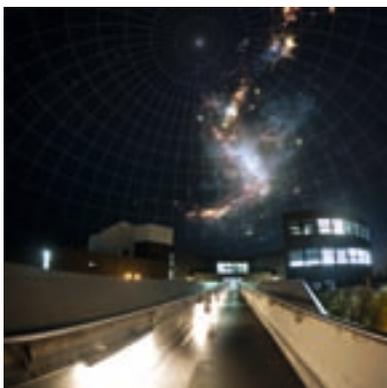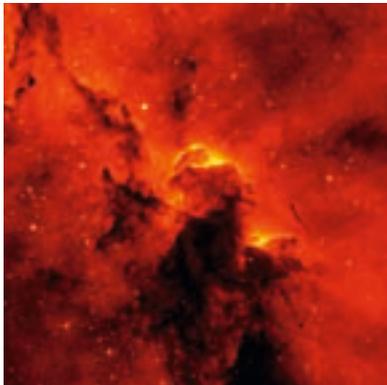
The Network of European Observatories in the North (NEON) is pleased to announce the NEON Observing Schools for 2008. The schools are sponsored by the European Community, Marie Curie Actions and supported by OPTICON and by the European Astronomical Society (EAS).

The purpose of the summer schools is to provide the opportunity for young researchers to gain practical experience in observational techniques, data reduction and analysis and the use of virtual observatory tools. Students will carry out small research projects, centred on selected astrophysical topics, in small groups under the supervision of experienced astronomers. These practical exercises will be complemented by lectures on general observational techniques and archival research for both ground- and space-based astronomy.

Figure 1 (upper): IC 1396B Nebula observed by the 2.5-m Isaac Newton Telescope. Nick Wright (UCL) and the IPHAS collaboration.
Figure 2 (lower): Montage of the NGC 1313 Galaxy over the ESO HQ in Garching.

The observing school at the telescopes on La Palma will largely concentrate on the skills required to execute an observing programme (imaging and spectroscopy) and instrumental developments. The Archive Observing School at ESO will concentrate on the quality appraisal of existing data and the research possible with large databases, combining ground and space data; emphasis will be on data-reduction techniques and the new tools now available within the Virtual Observatory.

The schools are principally open to astronomy PhD students and postdocs who are nationals of a Member State or an Associate State of the European Union. Applications from other European countries will also be considered.

The application deadline for both schools is 31 March 2008.

For details, see
http://www.eso.org/neon-2008
and
http://www.iap.fr/eas/neonNew.html

Personnel Movements

Arrivals (1 October–30 December 2007)

Europe

La Penna, Paolo (IT)	System Engineer/Physicist
Gonzalez, Juan Carlos (ES)	System Engineer
Jakob, Gerd (DE)	Engineer Cryogenic Systems
Burrows, Andrew (GB)	Systems Administrator
Vasisht, Gautam (IN)	Physicist
Bierwirth, Thomas (DE)	Software Engineer
Cayrel, Marc (FR)	Opto-Mechanical Engineer
Ziegler, Bodo (DE)	User Support Astronomer
Ramsay, Suzanne (GB)	Instrument Scientist
Battaglia, Giuseppina (IT)	Fellow
Neumayer, Nadine (DE)	Fellow
Bourtembourg, Reynald (FR)	Software Engineer
Nittel, Frank (DE)	Draftsman
Brogaard, Karsten (DK)	Student
Misgeld, Ingo (DE)	Student
Santangelo, Gina (IT)	Student

Chile

Hills, Richard (GB)	Alma Engineer/Scientist
Saldias, Antonio (CL)	Safety Officer
Segovia, Alex (CL)	Software Engineer
Urrutia, Josefina (CL)	Software Engineer
Pilquinao, Jorge (CL)	Electrical Engineer
Beltran, Juan (CL)	Laser Operator
Fox, Andrew (GB)	Fellow
De Ugarte Postigo, Antonio (ES)	Fellow

Departures (1 October–30 December 2007)

Europe

Ngoumou Yewondo, Judith Savina (DE)	Student
Korkiakoski, Visa (FI)	Student
Pedicelli, Silvia (IT)	Student
Kapadia, Amit (USA)	Student

Chile

Sepulveda, Jorge (CL)	Software Engineer
Alarcon, Hector (CL)	Telescope Instruments Operator
Roa, Luis (CL)	Mechanical Technician
Barrios, Emilio (CL)	Scientific Instruments Operator
Geissler, Kerstin (DE)	Student
Noterdaeme, Pasquier (BE)	Student
Vehoff, Stefan (DE)	Student

Fellows at ESO

Gaël James

Gaël James

Astronomy always interested me as a child, but the truth is that I had thought of many other professions before choosing this one. At least until I met two very enthusiastic astronomy professors while I was studying physics at Orsay University near Paris, in 1999. Not only did they pass on to me their passion for trying to understand the Universe, but, knowing about my origins and my growing interest to come back to South America, they also showed me the first pictures of the VLT while it was still being built and told me about its impressive first scientific achievements. The international aspect of the project and its foreseen impact on astronomy were definitively something of which I wanted to be a part.

I followed a Masters course at the Paris Observatory and had first contact with ESO for my thesis. After this, I obtained my PhD at the Paris Observatory studying chemical abundances of heavy elements in globular cluster stars. This work relied on high-resolution spectroscopic data taken at the VLT. During my PhD I also discovered the pleasure of observing in several observatories around the world, amongst which of course were La Silla and Paranal. I finally joined ESO as a fellow in October 2005 after completing my PhD and having spent a year as a teaching and research assistant in Paris.

Now, I work at the Paranal Observatory as a support astronomer. In particular,

I am the Instrument Fellow for UVES, the VLT high-resolution ultraviolet and visual échelle spectrograph. In a few months, I will take over as its 1st Instrument Scientist. This has given me a lot of experience with an instrument that I regularly use for my science. Coupled with the rare human experience of working with highly dedicated professionals in a challenging but friendly environment, this has made my experience at ESO a great success.

Lorenzo Monaco

I received my PhD in astronomy from Bologna University in 2004. Before joining ESO in June 2005, I also covered a post-doctoral position at the Trieste Observatory. Therefore, the position at ESO was going to be my first experience in an international institution and I was very much looking forward to it.

Working at ESO is a wonderful experience for a young astronomer. The number of seminars at the ESO Vitacura office in Santiago, together with the visiting scientist programme, provides the opportunity to meet a number of scientists working on very different fields. Furthermore, the environment is enriched by the continuous flow of people joining ESO, from senior astronomers to fellows and students. On the other hand, due to the observatory duties, some difficulties do exist in meeting colleagues in Santiago. Occasions like the traditional VVV, Vitacura Vino y Verbos, are thus

very stimulating. At the VVV everyone is invited to briefly present any news considered interesting. Being in charge of organising the VVV for about one and half years was a nice opportunity to be directly involved in the Vitacura science life.

My research activity is focussed on the study of resolved stellar populations in the Local Group with the main aim of understanding the processes which drive galaxy formation. In particular, recently I spent a large part of my time computing chemical abundances from high-resolution spectra of Red Giant Branch stars in the Sagittarius dwarf spheroidal galaxy, which certainly represents the most striking ongoing merger event in the Milky Way.

At the La Silla Observatory I spend most of my time working with the 3.6-m telescope instruments. Supporting these instruments is very instructive. With EFOSC2 I could use observing modes with which I was not familiar (e.g. low-resolution spectroscopy, polarimetry), while with HARPS I could refine my expertise with high-resolution spectroscopy. Taking care of an instrument is a very stimulating task.

Spending a few years at ESO allowed me to start many new collaborations. I could expand both my technical and science-related knowledge and I was able to start investigating fields to which I had not been exposed.

Lorenzo Monaco

A Long Night for ESO

Henri Boffin
Claus Madsen
(ESO)

Home, sweet home! In October, the Garching campus, that is home to the ESO headquarters in Germany, celebrated its golden anniversary. The campus has indeed existed since 1957, when the 'Garching Atom-egg' was inaugurated. It was the first nuclear installation in Germany and a pioneer in nuclear research.

Since then, the Garching Campus has developed extensively, welcoming several Max-Planck Institutes (Astrophysics, Extraterrestrial Physics, Plasma Physics, Quantum Optics), several institutes of the Bavarian Academy of Sciences, the Federal Research Institute for Food Chemistry, and the Bavarian Centre of Applied Energy Research, to name just a few. In the course of the years, also several departments of both Munich universities (Mathematics, Computer Science, Physics, Chemistry, Mechanical Engineering) settled here, conferring on Garching the title of a University city. There are now about 4 000 people who work on the campus, in addition to the 8 500 students, making the campus almost as populous as the town of Garching itself.

Albeit ESO only joined the Campus in 1980, it participated fully in the activities for the 50th Anniversary, organising or taking part in several public events. The set of activities started on 26 September, with a gala evening, featuring high-level politicians, including the then Prime Minister of Bavaria, Dr Edmund Stoiber, and the German Federal Secretary of State for Research, Dr Thomas Rachel (see Figure 1). On 2nd of October, ESO organised a round-table discussion on the topic of "Arts and Science". The discussion was moderated by a well-known space-science journalist, Dirk Lorenzen. Hans-Ulrich Käufl from ESO responded to Ernst-Peter Fischer, Dieter Ronte, and Elmar Zorn, on the interplay between the two very different sensitivities and how they can apprehend the world. The event, which was broadcast on Bavarian TV, was very successful, drawing participants

Figure 1: The Mayor of Garching, Manfred Solbrig, addressing the audience of invited guests at the gala event on 26 September.

from all over Germany and abroad, and allowed people to see the ESO Headquarters building in a new and unique setting: on this occasion, paintings by Rita Adolff-Wollfarth, a German painter who also participated in the discussion, were on display in the building.

Another round-table event took place eleven days later, this time organised by the whole campus. Under the title "From Garching to Europe, Science in a Globalised World", a panel of six science policy experts discussed how the Garching campus might evolve in the future, including its role in the international fabric of science.

On the same day, 13th October, the campus organised a 'Long Night of Science', running from 18:00 till midnight. As usual, ESO, with the participation of staff from all the divisions, set up a wide range of activities. The visitors could watch the latest ESO movie or attend short scientific talks on many subjects – from the history of the telescope to the principles of interferometry, from the study of exoplanets to the interaction of galaxies.

They could also glance at the exhibition, featuring panels and models, or talk with the many staff present. They could address their questions to Nancy Ageorges in Paranal over the video link, with Christian Hummel in Garching taking the role of moderator. Activities were also organised for the young, such as puzzles, a stamp quest, a quiz and a planetarium show. As the weather was fine and the skies clear, the members of the AGAPE observational astronomy group were able to share their enthusiasm with visitors (see photo on page 47). The Charity group also set up a very successful stand, selling a variety of food from different European countries that had been generously prepared by many ESO staff and their families. Particularly popular were the Belgian waffles, whose mouth-watering smell attracted many people.

By the end of the night, about 1 800 people had visited ESO's headquarters during the 6-hour period. A remarkable achievement, since at the same time, the national soccer team was playing a qualifying match for the European Championship!

Report on the

First ESO-EAAE Astronomy Summer School

held at ESO Headquarters, Garching, Germany, 19–23 July 2007

Douglas Pierce-Price[1]
Rosa Maria Ros[2]
Claus Madsen[1]

[1] ESO
[2] EAAE

The 1st ESO-EAAE Astronomy Summer School for teachers took place in the ESO Headquarters in Garching from 19th to 23rd July 2007. This summer school was based on ten years of successful schools organised around Europe by the EAAE (European Association for Astronomy Education), but 2007 marked increased involvement by ESO. In addition, the summer school was recognised as a Socrates course, allowing teachers to apply for funding through the Socrates programme, while some additional support for delegates was made available through ESO.

Fifty teachers and other educators from 16 countries around Europe, plus Chile, took part in the summer school, with the theme of "Strategies for effective teaching of astronomy". The aim was to promote active participation and the exchange of ideas, and the school was open to all teachers with an interest in astronomy.

The summer school included workshops from EAAE instructors, poster sessions on astronomy teaching activities and a series of general talks presented by scientists at ESO. In addition, there were amateur observing sessions kindly arranged by AGAPE, and a live video link to the VLT on Paranal.

In the opening session, participants were welcomed by Claus Madsen (Head of the ESO Public Affairs Department), Fernand Wagner (President of the EAAE), and Rosa M. Ros (Chair of the Summer School).

During the five days of the course, the participants took part in ten different workshops, on topics as diverse as educational exercises involving gravitational lenses, a study of Eta Carinae, and ways to make astronomical observations with a pinhole camera. A guide to ESO's educational programmes was also

Figure 1: Participants in the 1st ESO-EAAE Astronomy Summer School for teachers in the entrance hall of the ESO Headquarters.

presented by Douglas Pierce-Price, and Claus Madsen discussed science education in a European context. In addition, as a new feature of the joint ESO-EAAE Summer School, there was a series of extremely well-received talks by ESO astronomers about the latest work of the organisation. These included presentations on the European Extremely Large Telescope (E-ELT) by Roberto Gilmozzi, the Atacama Large Millimeter/submillimeter Array (ALMA) by Paola Andreani, and "Supernovae: the exploding stars" by Ferdinando Patat. In addition, delegates were able to share more information by presenting posters of their educational projects.

Also during the day, we were very fortunate to be able to make observations of the Sun, thanks to the help of the AGAPE team. Unfortunately, the weather in the evening was not good enough for night observations, but an excellent live video presentation from Paranal by Paul Lynam

proved a highlight of the summer school. At the weekend, a trip to the Deutsches Museum in Munich gave delegates a chance to visit its astronomy exhibits, and more.

At the end of the five-day-long Summer School, all delegates received a certificate of participation from ESO and the EAAE. However, of course, the most important things they took home were knowledge about the latest astronomical developments at ESO, an understanding of new and exciting ways to teach astronomy, memories of a great summer school, and new contacts with colleagues and friends.

Thanks are due to all the speakers, the AGAPE volunteers, and the organising committees, for making this first joint summer school such a resounding success. The next summer school, which is currently being planned, will take place in Granada in July 2008.

A String of Exhibitions

Ed Janssen, Luis Calçada,
Hans Hermann Heyer (ESO)

As part of its remit, ESO shares its endeavours and the discoveries made by its telescopes with as many of the general public as possible, particularly in the ESO member states. Press releases and publications are part of this communication, but as often as possible we try to take the message more directly to the public. For many years ESO has participated in exhibitions geared both to the general public and professional scientists. This year was no exception and ESO participated in a string of exhibitions in many countries.

An important event this year was JENAM, the Joint European and National Astronomy Meeting, which is organised annually in one of the European countries, jointly by the European Astronomical Society and the national astronomical society. This year, JENAM took place in Yerevan, Armenia, allowing many to discover a unique culture and country. ESO was present at this European astronomical event, also with an exhibition (see Figure 1).

In mid-2007, a French version of the ESO exhibition went on a real 'tour de France', travelling from Meursault to Paris, then to Meudon. At the end of May, the city of Meursault in Burgundy was renamed for five days 'Meursault les Etoiles', as it featured many astronomical activities for schools and the general public. In June, ESO participated for the third time in the European Research and Innovation Exhibition, held in Paris, an event that attracted about 25 000 visitors (see Figure 2). This year, ESO joined partners with three astronomical institutes from Paris that develop instruments together with ESO or make use of ESO telescopes: the Paris Observatory; the Institut d'Astrophysique; and CEA/Saclay. Staff from these institutes manned the ESO stand and interacted with the public. Many were former ESO staff and they shared their knowledge with visible pleasure. They also helped moderate the daily videoconferences that took place with Paranal, with Olivier Hainaut on the other end of the line. Later, in October, the ESO exhibition was featured at the Meudon site of the Paris Observatory

Figure 1: The ESO exhibition stand at the JENAM conference in Yerevan, Armenia was a focal point.

Figure 2: Henri Boffin (ESO) giving an interview to France 24 TV at the Salon Européen de la Recherche et de l'Innovation.

during Science Week. About 1 000 school children attended, while on the Sunday, 1 600 members of the general public visited.

France was not the only country visited of course, and ESO was also present at meetings in Switzerland, Germany and the Netherlands. In Switzerland, ESO participated in the first Swiss Astronomy day, which took place on the 20th of

September on the Üetliberg near Zurich (see Figure 3). One of the organisers, Ms. Barbara Burtscher, had won the Specially Donated EIROforum/ESO Prize at the 16th European Young Scientists Contest in 2004. Her reward was a trip to Paranal. The September event in Zurich featured Bruno Leibundgut as one of the speakers. Bruno also moderated several videoconferences with Paranal, this time with Thomas Szeifert. The event attracted some 1 500 visitors.

In Germany, ESO had a stand during the 80th Annual Scientific Meeting of the 'Astronomische Gesellschaft' (AG), which also hosted the 5th biennial Workshop on Astroparticle Physics. This event, where ESO's Director General presented the ASTRONET Science Vision, took place in Würzburg on 24–28 September and was attended by some 300 participants.

Finally, in the Netherlands, ESO was present with an information stand at the International Festival for Astronomy (IFA) that took place near Utrecht. This three-day event, which focuses on senior high school students and beyond, was organised by the Dutch Youth Working Group for Astronomy and the Royal Netherlands Society for Meteorology and Astronomy. Amongst many other interesting sessions, the winners of the Catch a Star 2007 competition, Jan Mestan and Jan Kotek from the Czech republic, gave a presentation of their trip to the Paranal Observatory.

Figure 3: Former ESA astronaut Claude Nicollier talking with Ed Janssen (ESO) in front of the ESO stand on the 1st Swiss astronomy day.

Distinguished Visitors to Paranal

Henri Boffin
Claus Madsen
(ESO)

As part of his first official trip to Brazil and Chile, the European Science and Research Commissioner, Janez Potočnik, visited the ESO Paranal Observatory on 27 November. The Commissioner was accompanied by, among others, Jaime Pérez Vidal, Head of the Delegation of the European Commission (EC) to Chile, Mary Minch and Cornelia Nauen, respectively Director and Principal Administrator of International Scientific Cooperation for the EC, and Hervé Peró, Head of EC Unit Research Infrastructures.

Figure 1: EC Commissioner Janez Potočnik at the Control-Console of the VLT.

Figure 2: A colour composite image of the spiral galaxy NGC 134 based on images obtained in B, V, R and H-α filters with FORS2 during the visit of Commissioner Potočnik.

The guests were welcomed by the ESO Director General, Tim de Zeeuw, the ESO Representative in Chile, Felix Mirabel, and the Director of the Paranal Observatory, Andreas Kaufer, and stayed overnight on Paranal. The Commissioner visited the VLT Control Room (see Figure 1) and participated in an observing sequence. He observed the warped spiral galaxy NGC 134 with the FORS2 instrument on Antu. Figure 2 shows a colour composite, based on the images, made after the event.

The Commissioner's visit was part of an official trip to Chile and Brazil. The EU has established a bilateral relationship with Chile and a Science and Technology agreement was signed in 2002. More information on the visit can be found in PR's 48/07 and 49/07.

A few weeks later the Regional Minister for Research of the Belgian French-speaking Community, Marie-Dominique Simonet, visited Paranal on 17th November. This was also part of a visit to Brazil and Chile, in which the Minister promoted the 'Competitivity Poles', as well as Research and Education. The Minister was accompanied by a delegation consisting of Claude Gonfroy and Jean-Luc Horward, both members of her Cabinet, Jean-Pierre Swings, former member of the ESO Council, Claude Jamar from the Centre Spatial de Liège, and Bill Collins, from the AMOS company which built the four Auxiliary Telescopes. Ten French-speaking Belgian journalists, including two TV crews, also joined the Minister for a day at Paranal. Felix Mirabel, Olivier Hainaut, Head of Science Operations at Paranal, and Ueli Weilenmann, were the ESO hosts.

The Minister visited the telescopes and facilities on site and was clearly interested, as evidenced by Figure 3. Her visit coincided with her birthday and, at the dinner, she was presented with a cake and flowers, as well as gifts from members of her delegation.

Figure 3: The Belgian Regional Minister of Research, Marie-Dominique Simonet, in discussion with Paranal staff inside the Kueyen dome with FORS1 in the background.

Contents

Front Cover Picture: VLT HAWK-I near-infrared image of part of the Serpens star-forming region, showing a wealth of evidence for emergence of young stars from their patental cloud. This colour composite image was formed from three 1-min exposures in *J*, *H* and *K* filters taken during instrument commissioning. (See ESO PR Photo 36c/07.)